AFWAL-TR-86-3007

STRUCTURAL EVALUATION OF HIGH STRAIN FIBER AND RESIN COMPOSITE MATERIAL SYSTEMS

AD-A170 464

D. L. BUCHANAN

P. S. McCLELLAN

McDonnell Aircraft Company
McDonnell Douglas Corporation
P.O. Box 516
St. Louis, Missouri 63166

APRIL 1986

Final Report for Period 18 September 1984 - 18 January 1986

FLIGHT DYNAMICS LABORATORY
AIR FORCE WRIGHT AERONAUTICAL LABORATORIES
AIR FORCE SYSTEMS COMMAND
WRIGHT-PATTERSON AIR FORCE BASE, OHIO 45433

NOTICE

When Government drawings, specifications, or other data are used for any purpose other than in connection with a definitely related Government procurement operation, the United States Government thereby incurs no responsibility nor any obligation whatsoever; and the fact that the government may have formulated, furnished, or in any way supplied the said drawings, specifications, or other data, is not to be regarded by implication or otherwise as in any manner licensing the holder or any other person or corporation, or conveying any rights or permission to manufacture use, or sell any patented invention that may in any way be related thereto.

This report has been reviewed by the Office of Public Affairs (ASD/PA) and is releasable to the National Technical Information Service (NTIS). At NTIS, it will be available to the general public, including foreign nations.

This technical report has been reviewed and is approved for publication.

DAVID L. GRAVES, 1LT, USAF
Project Engineer

FRANK D. ADAMS, Chief
Structural Integrity Branch
Structures & Dynamics Division

FOR THE COMMANDER

ROGER J. HEGSTROM, Col, USAF
Chief, Structures & Dynamics Division

If your address has changed, if you wish to be removed from our mailing list, or if the addressee is no longer employed by your organization please notify AFWAL/FIBEC, Wright-Patterson AFB OH 45433-6553 to help maintain a current mailing list.

Copies of this report should not be returned unless return is required by security considerations, contractual obligations, or notice on a specific document.

UNCLASSIFIED
SECURITY CLASSIFICATION OF THIS PAGE

AD-A170 464

REPORT DOCUMENTATION PAGE

1a. REPORT SECURITY CLASSIFICATION	1b. RESTRICTIVE MARKINGS
2a. SECURITY CLASSIFICATION AUTHORITY UNCLASSIFIED	3. DISTRIBUTION/AVAILABILITY OF REPORT Approved for public release; distribution unlimited
2b. DECLASSIFICATION/DOWNGRADING SCHEDULE	
4. PERFORMING ORGANIZATION REPORT NUMBER(S)	5. MONITORING ORGANIZATION REPORT NUMBER(S) AFWAL/TR-86-3007
6a. NAME OF PERFORMING ORGANIZATION McDonnell Aircraft Company McDonnell Douglas Corporation 6b. OFFICE SYMBOL (If applicable)	7a. NAME OF MONITORING ORGANIZATION Air Force Wright Aeronautical Laboratories (AFWAL/FIBEC)
6c. ADDRESS (City, State and ZIP Code) P.O. Box 516 St. Louis, Missouri 63166	7b. ADDRESS (City, State and ZIP Code) Wright-Patterson Air Force Base, Ohio 45433
8a. NAME OF FUNDING/SPONSORING ORGANIZATION 8b. OFFICE SYMBOL (If applicable)	9. PROCUREMENT INSTRUMENT IDENTIFICATION NUMBER Contract F33615-84-C-3231
8c. ADDRESS (City, State and ZIP Code)	10. SOURCE OF FUNDING NOS. PROGRAM ELEMENT NO.: 62201F; PROJECT NO.: 2401; TASK NO.: 01; WORK UNIT NO.: 92
11. TITLE (Include Security Classification) Struct. Eval of High Strain Fiber & Resin Composite Material Systems	
12. PERSONAL AUTHOR(S) David L. Buchanan and Paul S. McClellan	
13a. TYPE OF REPORT Final Technical Report 13b. TIME COVERED FROM Sep 1984 TO Jan 1986	14. DATE OF REPORT (Yr., Mo., Day) April 1986 15. PAGE COUNT 90
16. SUPPLEMENTARY NOTATION	

17. COSATI CODES

FIELD	GROUP	SUB. GR.
11	04	
13	13	

18. SUBJECT TERMS (Continue on reverse if necessary and identify by block number)
Composite Materials; Fatigue Life; Tough Resins; Stress Analysis; Static Strength; Low Energy Impact Damage Tolerance

19. ABSTRACT (Continue on reverse if necessary and identify by block number)

The subject of this program was structural evaluation of high strain fiber and resin composite material systems. The objective was to develop a combined analytical and experimental procedure for performing a structural evaluation, then use it to evaluate the effects of recently developed higher strain fibers and resin systems on strength, durability, and damage tolerance of advanced carbon/epoxy composite material systems.

Testing included evaluation of basic lamina properties, static and fatigue testing of laminates with and without stress concentrations, evaluation of tolerance to low energy impact damage, and static and fatigue testing of a multifastener metal-to-composite splice joint. Included in the structural evaluation were analytical methods to predict unnotched and notched laminate strength and mode of failure based on unidirectional ply mechanical properties.

(Continued on reverse)

20. DISTRIBUTION/AVAILABILITY OF ABSTRACT UNCLASSIFIED/UNLIMITED ☒ SAME AS RPT. ☐ DTIC USERS ☐	21. ABSTRACT SECURITY CLASSIFICATION UNCLASSIFIED
22a. NAME OF RESPONSIBLE INDIVIDUAL Lt. David L. Graves	22b. TELEPHONE NUMBER (Include Area Code) (513) 255-6104 22c. OFFICE SYMBOL AFWAL/FIBEC

DD FORM 1473, 83 APR EDITION OF 1 JAN 73 IS OBSOLETE.

UNCLASSIFIED
SECURITY CLASSIFICATION OF THIS PAGE

A

Program activities to accomplish these objectives were organized into three tasks. Under Task I - Technology Assessment and Evaluation Procedure Development, a review was conducted of data available on current and developmental higher strain fiber and resin composite systems to identify materials for evaluation. A procedure was developed detailing tests, test methods, and analysis methods required to conduct a structural evaluation.

During Task II - Test Program, an experimental program was formulated to demonstrate and complement the evaluation procedure. The test program covered three levels of structural evaluation: basic lamina properties, laminate design properties, and test of a multifastener composite-to-metal splice joint. Four high strain fiber and resin composite material systems were evaluated using results from 254 static and fatigue coupon tests.

In Task III - Theory/Test correlation, test results from Task II were correlated with analytical predictions of laminate stiffness, strength, and mode of failure. Analytical procedures to predict laminate unnotched and notched static tension and compression strength are described. Data trends are discussed relative to fatigue life, accumulation of hole elongation with fatigue, and mode of failure. Limitations in the test and analysis procedures are presented.

FOREWORD

The work reported herein was performed by the McDonnell Aircraft Company (MCAIR) of the McDonnell Douglas Corporation (MDC), St. Louis, Missouri, under Air Force Contract F33615-84-C-3231, for the Flight Dynamics Laboratory, Wright-Patterson Air Force Base, Ohio. This effort was conducted under Task I of Project No. 2401 "Structures and Dynamics", Task 240101 "Structural Integrity for Military Aerospace Vehicles," Work Unit 24010192 "Structural Evaluation of High Strain Fiber and Resin Composite Material Systems." Lt. David L. Graves (AFWAL/FIBEC) was the Air Force Project Engineer. The work described was conducted during the period 18 September 1984 through 18 January 1986.

The work was managed by the MCAIR Structural Research Department with James M. Ogonowski as Program Manager and David L. Buchanan as Principal Investigator. Program testing was conducted under the direction of Paul S. McClellan, MCAIR Nonmetallics and Chemical Processes Laboratory.

Distribution Statement A is correct for this report.
Per Lt. David L. Graves, AFWAL/FIBEC

TABLE OF CONTENTS

LIST OF FIGURES

List of Figures (Continued)

List of Figures (Continued)

Figure | Page

SECTION I

INTRODUCTION

The objective of this program was the structural evaluation of high strain fiber and resin composite material systems. The objective was to develop a combined analytical and experimental procedure for performing a structural evaluation, then use it to evaluate the effects of recently developed higher strain fibers and resin systems on strength, durability, and damage tolerance of advanced carbon/epoxy composite material systems. Testing included evaluation of basic lamina properties, static and fatigue testing of laminates with and without stress concentrations, evaluation of tolerance to low energy impact damage, and static and fatigue testing of a multifastener metal-to-composite splice joint. Included in the structural evaluation were analytical methods to predict unnotched and notched laminate strength and mode of failure based on unidirectional ply mechanical properties.

Program activities to accomplish these objectives were organized into three tasks. Under Task I - Technology Assessment and Evaluation Procedure Development, a review was conducted of data available on current and developmental higher strain fiber and resin composite materials to identify systems for evaluation. A procedure was developed detailing tests, test methods, and analysis methods required to conduct a structural evaluation.

During Task II - Test Program, an experimental program was formulated to demonstrate and complement the evaluation procedure. The test program covered three levels of structural evaluation: basic lamina properties, laminate design properties, and test of a multifastener composite-to-metal splice joint. Four high strain fiber and resin composite material systems were evaluated using results from 254 static and fatigue coupon tests.

In Task III - Theory/Test Correlation, test results from Task II were correlated with analytical predictions of laminate stiffness, strength, and mode of failure. Analytical procedures for predicting laminate unnotched and notched static tension and compression mechanical behavior are described. Data trends are discussed relative to fatigue life, accumulation of hole elongation with fatigue, and mode of failure. Limitations in the test and analysis procedures are presented.

SECTION II

SUMMARY AND CONCLUSIONS

A structural evaluation procedure was developed which identifies experimental and analytical approaches for providing early insight into the structural performance of high strain fiber and resin composite material systems. In demonstrating the evaluation procedure, a data base was established on four high strain fiber and resin material system combinations. Analytic methods were demonstrated which permit analysis of structural laminates, with and without stress concentrations, with minimal test data. Fatigue life data for bolted joint structures was developed for comparison with established AS-1/3501-6 data bases.

Under Task I - Technology Assessment and Evaluation Procedure Development, a review of data available on current and developmental high strain fiber and resin composite material systems identified four fiber/resin material system combinations for test in demonstrating the structural evaluation procedure. Selected as the baseline resin system was 3501-6, for which an extensive data base of AS-1/3501-6 carbon/epoxy material property data exists (References 1, 2). The resin system Cycom 907 was selected as a state-of-the-art tough epoxy; Cycom 1808 and Narmco 5245C were selected as systems with improved toughness and 250^{o}F hot/wet service temperature capability. These four resin systems were evaluated in combination with the high strain (18,000 μ in/in) Union Carbide T-700 carbon fiber.

An experimental program was defined to obtain basic lamina data, laminate notched and unnotched mechanical properties, and data for a multifastener structural splice joint. Emphasis was placed on demonstrating analytic and experimental procedures for conducting a structural evaluation.

Under Task II - Test Program and Task III - Theory/Test Correlation, three levels of testing and analysis were conducted, evaluating basic lamina data, laminate design properties, and a multifastener metal-to-composite splice joint. A total of 254 tests were conducted; 198 static and 56 fatigue. In the first level of evaluation unidirectional 0^{o} tension, 0^{o} compression, 90^{o} tension, and intralaminar shear mechanical properties were determined. Mechanical properties were determined for both room temperature/dry (RTD) and elevated temperature/wet (ETW) environmental conditions. Mode I fracture toughness of all four resin systems was determined.

In the second level of evaluation, unnotched and notched laminate static and fatigue tests were conducted, providing experimental data for methodology verification and to identify trends in fatigue life and in accumulation of hole elongation with fatigue. Two layups were used in this evaluation: a 10/80/10 (percent of $0^o/\pm45^o/90^o$ plies) matrix dominated layup and a 50/40/10 fiber dominated layup. Tests were conducted under both RTD and ETW environental conditions.

Static tension and compression tests were conducted for both unnotched and notched laminates. Unloaded hole and loaded hole tests were conducted in evaluation of notched laminate strength.

Initial verification of analysis was obtained by correlating strength and stiffness predictions with data obtained from unnotched specimens. Predictions of laminate strength were accurate to within 7 percent using unidirectional ply mechanical properties and the Tsai-Hill failure criterion. Laminate strength predictions using unidirectional allowables and a maximum stress failure criterion were generally unconservative.

Analyses were further verified by correlating strength predictions with data obtained from specimens with a single unloaded fastener hole. The "Bolted Joint Stress Field Model (BJSFM) (Reference 1) was used for strength predictions. This method is based upon anisotropic theory of elasticity and classical laminated plate theory to obtain laminate stress distributions, and a characteristic dimension (R_c) failure hypothesis. Test data requirements are minimized by extending the characteristic dimension failure hypothesis to a ply-by-ply analysis in conjunction with known material failure criteria. Unidirectional (lamina) stiffness and strength data are used with an empirical value of R_c to predict stress distributions, critical plies, failure location, and failure load. From results of theory/test correlation with a 50/40/10 layup, strength of a 10/80/10 layup was predicted within 6 percent using the characteristic dimension failure hypothesis. Value of the characteristic dimension was dependent upon material system.

Tests were performed to provide data on laminate unloaded hole and loaded hole fatigue life performance, accumulation of hole elongation with fatigue, and failure mode behavior. Constant amplitude fatigue tests were conducted for the fiber dominated 50/40/10 layup. Tension-compression ($R = -1$) and compression only ($R = -\infty$) cyclic loadings were used to establish a material data base and identify trends. The approach was to test specimens to laminate rupture or to a point of excessive hole elongation, even though there were conditions when high stress levels were required to prevent long lives due to the excellent fatigue characteristics of advanced composites.

Tolerance to low energy impact induced damage was evaluated nondestructively, inspecting damage size after impact, and by residual compression strength after impact. Both fiber and matrix dominated layups were used in this evaluation; effect of low energy impact on damage size and on reduction of compression strength was independent of layup. For the level of impact energy selected, compression strength for the Cycom 907 resin system was reduced by 37 percent; strength for both the Cycom 1808 and 5245C resin systems was reduced by 62 percent.

In the third level of evaluation, a multifastener metal-to-composite splice joint was tested both statically and in fatigue. Analytical methods were demonstrated to predict laminate strength under combined bearing and bypass loading.

SECTION III

BACKGROUND

Much of the current work in developing higher strain fiber and resin composite material systems has been to evaluate fiber/resin combinations for specific property improvements, such as low energy impact damage tolerance or fracture toughness. There has been little effort to identify the effect these systems may have on unnotched and notched laminate strength, durability under fatigue loading, failure mechanisms, and the ability of current analysis methods to predict such behavior. Physical properties necessary for improving laminate structural performance are generally agreed upon, however no single evaluation has accounted for the effect of these properties over a wide range of structural properties (e.g. unnotched and notched tension and compression strength and durability, failure mechanisms, toughness, low energy impact damage tolerance, etc.). This program provides an experimental and analytical procedure for determining such effects early in a material system development.

1. MATERIAL SYSTEMS SELECTION

The high strain fiber and toughened epoxy resin systems evaluated in this program were selected based on an evaluation of key mechanical properties relative to properties of current carbon/epoxy material systems. Test data available from industry literature and material suppliers was used in the material evaluation and selection. All data was compared with production carbon/epoxy systems; used for baseline comparison were AS-1/3501-6 and AS-4/3501-6 systems.

Summarized in Figure 1 are properties of carbon fibers considered for evaluation in this program. These fibers all have moduli of approximately 35 msi; candidate high strain fibers have 18,000 μ inch/inch strain capability and include Union Carbide T-700, Hercules AS-6, and Celanese Celion ST. The high strain Union Carbide T-700 fiber was selected and used for all tests.

The selection of high strain, toughened resin systems for test with the T-700 fiber was based on an evaluation of neat resin strength, strain to failure and strain energy. A graphical presentation of the resin evaluation and selection procedure is shown in Figure 2 (Reference 3). Strength and moduli axes are normalized with respect to a baseline material strength, S_O, and modulus, E_O. Four parameters are used to define upper and lower bounds for the region where overall composite structural efficiency improvements are expected. These parameters are normalized resin tensile strength, normalized resin strain energy, normalized resin strain to

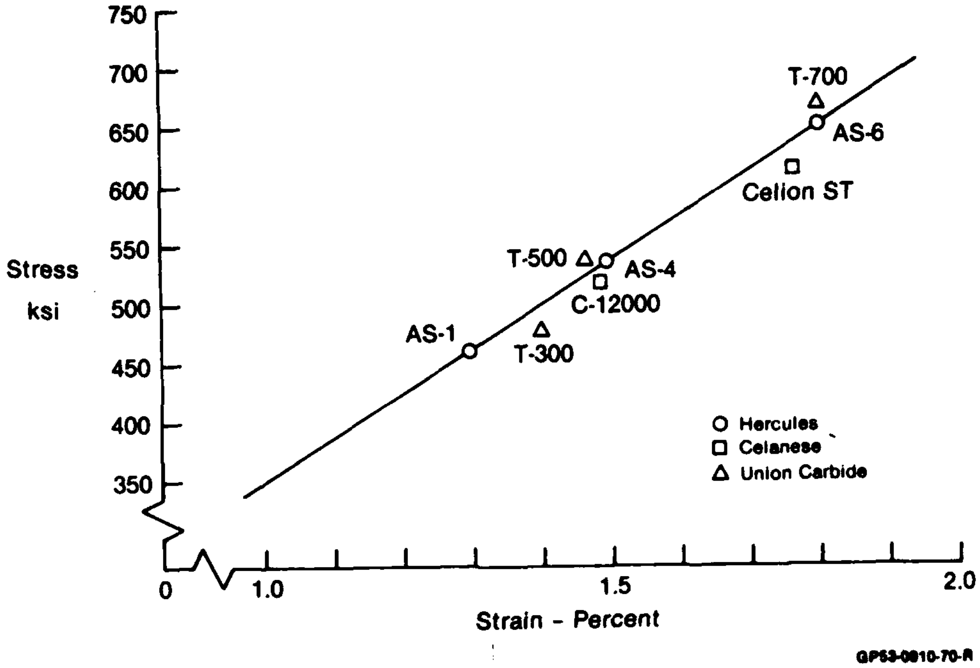

Figure 1. High Strain Carbon Fibers

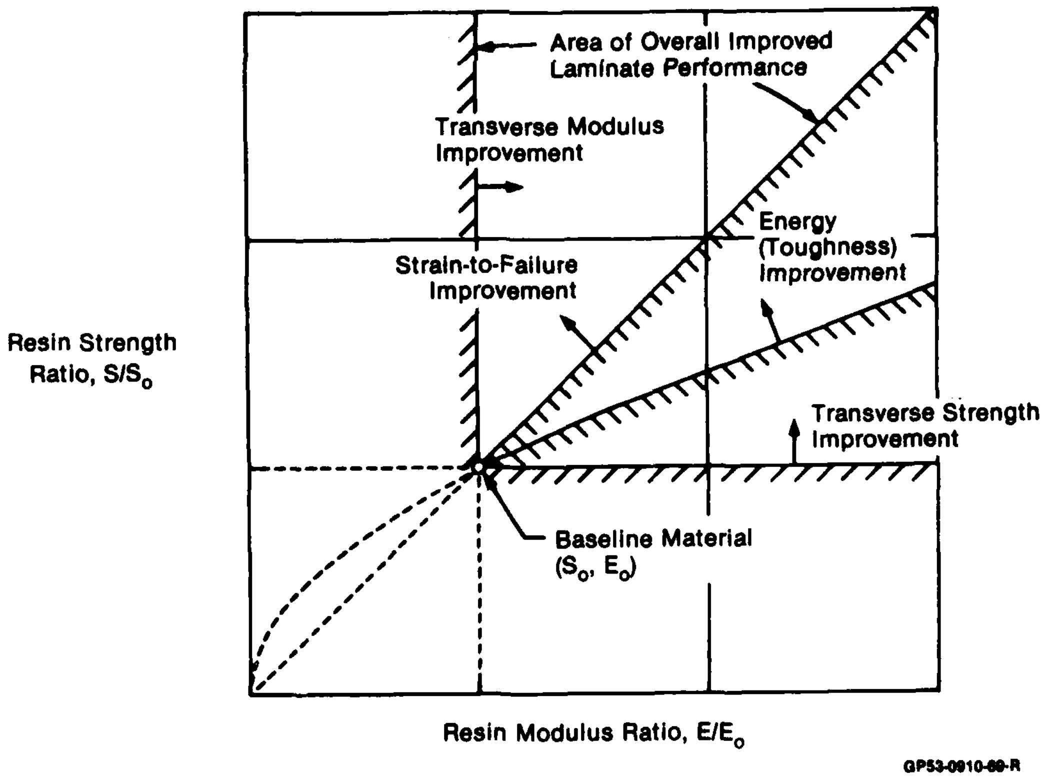

Figure 2. Resin Properties Necessary to Improve Laminate Properties

failure and normalized resin modulus. These normalized resin-related parameters bound the resin properties which result in improvements in laminate transverse strength, transverse modulus, strain energy (toughness) and matrix cracking.

Using this resin evaluation procedure, increasing the resin strength relative to a baseline is predicted to increase lamina transverse strength and interlaminar shear strength. Increasing the resin strain energy (toughness) increases laminate low energy impact resistance.

Global matrix cracking is controlled by resin strain allowables. Cyclic loading of laminates above the matrix cracking strain level is associated with rapid decrease in fatigue life, therefore composite durability is predicted to increase for resin systems with higher strain-to-failure.

The bound on composite material compressive performance is dictated by resin modulus. Longitudinal compression properties are improved with higher resin modulus due to greater fiber stabilization. Potentially, large benefits may be gained in toughness but at the expense of lower resin system modulus, resulting in lower longitudinal compression strength compared to the baseline material.

Previous work (Reference 4) has investigated these relationships between neat resin tensile stress-strain mechanical properties and their effect on impact damage tolerance and unidirectional compression strength, verifying this evaluation procedure. Based on this type of evaluation four resin systems were selected for test: (1) 3501-6, (2) Cycom 907, (3) Cycom 1808, and (4) 5245C. Typical neat resin tensile stress-strain test results for 3501-6, Cycom 907, and 5245C (Reference 5) are shown in Figure 3. A common characteristic of the tougher resin systems is their greater ductility and strain to failure compared to the currently used 3501-6 epoxy. However, the tougher resins have a lower modulus and would therefore be predicted to produce lower longitudinal compressive strengths

Final selection of the four resin systems was based on mechanical properties, processibility, and availability with the T-700 fiber in prepreg form. The 3501-6 resin system was selected for baseline comparison, for which an extensive data base of mechanical properties exist (References 1, 2) with AS-1 fibers. This epoxy resin has relatively high stiffness properties, but low toughness. The Cycom 907 system was selected for test since it represented a state-of-the-art toughened epoxy resin. Cycom 1808 and 5245C resin systems were selected for their improved toughness and also for their retention of mechanical properties in elevated temperature/wet operating environments.

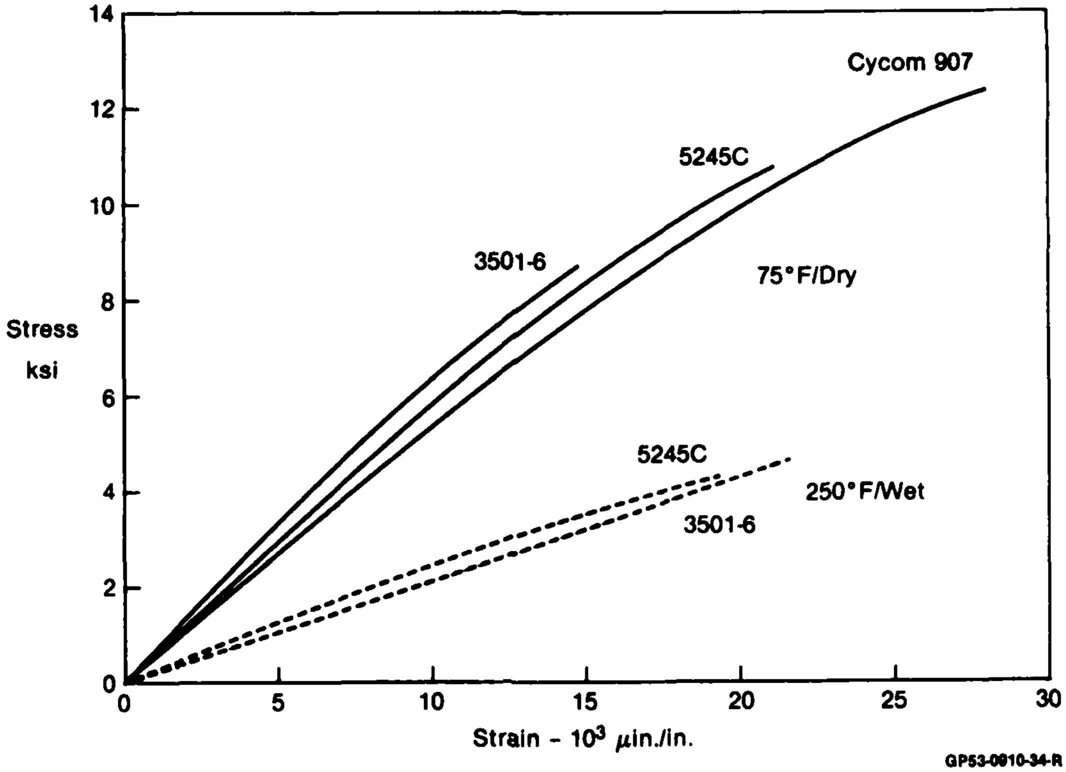

Figure 3. Neat Resin Stress/Strain Mechanical Properties

SECTION IV

STRUCTURAL EVALUATION: TEST AND ANALYSIS

The objective of the test program was to provide experimental data to describe unidirectional (lamina) mechanical properties, verify analytic predictions of notched and unnotched laminate stiffness and strength, and identify trends in fatigue durability and low energy impact damage tolerance.

1. TEST PLAN - In this program, a total of 198 static tests and 56 fatigue tests were performed, under both ambient and hot/wet environmental conditions. Tests were conducted to determine:

- o unidirectional material properties
- o resin interlaminar fracture toughness
- o unnotched laminate static tension and compression strength
- o unloaded hole laminate static tension and compression strength
- o loaded hole laminate static strength
- o laminate durability under cyclic loading
- o environmental effects on strength
- o layup effects on strength
- o structural performance of a multifastener splice joint

Specimens were tested per the requirements of the matrix shown in Figure 4. This matrix includes three levels of structural evaluation:

- o basic lamina data
- o laminate design allowables
- o multifastener structural component

The first group of tests used unidirectional and $\pm 45^{o}$ specimens to evaluate tensile, compressive, and shear behavior of the lamina. These material properties were used for ply-by-ply analysis of notched and unnotched laminate static strength.

The second and third levels of evaluation used tests of notched and unnotched laminates and bolted joints to verify predictions of strength and mode of failure, and establish a data base on fatigue life and accumulation of hole elongation with fatigue. Additionally, a data base on low energy impact damage tolerance was established.

Environmental testing was included on both the lamina and laminate levels to evaluate mechanical properties in room temperature/dry (RTD) and elevated temperature/wet (ETW)

Test Level of Evaluation	Aspect of Material System Being Evaluated	Specimen Test Condition	Specimen Type	Fiber/Resin Material System Combination: T700/3501-6 RTD	T700/CYCOM 907 RTD	T700/CYCOM 1808 RTD	T700/CYCOM 1808 ETW	T700/5245C RTD	T700/5245C ETW	Specimen Totals: Static	Fatigue
1 Basic Lamina Data	Fiber in Tension	0° Tension	Coupon	•	•	•	•	•	•	18	—
	Fiber/Resin in Compression	0° Compression	Coupon	•	•	•	•	•	•	18	—
	Resin in Tension	90° Tension	Coupon	•	•	•	•	•	•	18	—
	Fiber/Resin in Shear	± 45° Tension	Coupon	•	•	•	•	•	•	18	—
	Resin Toughness	Double Cantilever Beam (DCB)	Coupon	•	•	•	—	•	—	12	—

Test Level of Evaluation	Aspect of Material System Being Evaluated	Specimen Test Condition	Specimen Type	T700/CYCOM 907 50/40/10 RTD	T700/CYCOM 907 10/80/10 RTD	T700/CYCOM 1808 50/40/10 RTD	T700/CYCOM 1808 50/40/10 ETW	T700/5245C 50/40/10 RTD	T700/5245C 50/40/10 ETW	T700/5245C 10/80/10 RTD	Specimen Totals: Static	Fatigue
2 Laminate Design Allowables	Unnotched	Tension	Coupon	•	•	•	—	•	—	•	15	—
		Compression	Coupon	•	•	•	—	•	—	•	15	—
	Unloaded Hole	Tension	Coupon	• ★	•	• ★	•	• ★	•	•	21	24
		Compression	Coupon	•	•	•	•	•	•	•	21	—
	Loaded Hole	Bearing	Coupon	• ★	•	• ★	•	• ★	•	•	21	24
	Impact - Unnotched	Compression	Coupon	•	•	•	—	•	—	•	15	—
3 Aircraft Structural Component	Highly-Loaded Bolted Joint	Tension Composite-to-Metal Joint	Scarfed Three Fastener Joint	• ☆	—	• ☆	—	—	—	—	6	8
										Specimen Totals	198	56
											254	

• 3 static tests
★ 4 fatigue tests at R = - 1.0
4 fatigue tests at R = - ∞
4 fatigue tests at R = - 1.0

GP53-0810-31-R

Figure 4. Test Matrix

operating environments. Elevated temperature wet tests were conducted at 250°F for both the 5245C and Cycom 1808 resin systems. Specimens were preconditioned in 95 percent relative humidity and 180°F until an equilibrium (saturation) moisture content was reached. The rate of moisture absorption and saturation moisture content was recorded for all hot/wet tests.

2. <u>SPECIMEN FABRICATION</u> - The high strain Union Carbide T-700 carbon fiber was used for all test specimens. This fiber was supplied in unidirectional tape with four epoxy resin systems: 3501-6, Cycom 907, Cycom 1808, and 5245C. During fabrication a three phase procedure to assure quality of test specimens was performed.

First, material prepreg was physically tested for conformance with material specifications for resin content, resin flow, volatiles, resin tack and drape, and fiber aerial weight. A vendor certification was supplied with each shipment of prepreg to assure it had been found acceptable. Secondly, after fabrication, each panel was inspected using ultrasonic reflection plate techniques per MCAIR process specifications. Finally, the third phase of specimen quality assurance required that machining and drilling of each specimen be in conformance with MCAIR standards. Specimens used in this program were acceptable in all three phases of this quality assurance.

Panel processing procedures were followed according to either MCAIR or material supplier specifications. Processing of panels with the 3501-6 resin system was according to MCAIR specifications which have been established for production use on current aircraft. This processing cycle, with an eight hour post cure at 350°F, has been optimized for material properties including retention of those properties critical in elevated temperature/moisture saturated operating environments. Processing of the resin material systems Cycom 907 and Cycom 1808 followed specifications recommended by the supplier. Both systems do not require a post cure.

Processing of the 5245C resin system was based on recommendations of the supplier and an evaluation of the effect of post cure on strength. A summary of test results used to determine an optimum post cure cycle based on hot/wet interlaminar shear strength is shown in Figure 5. Moisture preconditioning was established with a 24 hour distilled water boil. Selection of an optimum post cure was based on a compromise between hot/wet strength and anticipated retention of improved toughness and impact damage tolerance. Based on test results, a post cure of 400°F for four hours was selected for the T-700/5245C system.

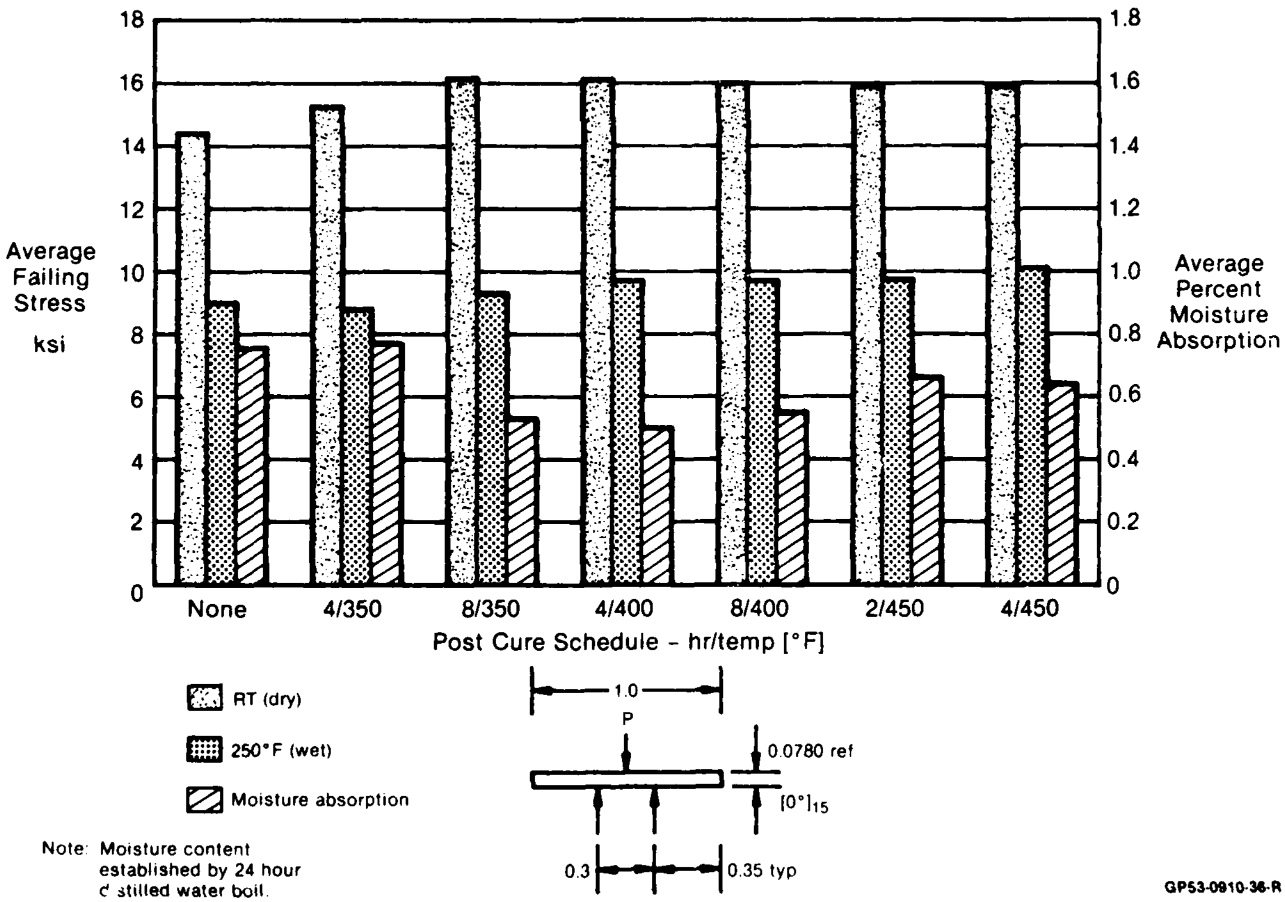

Figure 5. Post Cure Evaluation of T-700/5245C

Nineteen carbon/epoxy panels were required to fabricate test specimens to complete program testing. Specimens were machined from panels with each specimen uniquely numbered to identify material system, panel number, and individual specimen number according to the following code:

```
X - X - X
|   |   |
|   |   └─ Specimen Number
|   |
|   └─ Panel Number
|
└─ Material System
    (1) T-700/3501-6
    (2) T-700/Cycom 907
    (3) T-700/Cycom 1808
    (4) T-700/5245C
```

This coding facilitates tracing specimens back to its panel, material system, and location within the panel. Reserve space was allocated in all panels to permit duplication of specimens from the same data base as necessary.

Cured laminate resin content was determined for each material system, taken from panels used to fabricate the unidirectional 0° tension, 0° compression, and 90° tension test specimens. Results are shown in Figure 6. A nominal per ply thickness based on 63 percent fiber volume was determined using fiber aerial weight data, and has been used to summarize test results.

Resin System	Average Cured Per Ply Thickness (inch)	Specific Gravity (gm/cm^3)	Resin Content (% by weight)	Fiber Volume (%)	Fiber Aerial Weight (gm/m^2)	Nominal Per Ply Thickness (inch) (based on 63% fiber volume)
3501-6	0.0064	1.5772	33.60	57.9	149.0	0.0051
Cycom 907	0.0061	1.5471	33.11	57.2	150.5	0.0052
Cycom 1808	0.0057	1.5906	31.32	60.3	147.8	0.0051
5245C	0.0051	1.6090	26.81	65.1	141.0	0.0049

Resin System	Density (gm/cm^3)	Fiber System	Density (gm/cm^3)
3501-6	1.27	T-700	1.81
Cycom 907	1.22		
Cycom 1808	1.25		
5245C	1.25		

GP53-0910-80-R

Figure 6. Resin Content Summary

Specimens requiring moisture preconditioning were stored in environmental control chambers and their moisture content monitored by measuring weekly weight changes. The objective in preconditioning was to reach saturation and obtain a constant moisture content through the thickness of the laminate. Specimens were exposed to 95 percent relative humidity at 180°F until a near equilibrium moisture content was reached. Moisture preconditioning measurements of specimens used for basic lamina testing (16 ply laminates) are shown in Figure 7. Moisture equilibrium was reached in approximately 30 days. The equilibrium (saturation) moisture content for Cycom 1808 was 1.18 percent by weight; 5245C equilibrium moisture content was 0.69 percent by weight.

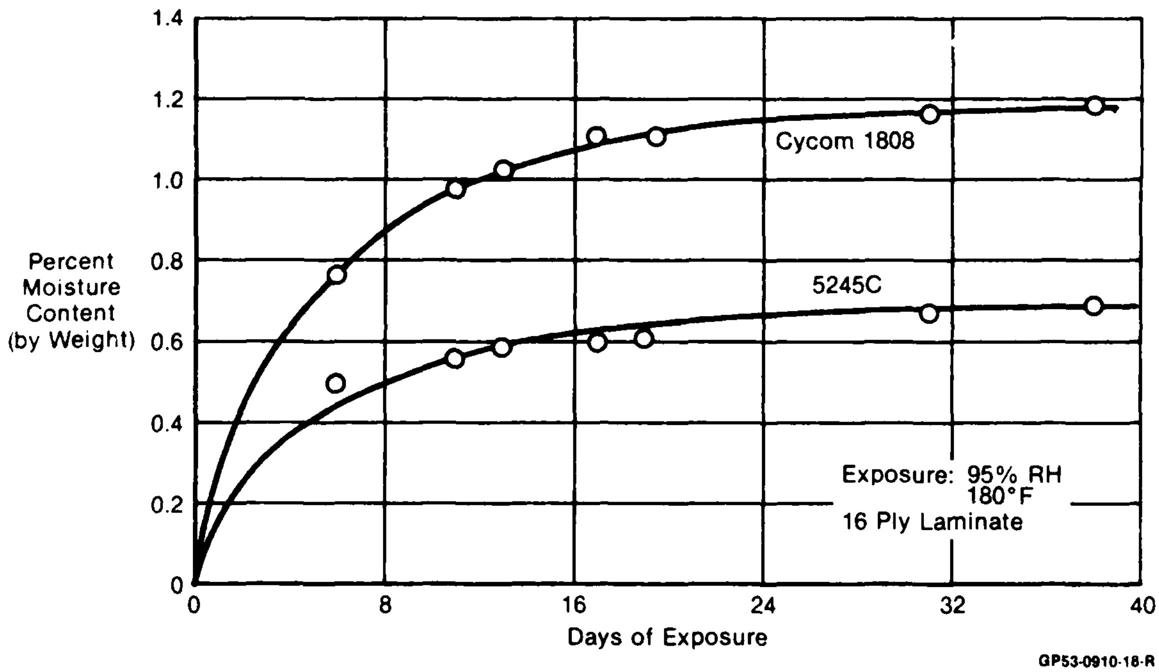

Figure 7. Moisture Preconditioning Results: 16 Ply Laminate

Moisture preconditioning measurements of specimens used in laminate design allowables testing (40 ply laminates) are shown in Figure 8. Specimens were tested after approximately 45 days of exposure. Specimens fabricated from the 5245C resin system had reached saturation when tested; specimens fabricated from the Cycom 1808 resin system had reached 80 percent of saturation.

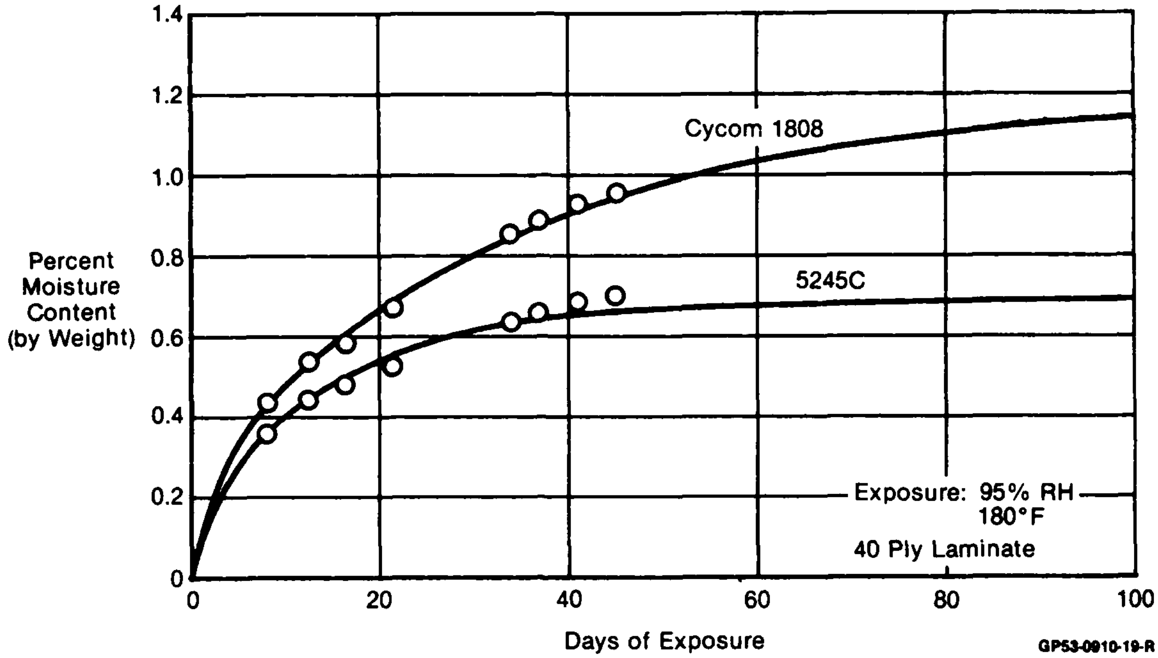

Figure 8. Moisture Preconditioning Results: 40 Ply Laminate

3. <u>BASIC LAMINA PROPERTIES</u> - This section contains test procedures, specimen configurations, test setups, specimen geometric data, failure loads, failure strains, and failure mode information for each specimen tested in this level of evaluation.

a. <u>Elastic Constants</u> - The 0° tension test specimen is shown in Figure 9. Test results are shown in Figure 10.

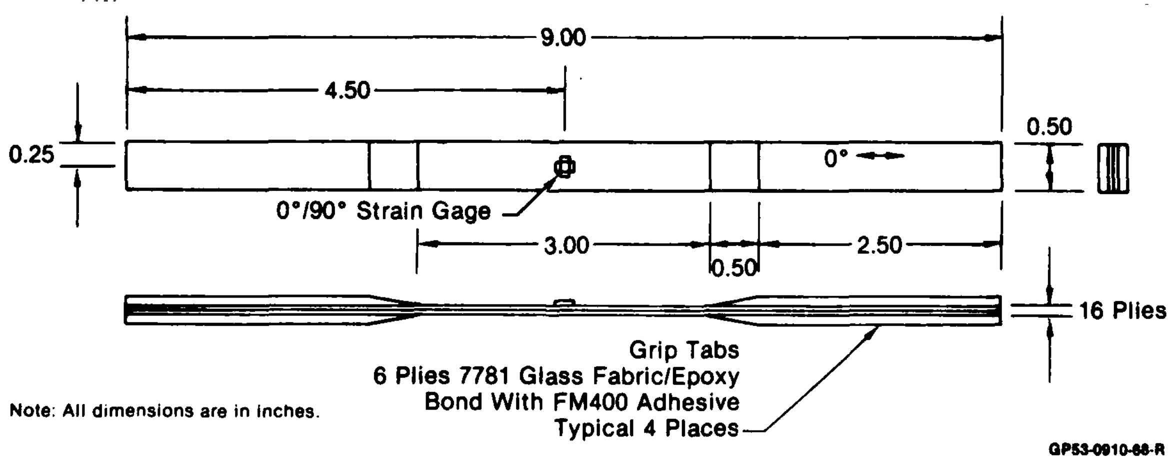

Figure 9. Unidirectional 0° Tension Test Specimen

Resin Specimen	Environment	Specimen Number	Thickness (inch)	Width (inch)	Failure Load (lb)	Failure Stress (ksi)		Failure Strain (μin/in)		Modulus (msi)		Poisson's Ratio
						Individual	Average	Individual	Average	Individual	Average	
		1-1-6	0.1000	0.5034	12,640	307.6		13,200		22.25		0.301
3501-6	RTD	1-1-7	0.0998	0.5061	10,000	242.1	275.8	11,040	12,200	21.01	21.76	0.365
		1-1-8	0.1036	0.5007	11,340	277.6		12,360		22.03		0.327
		2-1-6	0.0982	0.4985	13,050	314.6		13,340		22.06		0.330
Cycom 907	RTD	2-1-7	0.0985	0.4961	13,800	333.0	328.0	14,220	13,770	21.84	22.28	0.316
		2-1-8	0.0985	0.5040	14,080	336.3		13,740		22.94		0.339
		3-1-10	0.0921	0.5022	14,490	353.6		15,300		21.96		0.319
Cycom 1806	RTD	3-1-11	0.0927	0.5046	14,800	360.1	357.1	15,600	15,460	21.66	21.95	0.302
		3-1-12	0.0932	0.5029	14,670	356.5		15,480		22.94		0.312
		3-1-13	0.0930	0.5055	8,960	217.2		9,570		22.59		0.481
	ETW	3-1-14	0.0936	0.5055	9,000	218.2	229.2	9,300	9,560	22.34	22.63	0.404
		3-1-15	0.0932	0.5072	10,440	252.3		9,810		22.96		0.396
		4-1-10	0.0866	0.5081	15,350	385.3		16,200		22.28		0.322
5245C	RTD	4-1-11	0.0868	0.5108	16,470	411.3	397.6	17,160	16,700	21.97	21.92	0.296
		4-1-12	0.0866	0.5072	15,750	396.1		16,740		21.50		0.301
		4-1-13	0.0852	0.5060	11,250	283.6		11,180		22.28		0.375
	ETW	4-1-14	0.0856	0.5055	10,730	270.6	279.4	11,090	11,380	23.13	22.87	0.344
		4-1-15	0.0853	0.5054	11,250	283.9		11,880		23.21		0.386

GP53-0910-100-R

Figure 10. Unidirectional 0° Tension Test Results

Strength of the four fiber/resin system combinations indicate the relative capability of the resin to translate fiber strength (18,000 μ in/in) to the composite lamina. A typical failed specimen is shown in Figure 11. Results from ETW tests indicated a 35 percent reduction in tensile strength. This reduced strength may have been caused by tab failure, although no anomalies were observed in ETW specimen failures.

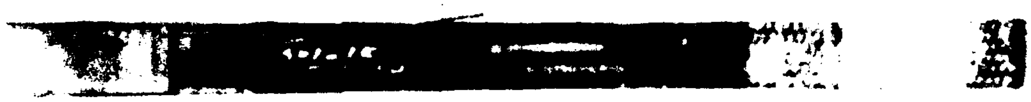

3-1-15

GP53-0910-50-R

Figure 11. Failed Unidirectional 0° Tension Test Specimen

The 90^{o} tension test specimen is shown in Figure 12, and results of static tests are shown in Figure 13. The three tough resin systems demonstrated a 50 to 70 percent increase in transverse tension strength relative to the 3501-6 resin. A typical failed specimen is shown in Figure 14.

0^{o} compression mechanical properties were determined using both unidirectional coupons and unidirectional sandwich beams, comparing the ability of each test method to accurately measure strength and stiffness. The 0^{o} compression coupon test specimen configurations are shown in Figure 15; two coupon configurations were used to determine stiffness and strength. The configuration without tabs was instrumented to measure modulus and Poisson's ratio. The tabbed specimen was used to determine material ultimate strength. The unsupported specimen length was chosen so that buckling would greatly exceed material compression strength. Due to the short gage length these tabbed specimens could not be instrumented.

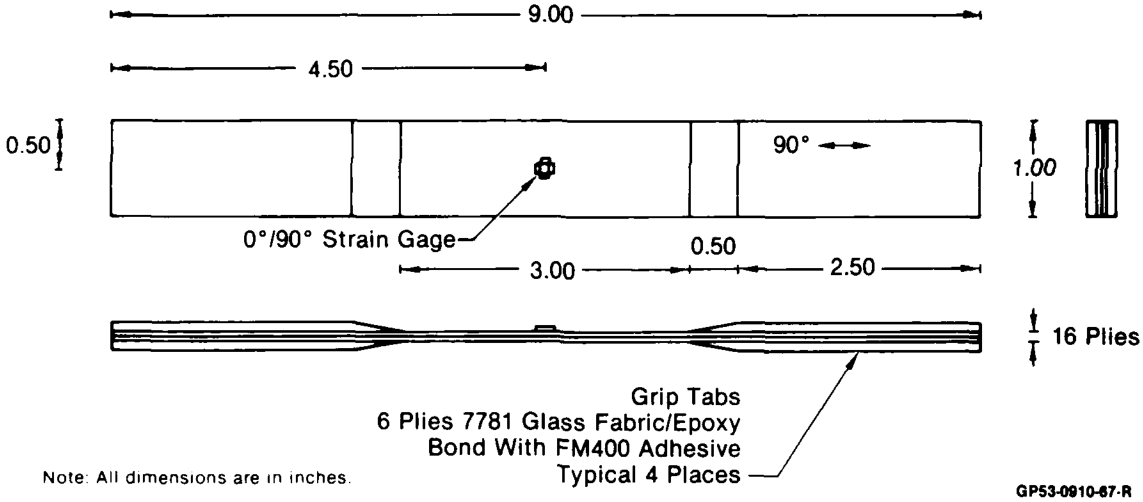

Figure 12. Unidirectional 90° Tension Test Specimen

Resin System	Environment	Specimen Number	Thickness (inch)	Width (inch)	Failure Load (lb)	Failure Stress (psi)		Failure Strain (μin/in)		Modulus (msi)		Poisson's Ratio
						Individual	Average	Individual	Average	Individual	Average	
		1-1-1	0.0975	0.9843	602	7,500		5,100		1.481		0.018
3501-6	RTC	1-1-2	0.1002	1.0068	625	7,610	7,270	5,110	4,890	1.494	1.493	0.021
		1-1-3	0.0986	1.0097	552	6,700		4,470		1.504		0.019
		2-1-1	0.0994	1.0023	960	11,510		8,280		1.469		0.020
Cycom 907	RTD	2-1-2	0.0994	1.0145	896	10,620	11,300	7,790	8,280	1.432	1.443	0.018
		2-1-3	0.0963	1.0074	987	11,780		8,780		1.428		0.018
		3-1-1	0.0911	1.0108	731	8,690		6,940		1.311		0.019
Cycom 1808	RTD	3-1-2	0.0940	1.0109	679	8,070	9,100	6,570	7,470	1.268	1.271	0.019
		3-1-3	0.0935	1.0057	882	10,540		8,890		1.241		0.017
		3-1-4	0.0926	1.0024	225	2,750		4,760		0.703		0.063
	ETW	3-1-5	0.0938	1.0034	260	3,180	2,890	5,260	4,970	0.704	0.669	0.044
		3-1-6	0.0938	1.0036	224	2,740		4,880		0.601		0.044
		4-1-1	0.0845	0.9899	843	10,860		8,020		1.398		0.020
5245C	RTD	4-1-2	0.0895	0.9960	812	10,400	10,990	7,490	8,070	1.458	1.425	0.018
		4-1-3	0.0852	1.0083	925	11,700		8,700		1.420		0.017
		4-1-4	0.0850	1.0096	340	4,300		7,720		0.854		0.049
	ETW	4-1-5	0.0853	1.0079	375	4,750	4,510	6,200	6,740	1.062	0.919	0.050
		4-1-6	0.0833	1.0084	355	4,490		6,300		0.842		0.046

GP53-0910-96-R

Figure 13. Unidirectional 90° Tension Test Results

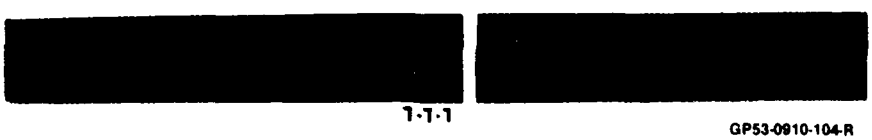

Figure 14. Failed Unidirectional 90° Tension Test Specimen

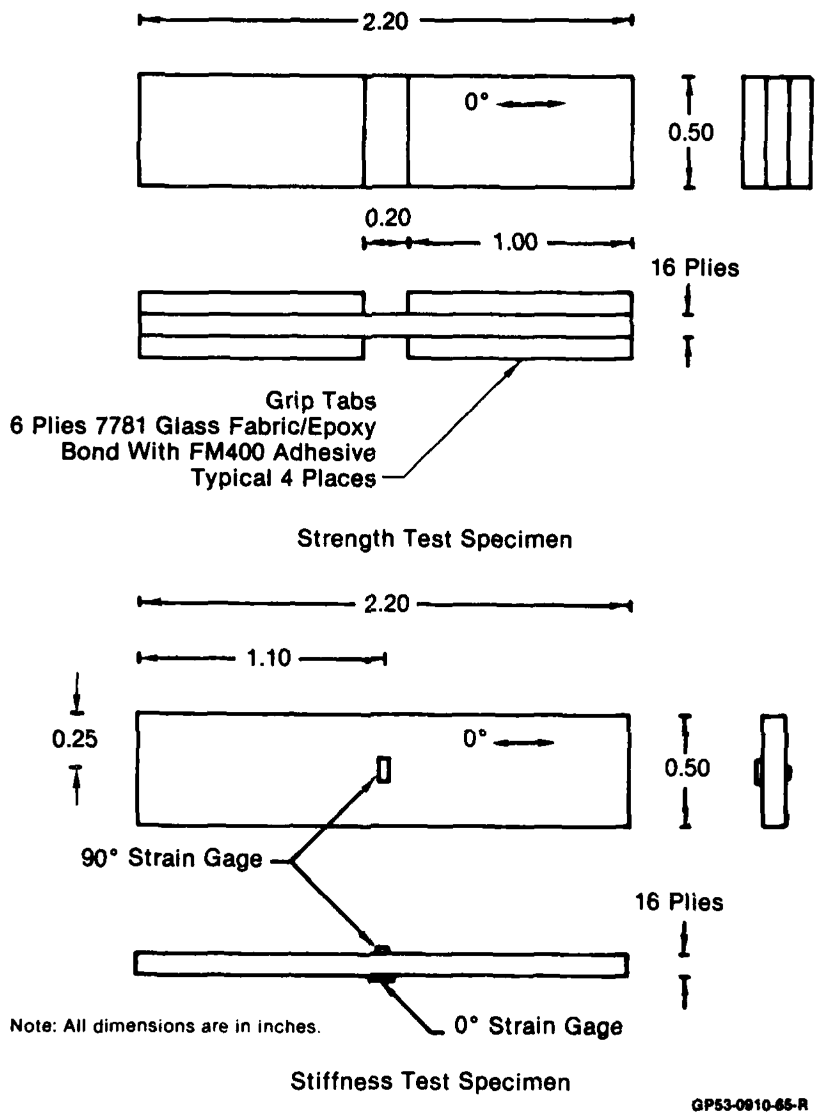

Figure 15. Unidirectional 0° Compression Coupon Test Specimens

Specimens were tested in a specially designed loading fixture shown in Figure 16. This test fixture includes two vertical alignment pins assuring loading directly along the axis of the specimen precluding eccentric loading and premature buckling of the specimen. Blocks at the grip ends provided lateral support and compression loading was introduced on the ends of the specimen.

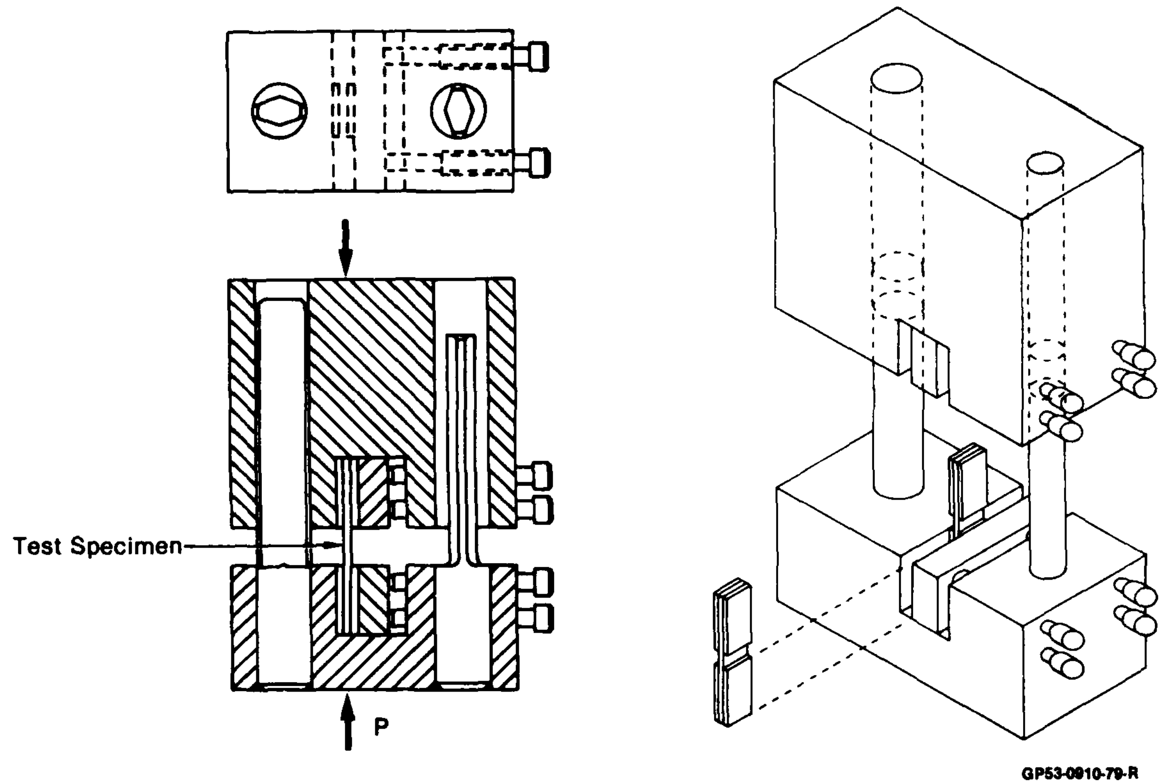

Figure 16. Compression Test Fixture

Unidirectional compression test results are shown in Figure 17. The tabbed specimens generally failed in shear across a 45° plane through the laminate thickness, rather than as a 0° fiber compression failure. A typical failed test specimen is shown in Figure 18.

The unidirectional 0° compression sandwich beam test specimen is shown in Figure 19; test results are shown in Figure 20. Inspection of a failed sandwich beam specimen, such as the one shown in Figure 21, indicated a 0° fiber compression mode of failure. This mode of failure is reflected in the higher strength and strain-to-failure compared to results obtained with the compression coupon. The sandwich beam test also resulted in a slightly higher unidirectional compression modulus (8 to 17 percent) compared to coupon test results. As will be demonstrated in the evaluation of laminate design allowables, strength predictions correlate well with test results using sandwich beam strength allowables; however, coupon test results provided better correlation with predictions of laminate modulus.

Resin System	Environment	Specimen Number	Thickness (inch)	Width (inch)	Failure Load (lb)	Failure Stress (ksi) Individual	Failure Stress (ksi) Average	Modulus (msi) Individual	Modulus (msi) Average	Poisson's Ratio	Mode of Failure
3501-6	RTD	1-1-11	0.101	0.502	-	-		21.65		0.320	-
		1-1-12	0.098	0.503	-	-	-	21.15	20.74	0.297	-
		1-1-13	0.102	0.503	-	-		19.42		0.338	-
		1-1A	0.101	0.505	6,350	151.1		-		-	1-2
		1-1B	0.102	0.504	7,250	172.9		-		-	1
		1-1C	0.098	0.502	5,130	122.7	160.4	-	-	-	2
		1-1D	0.103	0.503	8,490	202.8		-		-	1
		1-1I	0.099	0.503	6,380	152.3		-		-	2
Cycom 907	RTD	2-1-11	0.098	0.502	-	-		18.16		0.354	-
		2-1-12	0.098	0.500	-	-	-	19.44	18.79	0.366	-
		2-1-13	0.097	0.501	-	-		18.78		0.381	-
		2-1A	0.097	0.506	3,960	94.1		-		-	2
		2-1B	0.098	0.510	3,750	88.4		-		-	2
		2-1C	0.096	0.502	3,540	84.7	84.5	-	-	-	2
		2-1D	0.097	0.505	3,100	73.8		-		-	2
		2-1I	0.097	0.510	3,460	81.6		-		-	2
Cycom 1808	RTD	3-1-19	0.091	0.504	-	-		20.58		0.350	-
		3-1-20	0.092	0.504	-	-	-	20.22	20.45	0.365	-
		3-1-21	0.092	0.503	-	-		20.55		0.327	-
		3-1A	0.091	0.505	4,500	107.1		-		-	2
		3-1B	0.091	0.508	4,730	111.8		-		-	2
		3-1C	0.092	0.502	7,190	172.1	117.9	-	-	-	1
		3-1D	0.091	0.505	4,980	118.5		-		-	2
		3-1I	0.091	0.507	3,380	80.0		-		-	2
	ETW	3-1-22	0.092	0.504	-	-		27.43		0.363	-
		3-1-23	0.092	0.505	-	-	-	19.51	20.75	0.299	-
		3-1-24	0.092	0.503	-	-		21.98		0.338	-
		3-1E	0.091	0.499	1,950	47.9		-		-	2
		3-1F	0.091	0.503	2,850	69.4	58.3	-	-	-	2
		3-1G	0.091	0.504	2,440	59.3		-		-	2
		3-1H	0.091	0.509	2,350	56.6		-		-	2
5245C	RTD	4-1-19	0.088	0.503	-	-		20.69		0.295	-
		4-1-20	0.086	0.504	-	-	-	19.98	20.09	0.306	-
		4-1-21	0.089	0.503	-	-		19.59		0.345	-
		4-1A	0.091	0.510	5,630	132.6		-		-	2
		4-1B	0.091	0.500	3,590	86.2		-		-	2
		4-1C	0.092	0.499	4,340	104.5	119.7	-	-	-	2
		4-1D	0.091	0.508	5,700	134.9		-		-	2
		4-1I	0.091	0.503	5,880	140.4		-		-	1-2
	ETW	4-1-22	0.085	0.504	-	-		22.71		0.334	-
		4-1-23	0.089	0.501	-	-	-	21.58	22.15	0.409	-
		4-1-24	0.088	0.503	-	-		26.29		0.259	-
		4-1E	0.085	0.507	3,990	100.4		-		-	1
		4-1F	0.085	0.504	4,840	122.5	111.3	-	-	-	1
		4-1G	0.084	0.505	3,650	92.2		-		-	1
		4-1H	0.086	0.504	5,140	130.1		-		-	1

MODE OF FAILURE LEGEND :   1 FIBER COMPRESSION   2 SHEAR ACROSS THE THICKNESS

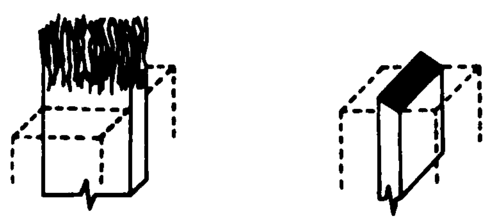

GP53-0910-98-R

Figure 17. Unidirectional 0° Compression Coupon Test Results

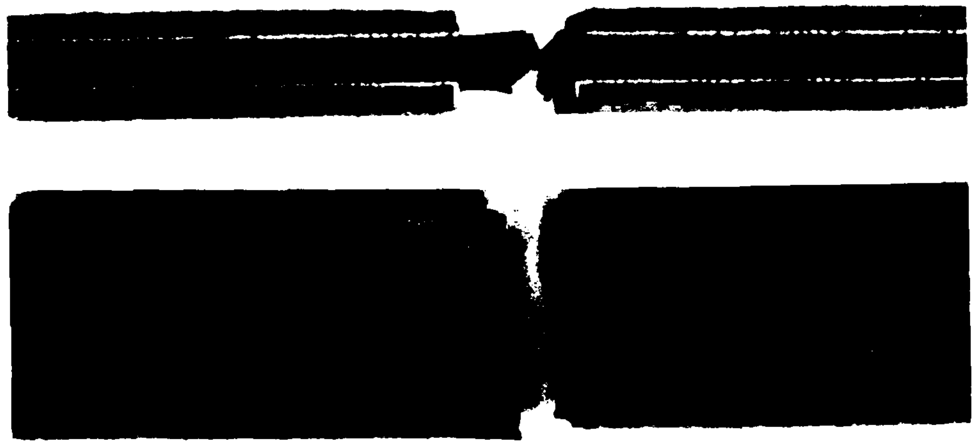

(1-1C)

GP53-0910-47-R

Figure 18. Failed Unidirectional 0° Compression Coupon Test Specimen

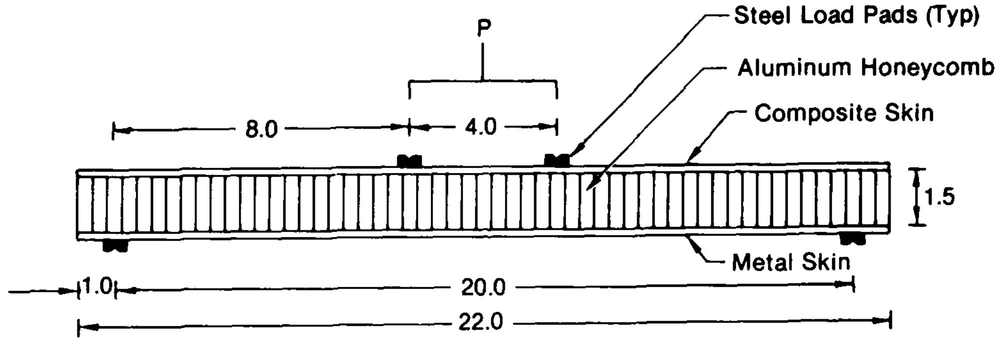

Composite Skin: 1.00 in. Wide; 22.0 in. Long; 6 Plies Thick
Metal Skin: 1.00 in. Wide; 22.0 in. Long; 0.090 in. Thick; 6Al-4V Annealed Titanium
Aluminum Honeycomb: 1.25 in. Wide; 22.0 in. Long; 1.50 in. Thick
Data Reduction:

$$\sigma = \frac{P\,L}{2\,w\,t\left(C + \frac{t + T}{2}\right)}$$

Where: σ = Uniaxial Compression Stress
P = Applied Load
w = Composite Skin Width (1.00 in.)
t = Nominal Composite Skin Thickness (6 Plies)
C = Honeycomb Core Height (1.50 in.)
T = Metal Skin Thickness (0.090 in.)
L = Moment Arm Between Applied Load and Reaction Support (8.0 in.)

GP53-0910-64-R

Figure 19. Unidirectional 0° Compression Sandwich Beam Test Arrangement

Resin System	Environment	Specimen Number	Thickness (inch)	Width (inch)	Failure Load (lb)	Failure Stress (ksi)		Failure Strain (μin/in)		Modulus (msi)	
						Individual	Average	Individual	Average	Individual	Average
		1-S-1	0.032	1.008	2,560	210.5		11,510		22.64	
3501-6	RTD	1-S-2	0.032	1.007	2,440	200.6	213.9	9,520	11,040	23.05	22.56
		1-S-3	0.032	1.007	2,810	230.6		12,100		21.99	
		2-S-1	0.036	1.008	1,750	141.2		6,730		22.17	
Cycom 907	RTD	2-S-2	0.035	1.007	1,510	122.0	135.3	5,740	6,490	22.09	22.01
		2-S-3	0.035	1.009	1,770	142.6		7,000		21.78	
		4-S-1	0.029	1.004	2,430	208.1		10,820		21.90	
5245C	RTD	4-S-2	0.029	1.004	2,360	202.3	193.6	10,450	10,040	21.83	21.63
		4-S-3	0.029	1.004	1,990	170.3		8,860		21.15	
		4-S-4	0.029	1.005	1,010	86.1		4,220		21.28	
	ETW	4-S-5	0.029	1.004	1,040	88.8	88.1	4,220	4,350	21.42	20.99
		4-S-6	0.029	1.004	1,050	89.5		4,600		20.27	

GP53-0910-97-R

Figure 20. Unidirectional 0° Compression Sandwich Beam Test Results

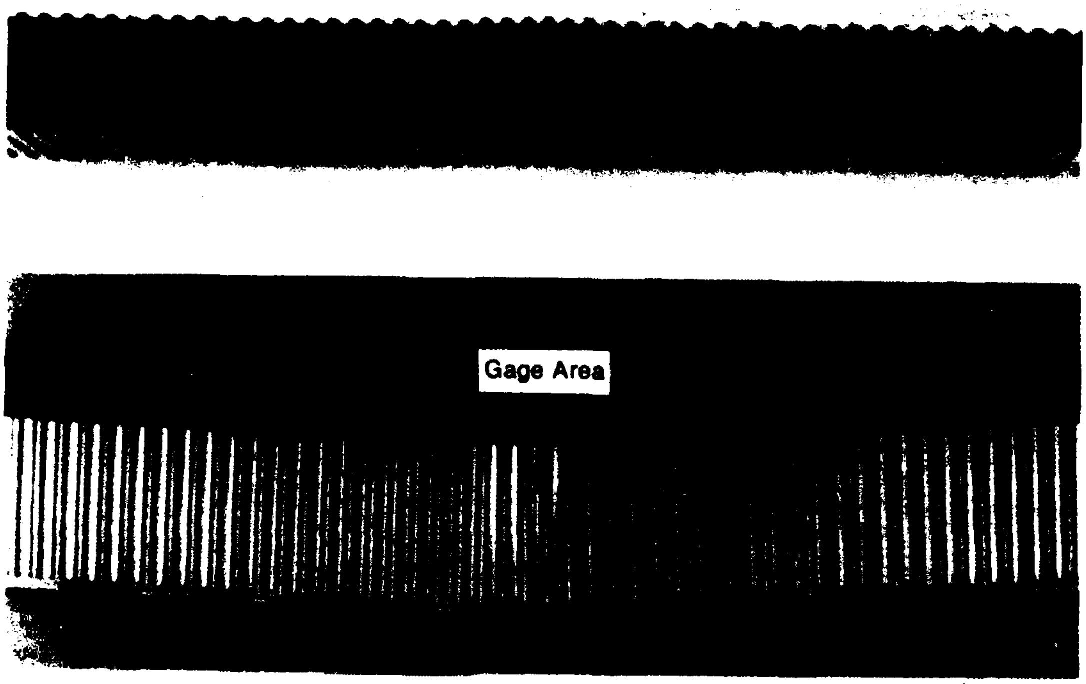

GP53-0910-48-R

Figure 21. Failed Unidirectional 0° Compression Sandwich Beam Test Specimen

Intralaminar shear mechanical behavior was evaluated using the $\pm 45^{\circ}$ test specimen shown in Figure 22. Test results are summarized in Figure 23, with complete shear stress-strain curves for each resin system shown in Figures 24 through 27. Typical failed test specimens are shown in Figure 28.

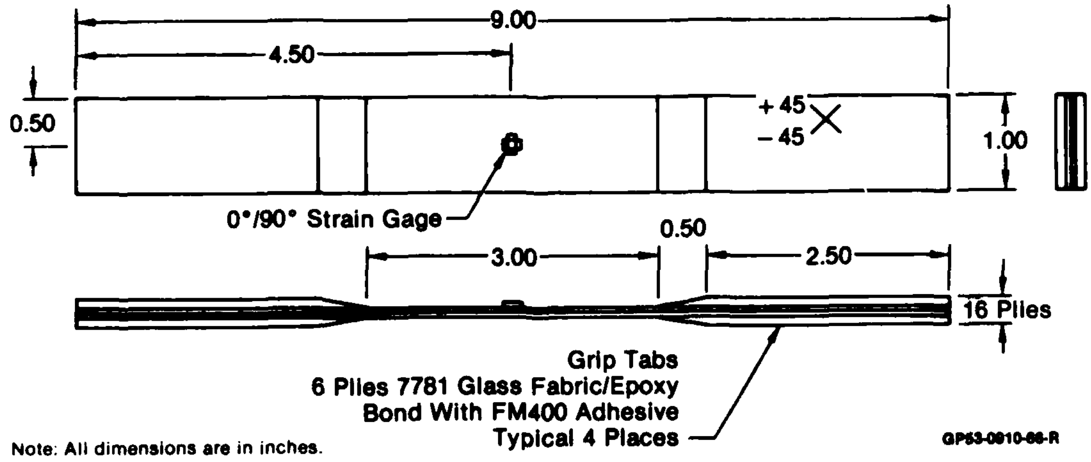

Figure 22. ±45° Intralaminar Shear Test Specimen

Resin System	Environment	Specimen Number	Thickness (inch)	Width (inch)	Failure Shear Stress (psi) Individual	Failure Shear Stress (psi) Average	Failure Shear Strain (μin/in)	Shear Modulus (msi) Individual	Shear Modulus (msi) Average
		1-2-1	0.1055	1.0057	14,530		26,200	0.876	
3501-6	RTD	1-2-2	0.1080	1.0057	14,070	14,510	24,470	0.879	0.877
		1-2-3	0.1076	1.0063	14,920		27,490	0.878	
		2-2-1	0.0971	1.0022	21,440		>72,000	0.798	
Cycom 907	RTD	2-2-2	0.0964	1.0064	18,180	19,580	>72,000	0.673	0.743
		2-2-3	0.0967	1.0068	19,130		>72,000	0.758	
		3-2-1	0.0859	1.0081	11,850		>72,000	0.623	
Cycom 1808	RTD	3-2-2	0.0878	1.0076	11,860	11,860	>72,000	0.627	0.636
		3-2-3	0.0880	1.0075	11,860		>72,000	0.659	
		3-2-4	0.0879	1.0066	10,350		>36,000	0.198	
	ETW	3-2-5	0.0884	1.0067	8,610	9,260	>36,000	0.210	0.218
		3-2-6	0.0878	1.0087	8,810		>36,000	0.247	
		4-2-1	0.0797	1.0035	12,710		>72,000	0.730	
5245C	RTD	4-2-2	0.0804	0.9966	12,160	12,320	>72,000	0.730	0.749
		4-2-3	0.0805	1.0021	12,080		>72,000	0.789	
		4-2-4	0.0805	0.9976	10,770		>36,000	0.334	
	ETW	4-2-5	0.0809	0.9993	11,250	11,000	>36,000	0.391	0.363
		4-2-6	0.0806	0.9984	10,990		-	-	

GP53-0910-95-R

Figure 23. Intralaminar Shear Test Results

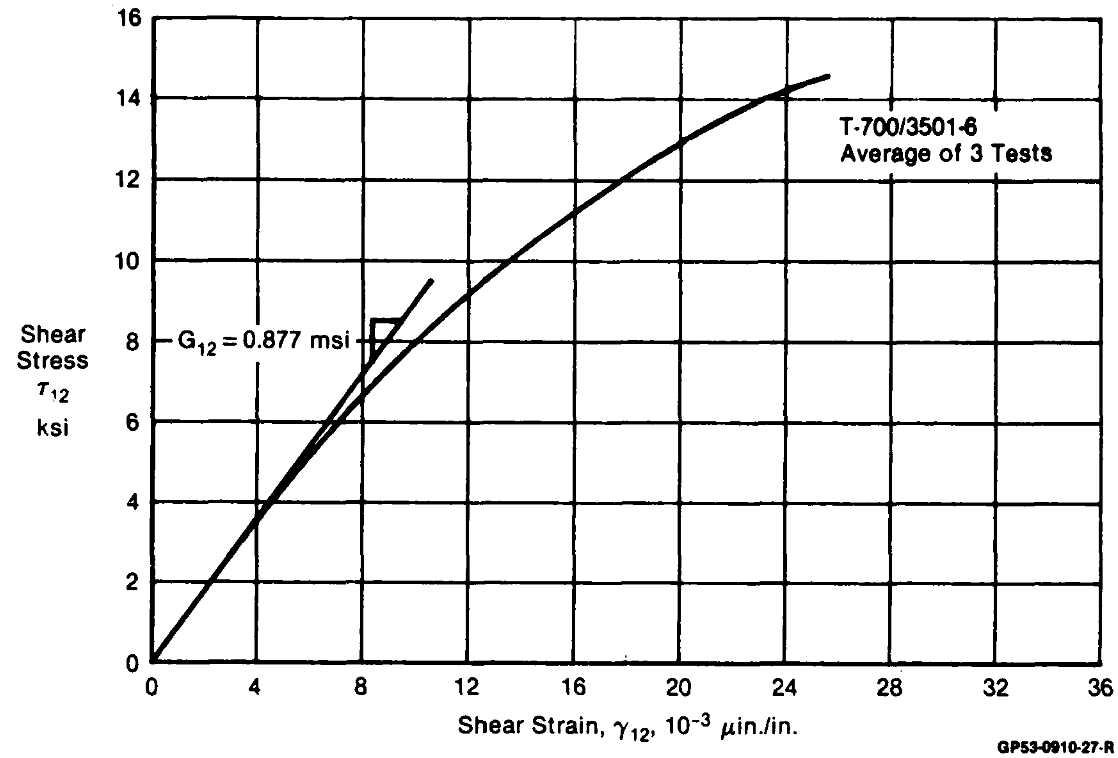

Figure 24. Intralaminar Shear Mechanical Behavior: 3501-6 Resin System

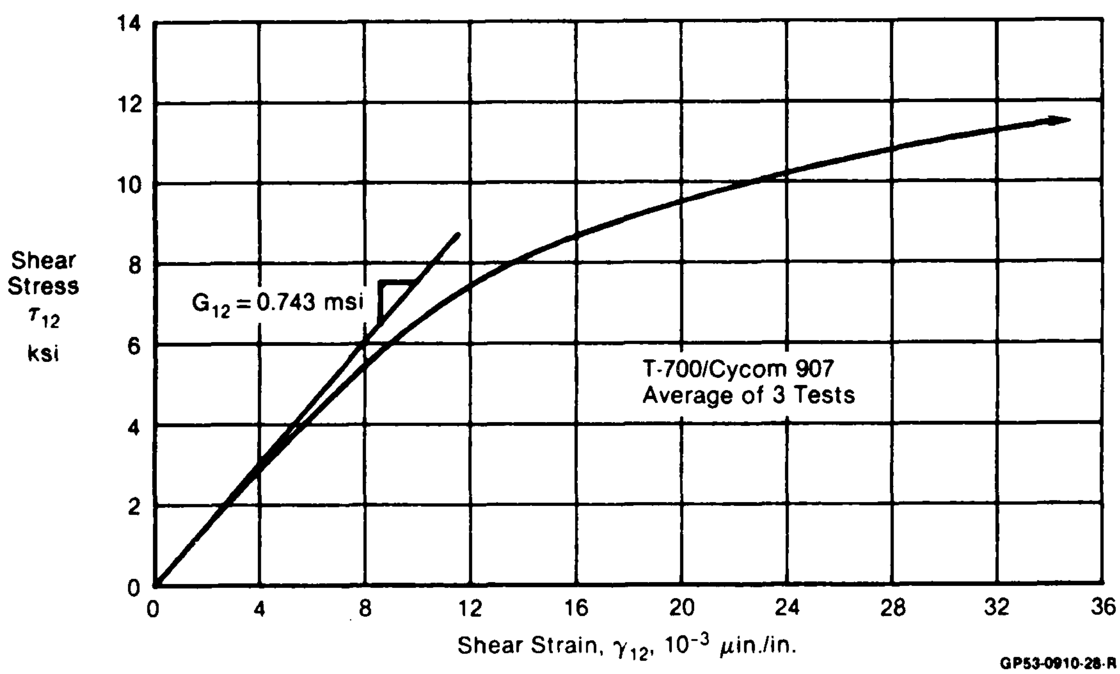

Figure 25. Intralaminar Shear Mechanical Behavior: Cycom 907 Resin System

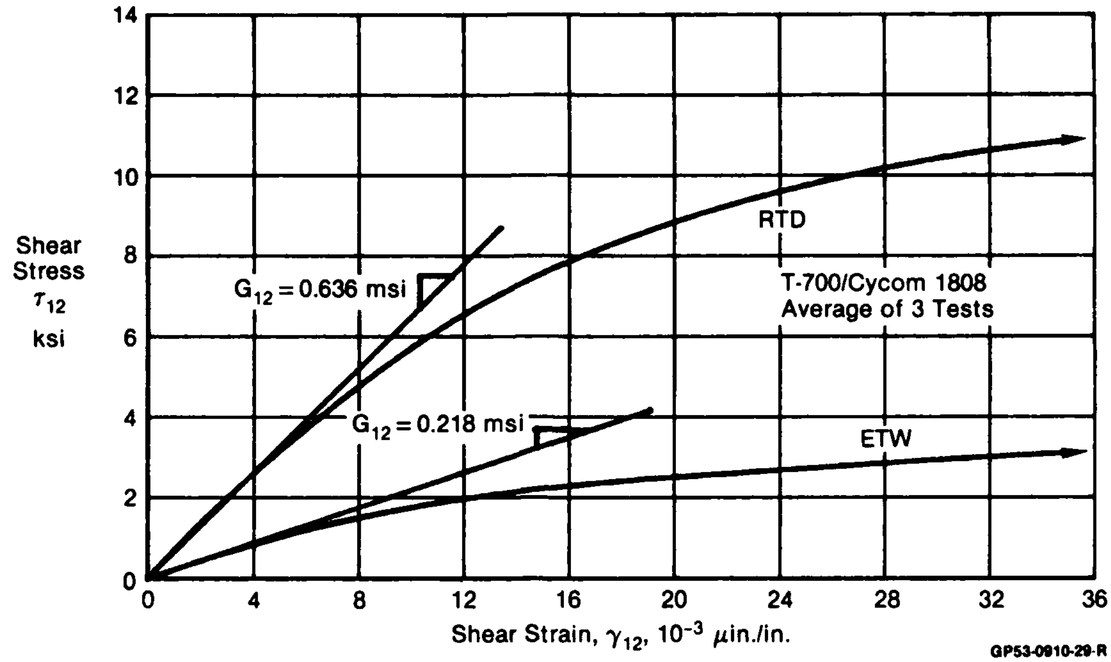

Figure 26. Intralaminar Shear Mechanical Behavior: Cycom 1808 Resin System

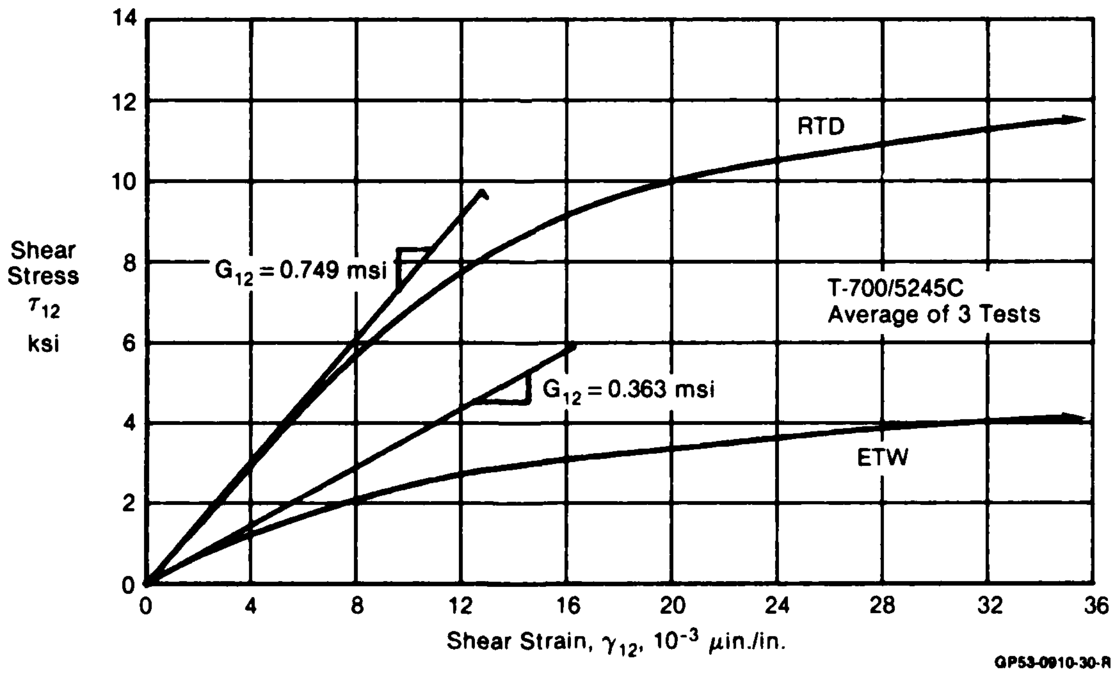

Figure 27. Intralaminar Shear Mechanical Behavior: 5245C Resin System

1-2-3: RTD

3-2-4: ETW

GP53-0910-105-R

Figure 28. Failed ± 45° Intralaminar Shear Test Specimens

Shear stress-strain mechanical behavior was obtained from measurements of load versus longitudinal and transverse strain using the following relations (Ref. 7):

$$G_{12} = \sigma_x/2(\varepsilon_x - \varepsilon_y) \quad (1)$$
$$\tau_{12} = \sigma_x/2 \quad (2)$$
$$\gamma_{12} = \varepsilon_x - \varepsilon_y \quad (3)$$

There are two important approximations inherent with this test and data reduction procedure (Ref 8). One approximation is caused by the lack of a pure shear stress or strain state in each ply of the ±45° test specimen. From test results in Figure 29, it is shown that the laminate Poisson's ratio is not exactly unity. Since the longitudinal strain is not quite equal to the negative of the transverse strain, the strain state in each ply at 45° to the laminate axes is not quite pure shear. If laminate strains are plotted on a Mohr's strain circle, results shown in Figure 30 are obtained. Small tensile strains exist in addition to the relatively large shear strains in the principal directions of the lamina. From test results shown in Figure 29, this tensile strain is computed to be approximately 7 percent of the shear strain. The tensile strains across the transverse direction of the lamina result in a slightly reduced shear modulus and contribute to laminate failure.

Resin System	Environment	Specimen Number	Thickness (inch)	Width (inch)	Step Number	Load (lb)	σ_x (psi)	E_x (msi)	ε_x (uin/in)	ε_y (uin/in)	ν_{xy}	τ_{12} (psi)	γ_{12} (μin/in)	G_{12} (msi)
5245C	RTD	4-2-1	0.0797	1.0035	1	260	3,310	2.50	1,320	960	0.727	1,650	2,280	0.725
					2	520	6,610	2.62	2,580	1,920	0.744	3,310	4,500	0.744
					3	780	9,910	2.20	4,080	3,060	0.750	4,960	7,140	0.626
					4	1,040	13,220	1.97	5,760	4,380	0.760	6,610	10,140	0.551
					5	1,300	16,520	1.53	7,920	6,180	0.780	8,260	14,100	0.417
					6	1,560	19,830	0.93	11,460	9,120	0.796	9,910	20,580	0.255
					7	1,820	23,130	0.46	18,600	15,360	0.826	11,570	33,960	0.124
					8	2,000	25,420	-	>36,000	>36,000	-	12,710	>72,000	-

GP53-0910-94-R

Figure 29. Intralaminar Shear Test Results

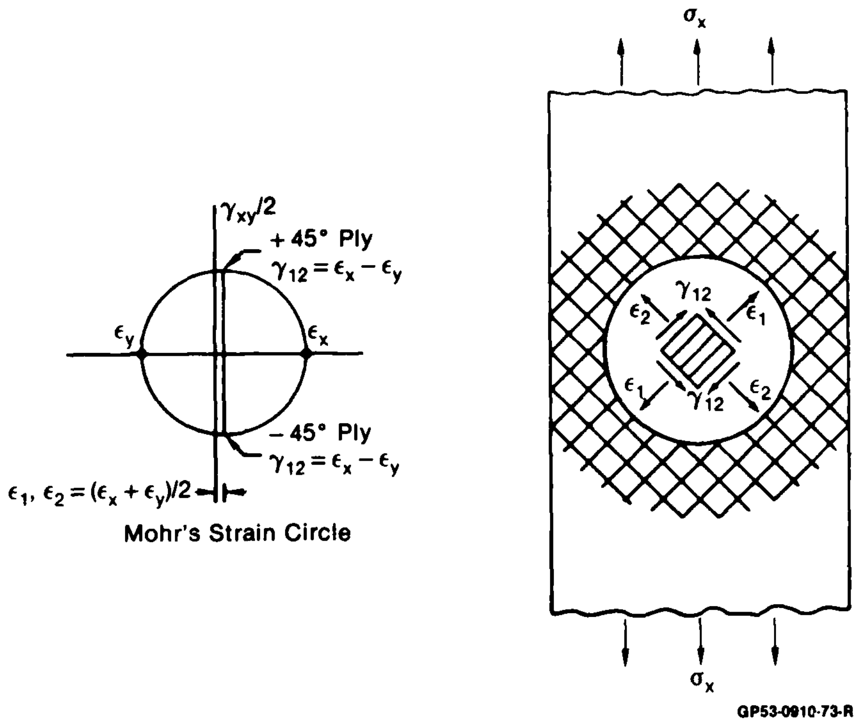

Figure 30. Strain State in ±45° Intralaminar Shear Test Specimen

The second approximation is due to the existence of large free edge stresses in the region near the boundary of the $\pm 45^{\circ}$ test specimen. Analytical predictions of free edge stresses in $\pm 45^{\circ}$ laminates have been discussed in the literature (Ref 9); results are reproduced in Figure 31. Failure of the $\pm 45^{\circ}$ intralaminar shear test specimen is influenced by damage growth caused by these large free edge stresses. Damage growth is primarily a Mode II fracture due to the interlaminar shear stress state at the laminate free edge. The toughness of the Cycom 907 resin system inhibits growth of this free edge damage and accounts for its high shear strength relative to the other three resin systems as measured using the $\pm 45^{\circ}$ test specimen. Recognizing the limitations of the $\pm 45^{\circ}$ test method for measuring lamina shear mechanical properties, lamina shear strength test results and hence laminate strength predictions will in general be conservative.

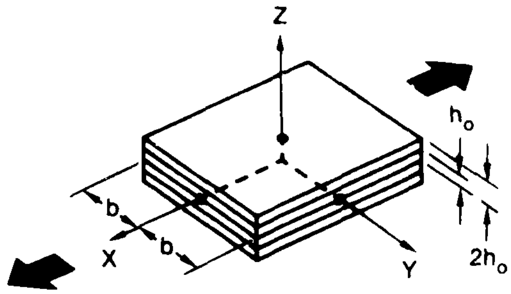

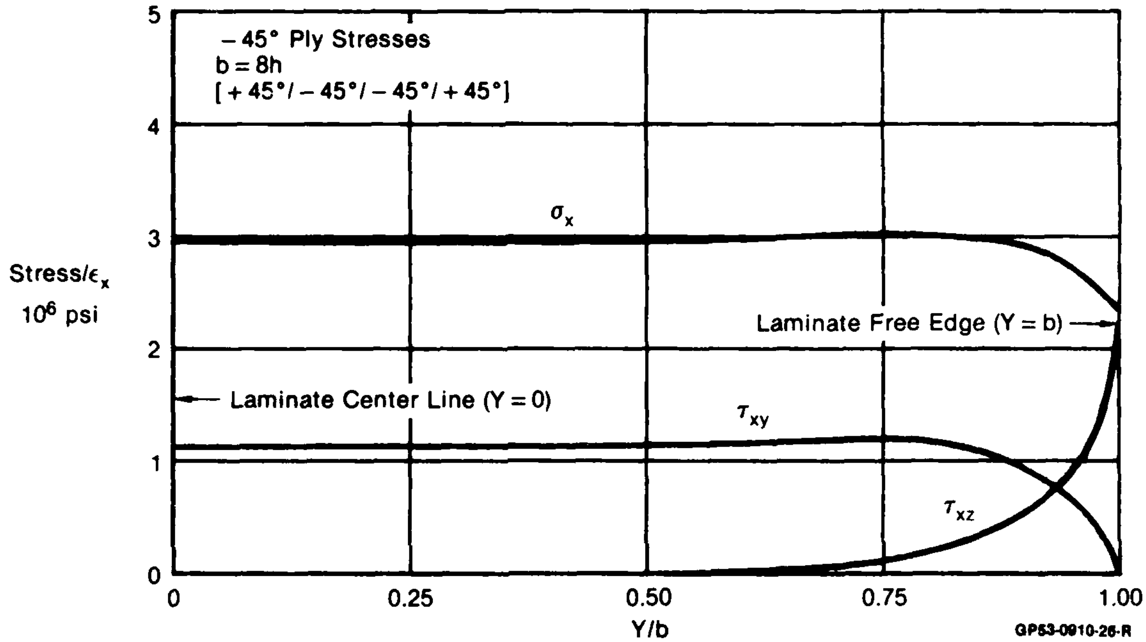

Figure 31. Interfacial Stresses in ±45° Intralaminar Shear Test Specimen

b. Mode I Fracture Toughness - The Mode I fracture toughness test specimen is shown in Figure 32. Critical strain energy release rates were obtained from measurements of crack length, failure load, compliance and crack opening deflections. The fracture toughness test arrangement is shown in Figure 33. The nomenclature describing the double cantilever beam is given in Figure 34.

Several tests were performed on each specimen. Opening displacement was applied to initiate crack growth in the starter film and increased until the crack extended some distance from the loading blocks. Displacement was then returned to zero. For each test measurement, displacement was applied to initiate crack growth, and the displacement was then increased until the crack propagated some arbitrary distance along the specimen. Crack length measurements were taken visually on the specimen edge with a traveling microscope. Displacement was returned to zero and the process repeated. Sample test data is shown in Figure 35 for the 5245C resin system.

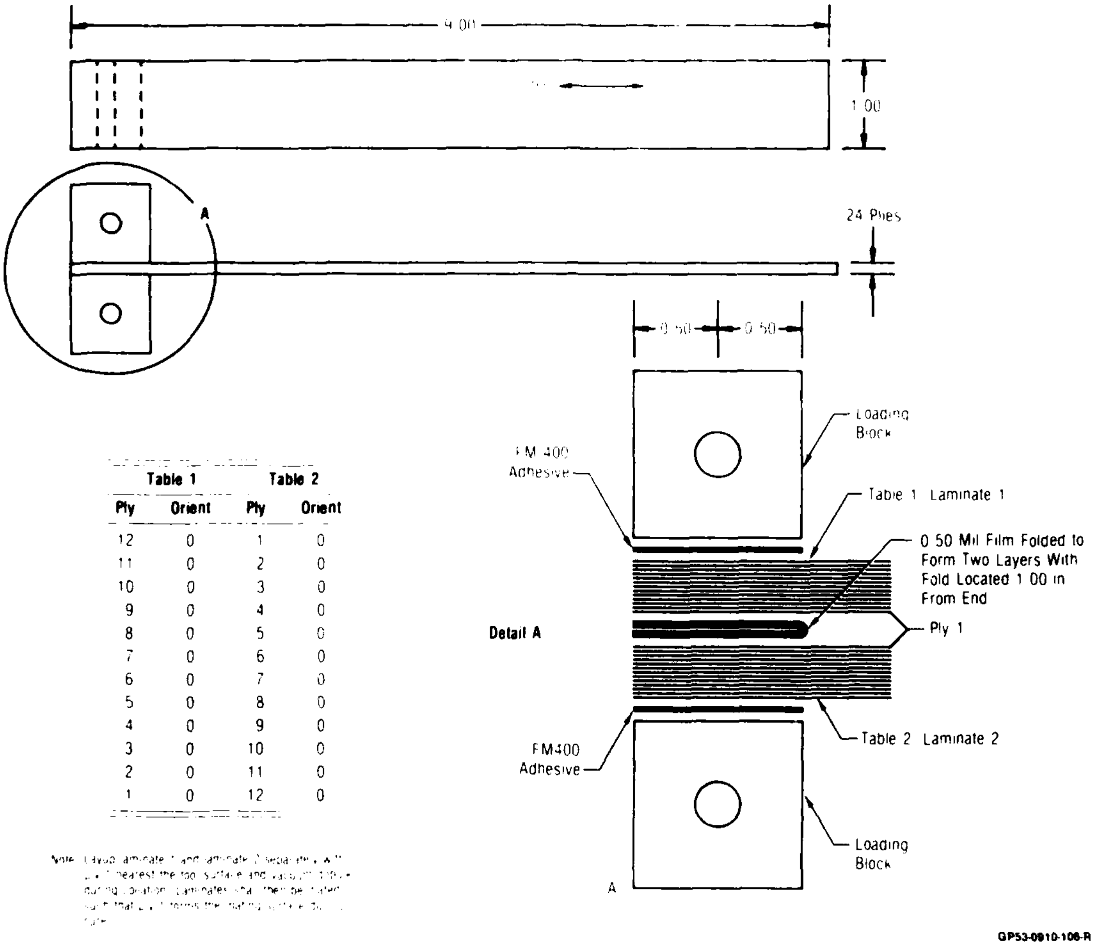

Table 1		Table 2	
Ply	Orient	Ply	Orient
12	0	1	0
11	0	2	0
10	0	3	0
9	0	4	0
8	0	5	0
7	0	6	0
6	0	7	0
5	0	8	0
4	0	9	0
3	0	10	0
2	0	11	0
1	0	12	0

Figure 32. Mode I Fracture Toughness Test Specimen

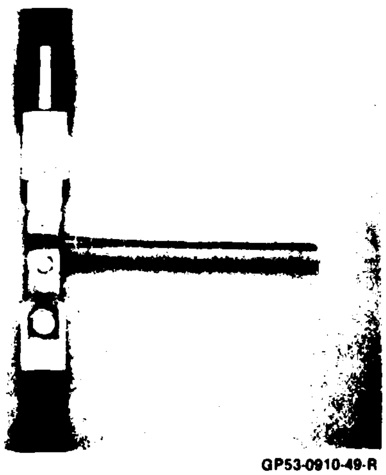

Figure 33. Mode I Fracture Toughness Test Arrangement

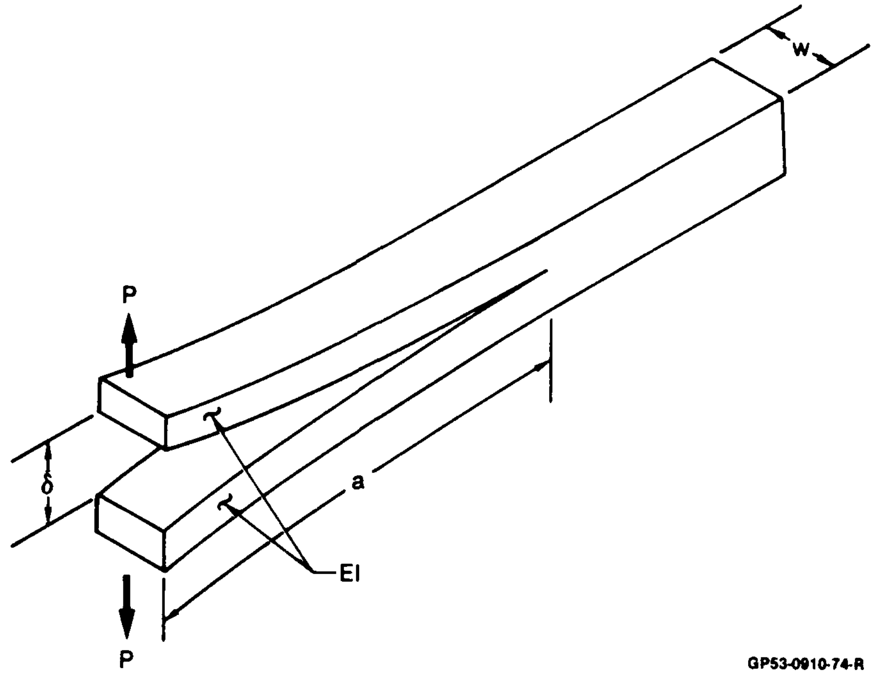

Figure 34. Double Cantilever Beam

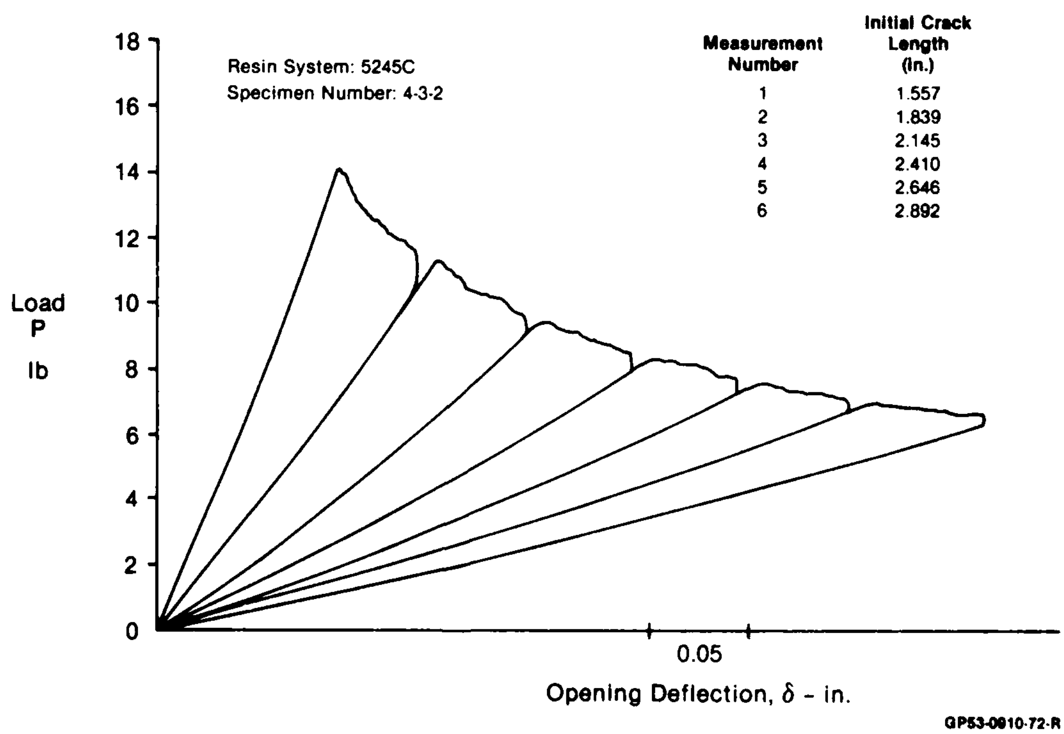

Figure 35. Mode I Fracture Toughness Test Data: 5245C Resin System

Critical strain energy release rates, G_{IC}, which is a measure of energy required by the action of external loads for a unit forward displacement of a crack surface, were computed from these test data using two methods. The first method used, called the Area-Integration Method, is shown in Figure 36. To compute the energy required to extend the crack, three separate energies are considered. Initial opening displacement

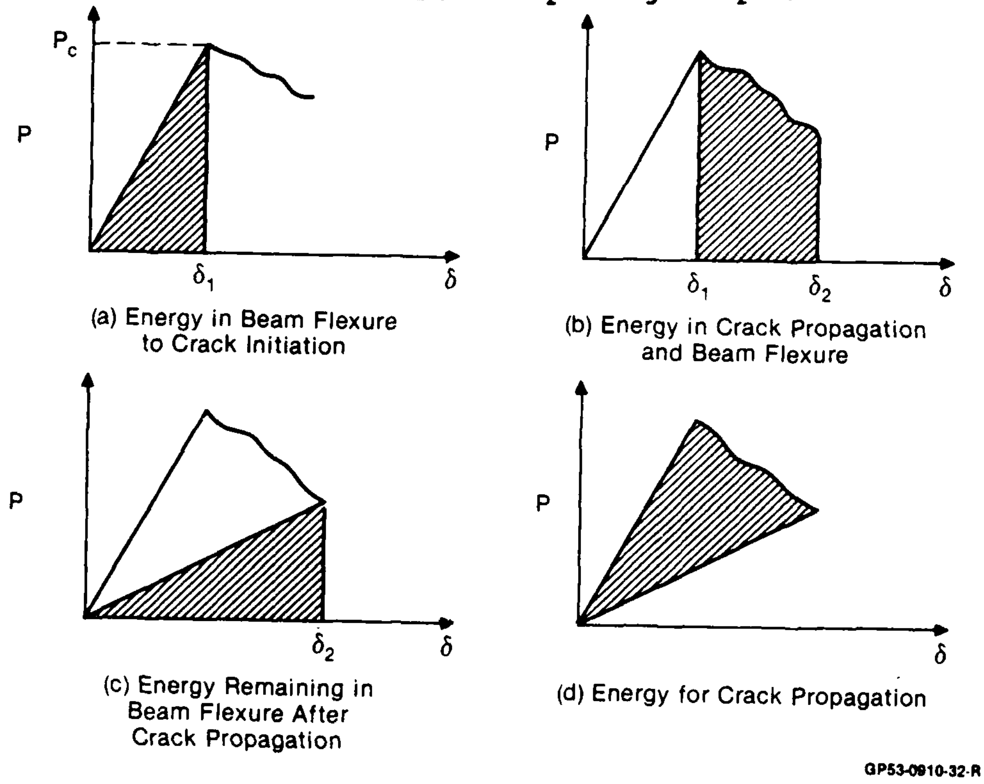

Figure 36. Area Integration Method for Calculating Mode I Fracture Toughness

represents the energy stored in the beam prior to crack growth (Figure 36a). Additional energy is required to propagate the crack and further flex the beam (Figure 36b). Unloading to zero displacement represents energy remaining in the beam after crack propagation (Figure 36c). The first two energies minus the third is the total energy required to propogate the crack. The critical strain energy release rate is this energy divided by the area created by the crack extension. Measurements required to calculate G_{IC} by this method are load, deflection, initial and final crack lengths, and specimen width. Using a linear approximation of load-deflection test results, fracture toughness can be computed using the relation:

$$G_{IC} = \frac{(P_1\delta_2 - P_2\delta_1)}{2W(a_2-a_1)}$$

Sample results using the Area-Integration Method are shown in Figure 37.

Resin System	Specimen Number	Width (inch)	Measurement Number	Load (lb)		Crack Length (inch)		Opening Deflection (inch)		Mode I Fracture Toughness (in-lb/in^2)	
				Initial	Final	Initial	Final	Initial	Final	Individual	Average
5245C	4-3-2	1.008	1	14.1	10.8	1.557	1.839	0.086	0.126	1.498	
			2	11.3	9.12	1.839	2.145	0.126	0.172	1.287	
			3	9.41	7.98	2.145	2.410	0.172	0.224	1.245	1.288
			4	8.28	7.23	2.410	2.646	0.224	0.272	1.235	
			5	7.54	6.69	2.646	2.892	0.272	0.316	1.148	
			6	6.97	6.24	2.892	3.124	0.316	0.370	1.306	

GP53-0910-92-R

Figure 37. Mode I Fracture Toughness Using Area-Integration Method

The second method for computing G_{IC} from test results, called the Compliance Calibration Method (Ref 10), uses the relationship:

$$G_{IC} = 3A_1A_2^2/2W.$$

A_1 and A_2 are given by the relations:

$$C = \delta/P = A_1a^3$$

$$P_c = A_2a^{-1}$$

where P_c is the critical load required to initiate crack growth. Sample data reduction results are shown in Figure 38; sample calculations are summarized in Figure 39.

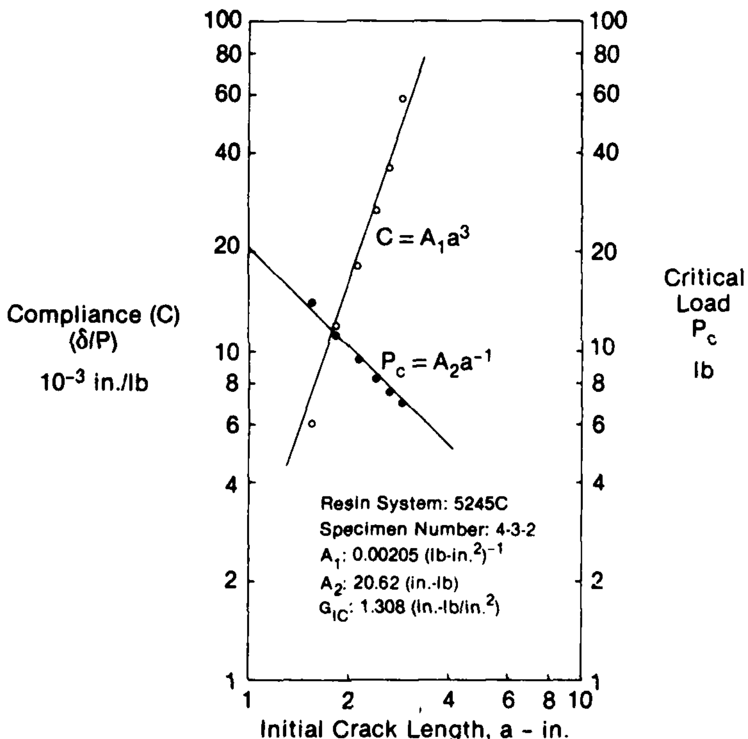

GP53-0910-71-R

Figure 38. Compliance Calibration Data Reduction: 5245C Resin System

Resin System	Specimen Number	Width (inch)	Measurement Number	Crack Length (inch)	Failure Load (lb)	Compliance (10^{-3} in/lb)	A_1 (lb-in^2)$^{-1}$	A_2 (in-lb)	Mode I Fracture Toughness (in-lb/in^2)
5245C	4-3-2	1.008	1	1.557	14.1	6.04	0.00205	20.62	1.308
			2	1.839	11.3	12.0			
			3	2.145	9.41	18.0			
			4	2.410	8.28	26.7			
			5	2.646	7.54	35.9			
			6	2.892	6.97	58.3			

GP53-0910-91-R

Figure 39. Mode I Fracture Toughness Using Compliance-Calibration Method

Mode I fracture toughness test results are summarized in Figure 40 for all four resin systems; results using both methods of data reduction are compared. The Area Integration Method generally gave higher values of toughness, while the Compliance Calibration Method generally gave more consistent results.

Resin System	Specimen Number	Thickness (inch)	Width (inch)	Mode I Fracture Toughness (in-lb/in^2): Area Integration Method, Individual	Area Integration Method, Average	Compliance Method, Individual	Compliance Method, Average
3501-6	1-3-1	0.147	1.005	0.876	0.807	0.867	0.812
	1-3-2	0.150	1.005	0.808		0.808	
	1-3-3	0.150	0.999	0.736		0.740	
Cycom 907	2-3-1	0.146	1.004	3.264	3.103	2.850	2.699
	2-3-2	0.148	1.000	2.804		2.497	
	2-3-3	0.148	0.996	3.240		2.748	
Cycom 1808	3-3-1	0.137	1.005	1.892	1.892	1.736	1.774
	3-3-2	0.139	1.008	1.676		1.572	
	3-3-3	0.142	1.006	2.109		2.014	
5245C	4-3-1	0.121	1.007	1.545	1.506	1.465	1.397
	4-3-2	0.121	1.008	1.286		1.308	
	4-3-3	0.121	1.008	1.688		1.419	

GP53-0910-93-R

Figure 40. Mode I Fracture Toughness Test Results

4. <u>LAMINATE PROPERTIES</u> - Lamina mechanical properties used for ply-by-ply analysis of laminates tested under this phase of program testing are summarized in Figure 41.

Properties	T-700/3501-6 RTD	T-700/Cycom 907 RTD	T-700/Cycom 1808 RTD	T-700/Cycom 1808 ETW	T-700/5245C RTD	T-700/5245C ETW
Elastic Constants						
E_1^t (msi)	21.76	22.28	21.95	22.63	21.92	22.87
E_1^c (msi)	20.74	19.74	20.45	20.75	20.09	20.99
E_2^t (msi)	1.493	1.443	1.271	0.669	1.425	0.919
G_{12} (msi)	0.877	0.743	0.636	0.218	0.749	0.363
ν_{12}	0.311	0.328	0.311	0.427	0.306	0.368
Allowables						
ϵ_1^{tu} (μin/in)	12190	13760	15460	9561	16700	11381
ϵ_1^{cu} (μin/in)	11040	6409	10491	-	10044	4348
ϵ_2^{tu} (μin/in)	4893	8283	7468	4967	8069	6739
γ_{12} (μin/in)	26050	>72000	>72000	>36000	>72000	>36000
F_1^{tu} (ksi)	275.8	328.0	357.1	229.2	397.6	279.4
F_1^{cu} (ksi)	213.9	135.3	214.5	-	193.6	88.1
F_2^{tu} (ksi)	7.27	11.30	9.10	2.89	10.99	4.51
F_{12}^{u} (ksi)	14.51	19.58	11.86	9.26	12.32	11.00

GP53-0910-101-R

Figure 41. Lamina Mechanical Properties

Both a fiber and matrix dominated layup were used to establish a data base on static and fatigue laminate mechanical properties. Laminate stacking sequences are shown in Figure 42. Laminate tests were performed to determine: (1) unnotched laminate static tension and compression strength, (2) unloaded hole static tension and compression strength, (3) unloaded hole constant amplitude fatigue life, (4) loaded hole pure bearing static strength, (5) accumulation of hole elongation with fatigue, (6) low energy impact damage tolerance, and (7) multifastener metal-to-composite strength and constant amplitude fatigue life. The following sections describe test results and correlation of analytical predictions with test results.

Ply Number (to Centerline)	Percent of 0°/±45°/90° Plies 50/40/10	10/80/10
1	+45	+45
2	0	−45
3	−45	+45
4	0	−45
5	90	90
6	0	+45
7	+45	−45
8	0	0
9	−45	+45
10	0	−45
11	+45	+45
12	0	−45
13	−45	+45
14	0	−45
15	90	90
16	0	+45
17	+45	−45
18	0	0
19	−45	+45
20	0	−45
Centerline		

Stacking Sequence Is Symmetric About Centerline

GP53-0910-75-R

Figure 42. Laminate Stacking Sequence

a. <u>Unnotched: Static and Fatigue</u> - The unnotched tension test specimen is shown in Figure 43; test results are shown in Figure 44. Unnotched tension test specimen failures for both the 10/80/10 and 50/40/10 layups are shown in Figure 45.

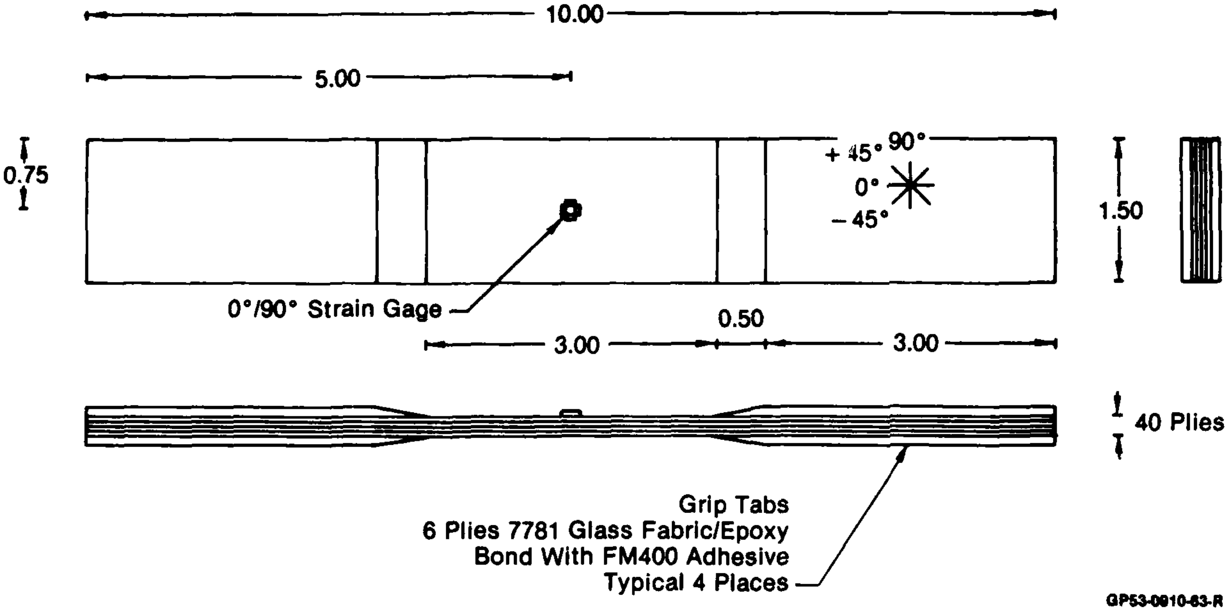

GP53-0910-63-R

Figure 43. Unnotched Tension Test Specimen

Resin System	Layup	Specimen Number	Thickness (inch)	Width (inch)	Failure Load (lb)	Failure Stress (ksi) Individual	Failure Stress (ksi) Average	Failure Strain (μin/in) Individual	Failure Strain (μin/in) Average	Modulus (msi) Individual	Modulus (msi) Average	Poisson's Ratio
		2-4-21	0.246	1.510	55,650	177.2		12,250		12.63		0.413
Cycom 907	50/40/10	2-4-22	0.247	1.497	57,500	184.7	182.4	13,620	13,340	12.87	12.62	0.410
		2-4-23	0.244	1.509	58,200	185.4		14,160		12.37		0.401
		2-5-1	0.250	1.502	23,300	74.6		16,800		5.11		0.518
	10/80/10	2-5-2	0.251	1.505	23,700	75.7	76.3	17,370	17,190	5.19	5.13	0.524
		2-5-3	0.251	1.503	24,550	78.5		17,400		5.09		0.632
		3-4-29	0.237	1.502	52,400	171.0		13,020		12.27		0.410
Cycom 1808	50/40/10	3-4-30	0.239	1.509	51,800	169.1	167.2	12,900	12,660	12.20	12.44	0.410
		3-4-31	0.238	1.502	49,500	161.5		12,060		12.85		0.425
		4-4-29	0.205	1.511	58,500	197.5		-		11.98		0.396
5245C	50/40/10	4-4-30	0.204	1.508	57,600	194.9	195.1	-	-	12.02	11.95	0.408
		4-4-31	0.204	1.507	57,000	193.0		15,600		11.85		0.405
		4-5-1	0.208	1.505	21,650	73.4		17,580		4.93		0.507
	10/80/10	4-5-2	0.207	1.505	21,550	73.1	72.4	17,730	17,610	5.04	4.99	0.516
		4-5-3	0.207	1.506	20,900	70.8		17,520		5.00		0.503

GP53-0910-90-R

Figure 44. Unnotched Laminate Tension Test Results

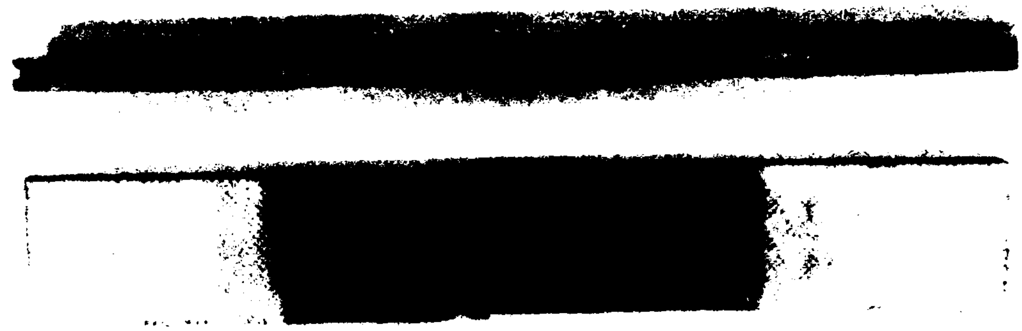

(10/80/10 Layup)

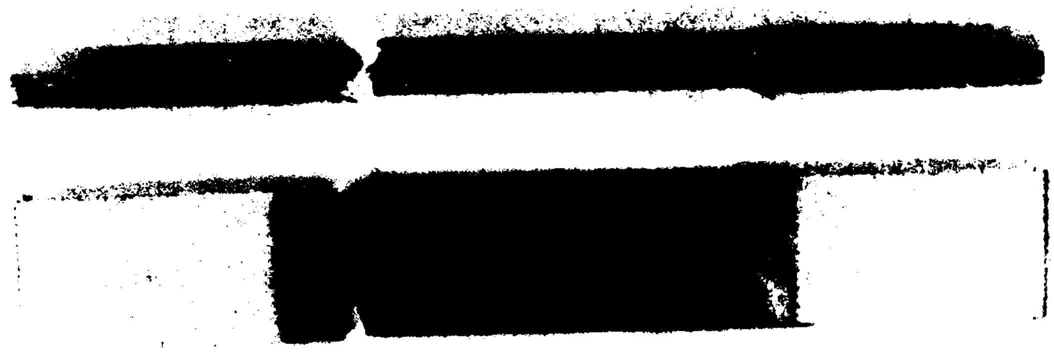

(50/40/10 Layup)

GP53-0910-45-R

Figure 45. Failed Unnotched Tension Test Specimens

Correlation of predicted laminate tension modulus, using classical laminated plate theory, with test results are shown in Figure 46. Predictions were generally within 7 percent of test results.

Unnotched laminate stresses were computed using classical lamination plate theory. Laminate failure was predicted by comparing elastic stresses with material failure criteria on a ply-by-ply basis. Typical material failure criteria are shown in Figure 47. The maximum stress and Tsai-Hill failure criteria were evaluated in correlating predicted strength with test results. The maximum stress failure criteria evaluates each of the three stress components independently:

$$\frac{\sigma_1}{F_1} = 1, \quad \frac{\sigma_2}{F_2} = 1, \quad \frac{\tau_{12}}{F_{12}} = 1.$$

When any of these ratios reach unity, failure is predicted. The Tsai-Hill failure criteria evaluates each of the stress components interactively:

$$\left(\frac{\sigma_1}{F_1}\right)^2 + \left(\frac{\sigma_2}{F_2}\right)^2 + \left(\frac{\tau_{12}}{F_{12}}\right)^2 - \left(\frac{\sigma_1 \sigma_2}{F_1{}^2}\right) = 1.$$

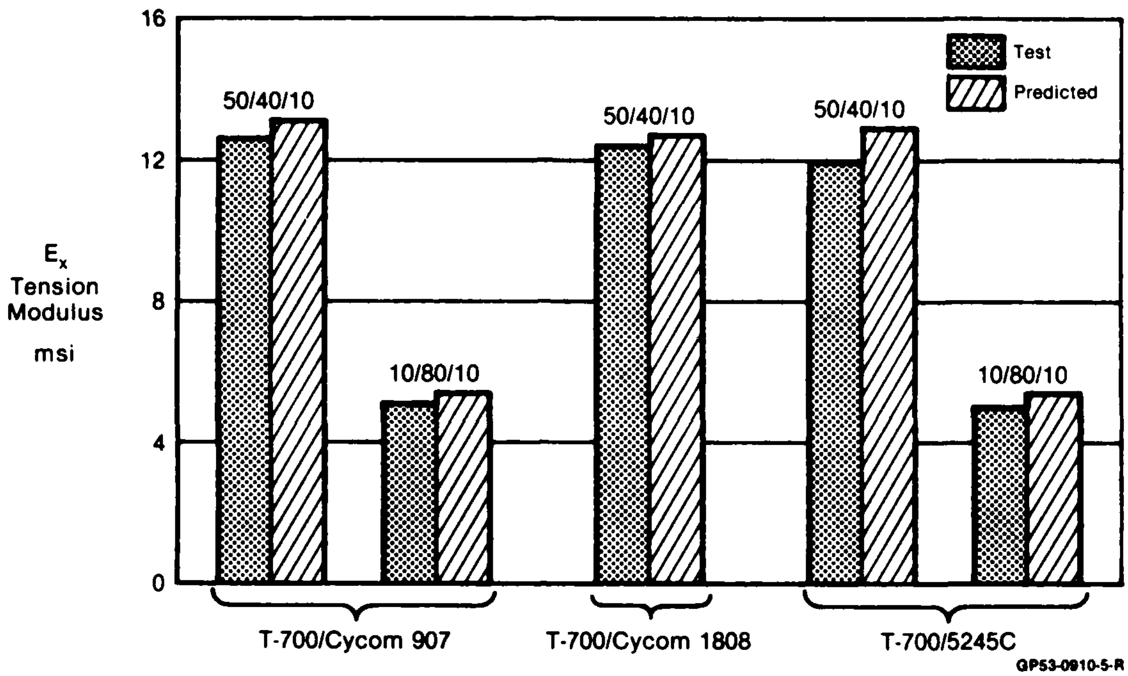

Figure 46. Correlation of Laminate Tension Modulus Test Results With Prediction

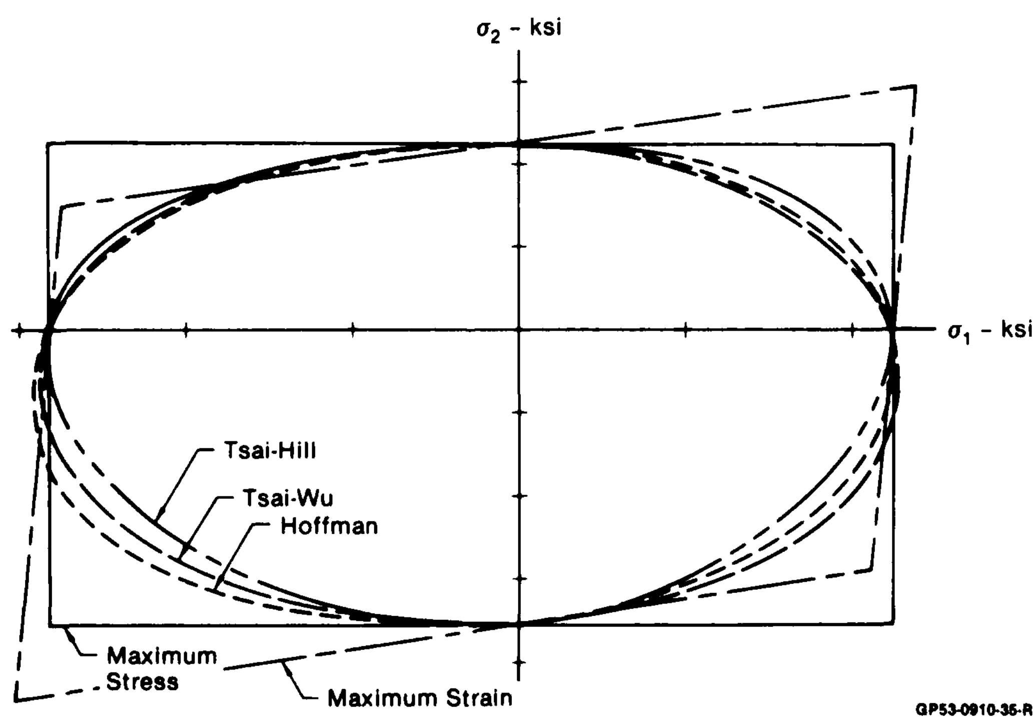

Figure 47. Failure Criteria Comparison

Predicted strength varies greatly between failure criteria depending on the magnitude of each stress component.

Correlation of unnotched laminate tension strength test results with predicted first ply failure is shown in Figure 48. The maximum stress failure criteria generally over predicted strength while predictions using the Tsai-Hill failure criteria were generally conservative. Predictions were conservative primarily because of the intralaminar shear strength allowable. Correlation of predicted stress-strain behavior with test results for both the 50/40/10 and 10/80/10 layups of the T-700/Cycom 907 material system are shown in Figure 49. Correlation was nearly exact up to the points of predicted first ply failure.

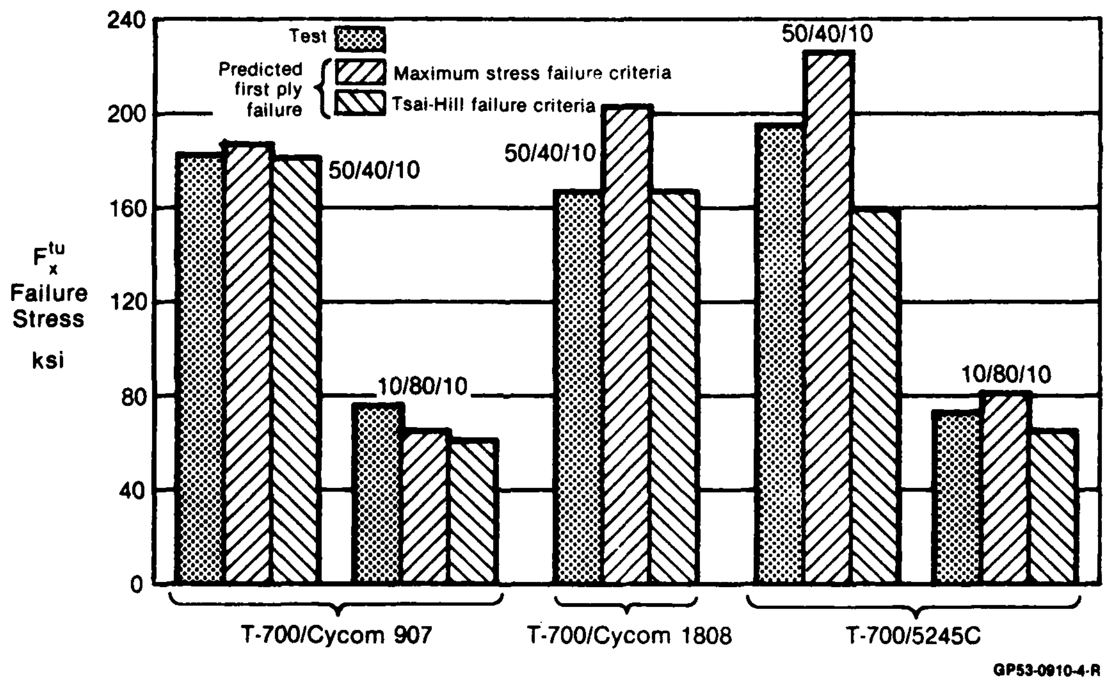

Figure 48. Correlation of Laminate Unnotched Tension Strength Test Results With Predicted First Ply Failure

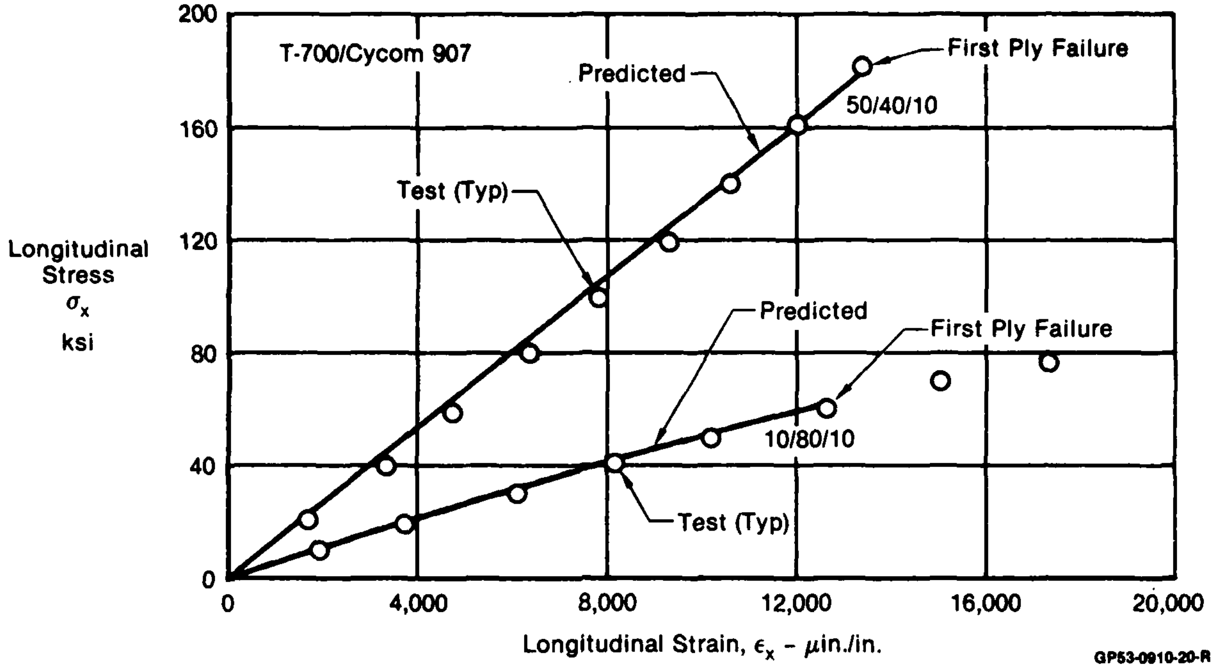

Figure 49. Correlation of Laminate Tension Stress/Strain Test Results With Prediction

The unnotched compression test specimen is shown in Figure 50; test results are shown in Figure 51. Typical test specimen failures for both 50/40/10 and 10/80/10 layups are shown in Figure 52.

Excellent agreement between predicted compression modulus and test results was obtained, as shown in Figure 53. Correlation of predicted first ply failure with test results are shown in Figure 54. Predictions for the Cycom 907 resin system were very conservative using unidirectional lamina strengths. Predicted strengths of the 50/40/10 layup for both the Cycom 1808 and 5245C resin systems correlated well with test results. Predicted strength of the 10/80/10 layup for the 5245C system was conservative by 30 percent, due to the nonlinearity in specimen failure and conservatism in ply intralaminar shear strength.

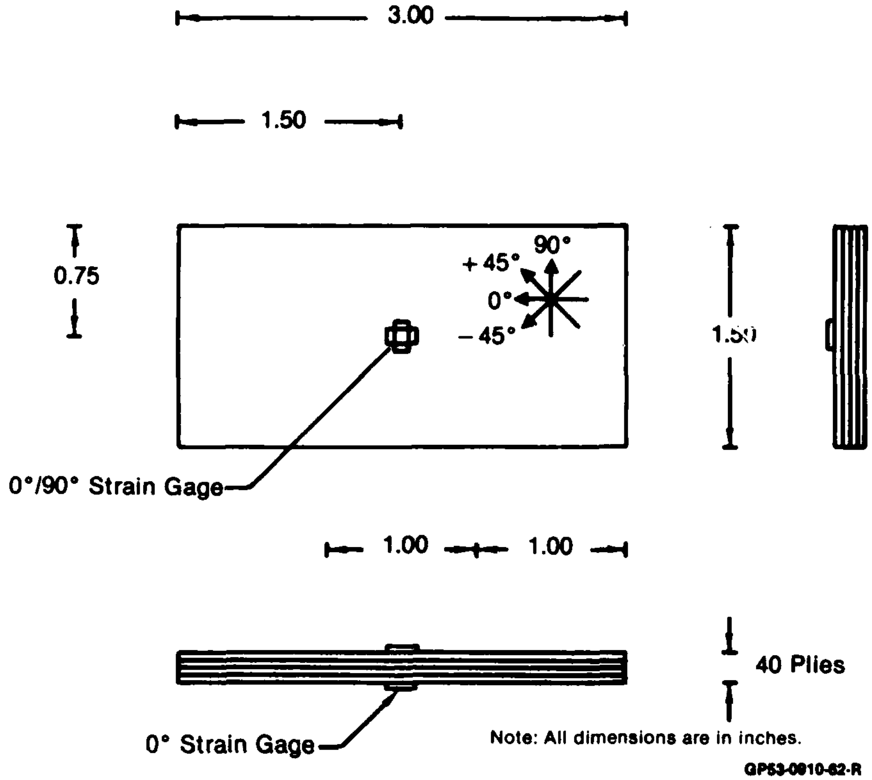

Figure 50. Unnotched Compression Test Specimen

Resin System	Layup	Specimen Number	Thickness (inch)	Width (inch)	Failure Load (lb)	Failure Stress (ksi) Individual	Failure Stress (ksi) Average	Failure Strain (μin/in) Individual	Failure Strain (μin/in) Average	Modulus (msi) Individual	Modulus (msi) Average	Poisson's Ratio
		2-4-18	0.246	1.507	36,890	117.7		10,350		11.81		0.469
Cycom 907	50/40/10	2-4-20	0.243	1.510	33,860	107.8	112.2	10,190	10,370	11.88	11.84	0.435
		2-4-41	0.243	1.509	34,860	111.1		10,580		11.84		0.446
		2-5-19	0.254	1.497	23,190	74.5		19,090		5.20		0.572
	10/80/10	2-5-20	0.253	1.498	23,625	75.8	74.3	18,690	18,790	5.40	5.28	0.557
		2-5-21	0.249	1.495	22,590	72.6		18,590		5.24		0.575
		3-4-37	0.243	1.501	40,110	125.3		12,530		11.60		0.434
Cycom 1808	50/40/10	3-4-38	0.238	1.501	36,550	119.4	121.7	11,280	11,720	11.73	11.60	0.459
		3-4-39	0.238	1.501	36,860	120.4		11,350		11.48		0.427
		4-4-37	0.206	1.508	36,720	122.7		11,980		11.74		0.412
5245C	50/40/10	4-4-38	0.205	1.507	32,070	108.6	116.5	10,900	11,580	11.49	11.20	0.427
		4-4-39	0.205	1.509	34,980	118.3		11,860		10.86		0.439
		4-5-19	0.202	1.511	20,680	69.8		18,180		4.88		0.568
	10/80/10	4-5-20	0.204	1.511	19,010	64.2	69.1	16,100	17,870	4.88	4.91	0.559
		4-5-21	0.206	1.510	21,650	73.8		19,340		4.96		0.558

GP53-0910-89-R

Figure 51. Unnotched Laminate Compression Test Results

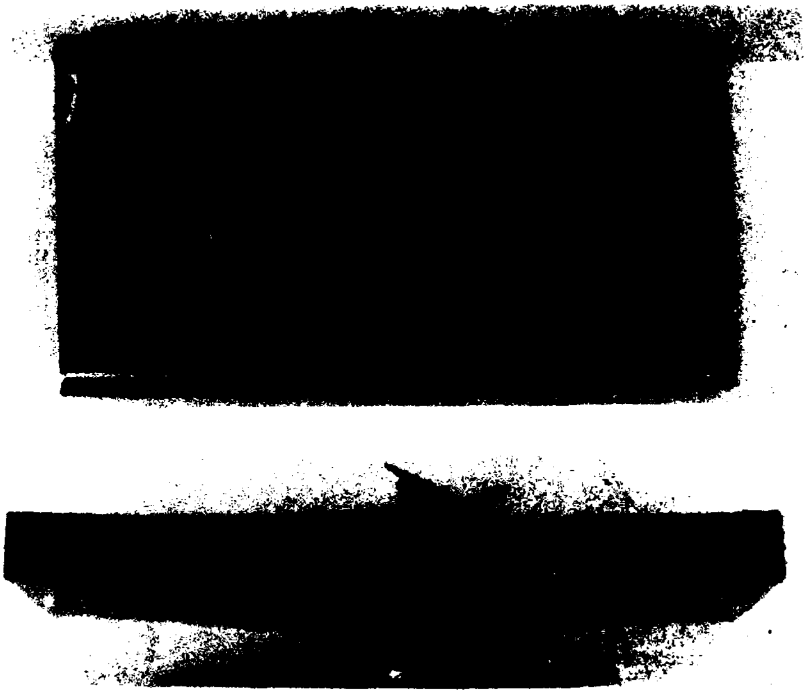

(10/80/10 Layup)

(50/40/10 Layup)

GP53-0810-43-R

Figure 52. Failed Unnotched Compression Test Specimens

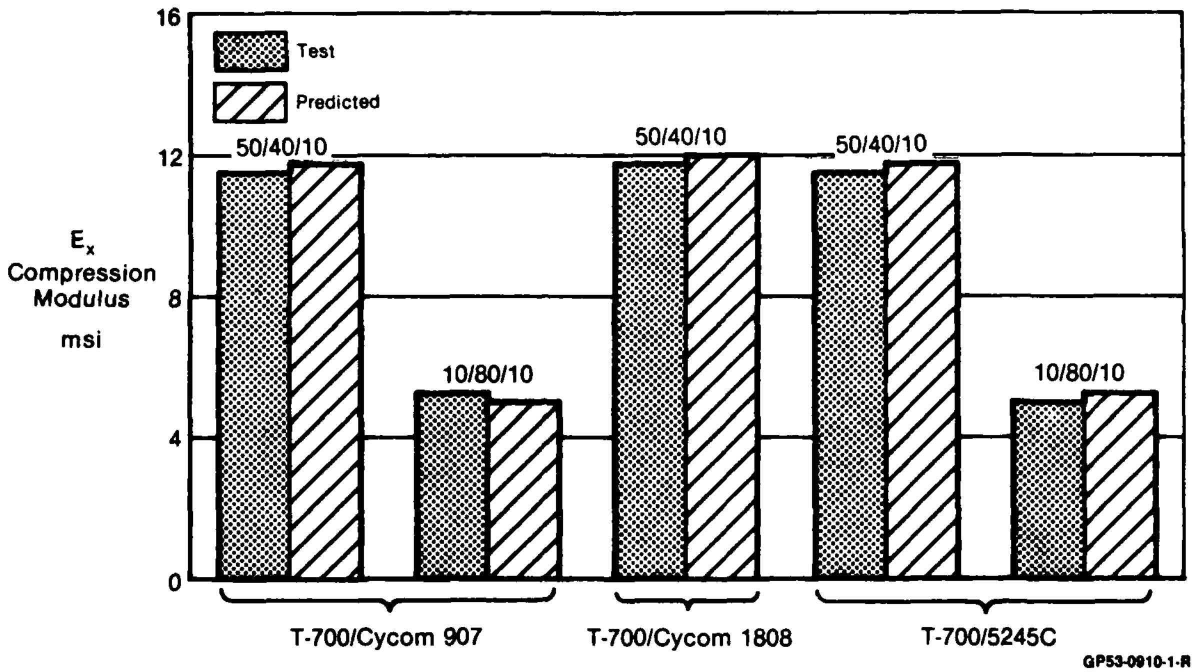

Figure 53. Correlation of Laminate Compression Modulus Test Results With Prediction

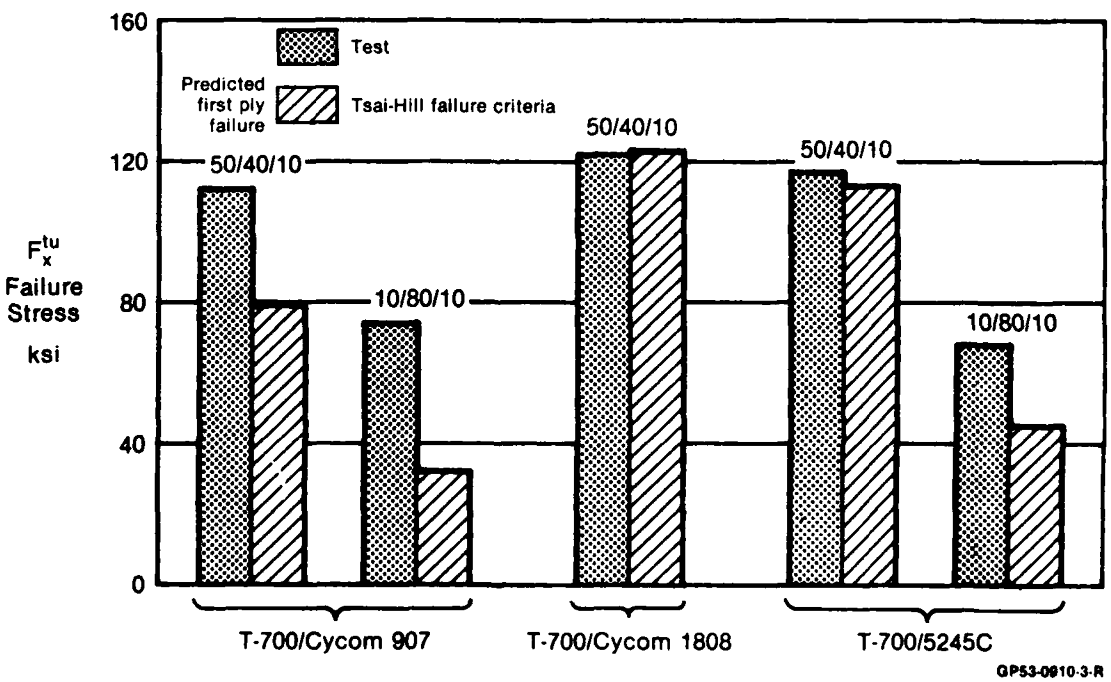

Figure 54. Correlation of Laminate Unnotched Compression Strength Test Results With Predicted First Ply Failure

b. Unloaded Hole: Static and Fatigue - The unloaded hole tension and compression static test specimen is shown in Figure 55. Compression test specimens were stabilized to prevent buckling. Unloaded hole tension test results are shown in Figure 56; typical test specimen failures are shown in Figure 57.

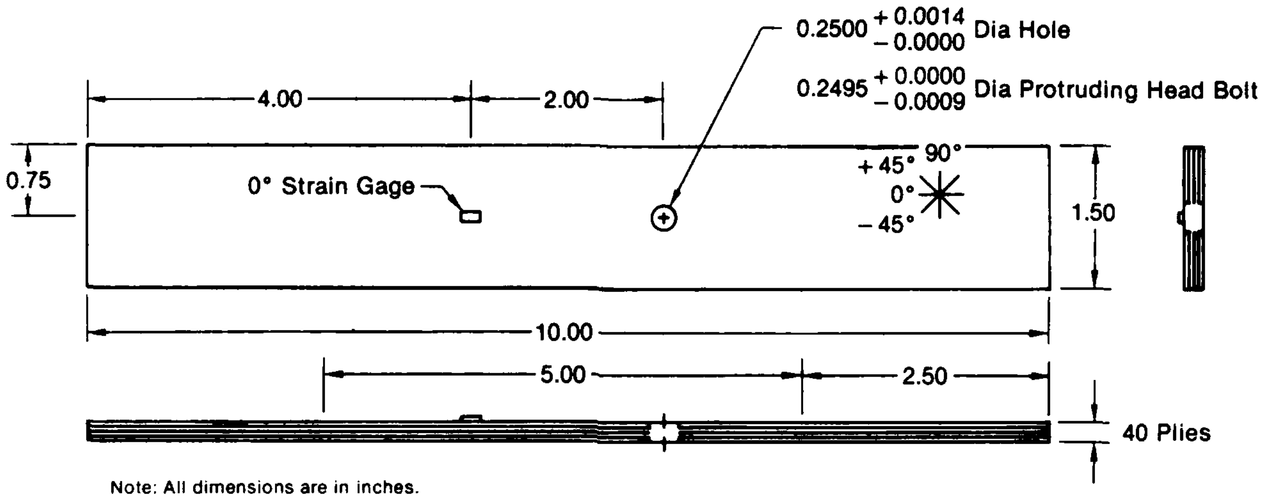

GP53-0910-61-R

Figure 55. Unloaded Hole Tension and Compression Static Test Specimen

Resin System	Environment	Layup	Specimen Number	Thickness (inch)	Width (inch)	Hole Diameter (inch)	Failure Load (lb)	Failure Stress (psi) Individual	Failure Stress (psi) Average	Failure Strain (μin/in) Individual	Failure Strain (μin/in) Average	Modulus (msi)
			2-4-24	0.244	1.509	0.250	28,850	91,920		7,130		11.80
Cycom 907	RTD	50/40/10	2-4-25	0.245	1.509	0.250	29,650	94,470	94,200	7,170	7,200	12.74
			2-4-26	0.245	1.509	0.250	30,200	96,220		7,290		12.55
			2-5-4	0.249	1.504	0.250	15,700	50,190		10,650		5.05
	RTD	10/80/10	2-5-9	0.249	1.504	0.250	16,400	52,460	51,540	11,070	10,830	5.17
			2-5-10	0.250	1.503	0.250	16,250	51,980		10,760		5.30
			3-4-32	0.240	1.495	0.270	28,750	94,720		6,990		13.12
Cycom 1808	RTD	50/40/10	3-4-33	0.240	1.500	0.250	28,450	92,970	91,670	6,750	6,860	13.25
			3-4-34	0.240	1.502	0.250	27,900	87,770		6,840		12.74
			3-4-45	0.240	1.493	0.250	29,700	97,510		6,290		14.72
	ETW		3-4-46	0.239	1.502	0.250	30,400	99,210	98,360	7,140	6,600	13.08
			3-4-47	0.239	1.500	0.250	30,100	98,370		6,380		14.69
			4-4-32	0.204	1.509	0.250	26,850	87,220		7,230		12.17
5245C	RTD	50/40/10	4-4-33	0.205	1.507	0.250	27,000	87,830	88,470	7,130	7,250	12.08
			4-4-34	0.205	1.508	0.250	27,800	90,370		7,400		11.83
			4-4-45	0.203	1.507	0.250	27,050	91,580		7,030		12.06
	ETW		4-4-46	0.206	1.507	0.250	28,250	95,640	94,530	6,990	7,220	13.10
			4-4-47	0.205	1.506	0.250	28,450	96,380		7,650		11.99
			4-5-4	0.206	1.507	0.250	14,200	48,080		10,010		5.22
	RTD	10/80/10	4-5-9	0.206	1.507	0.250	13,850	46,890	47,620	9,780	9,990	5.10
			4-5-10	0.205	1.507	0.250	14,150	47,910		10,190		5.03

GP53-0910-88-R

Figure 56. Unloaded Hole Tension Test Results

(50/40/10 Layup)

Figure 57. Failed Unloaded Hole Tension Test Specimens

Unloaded hole strength predictions were performed using the "Bolted Joint Stress Field Model" (BJSFM)(Reference 1), outlined in Figure 58. This methodology is based upon classical lamination plate theory and anisotropic theory of elasticity to obtain laminate stress and strain distributions, and a characteristic dimension (R_C) failure hypothesis. Test data requirements are minimized by extending the characteristic dimension failure hypothesis to a ply-by-ply analysis in conjunction with known material failure criteria. Unidirectional (lamina) stiffness and strength data were used with an empirical value of R_C to predict stress distributions, critical plies, failure location, and failure load. The utility in this analysis procedure is the use of a single characteristic dimension for various layups, made possible since failure is predicted on a ply-by-ply basis.

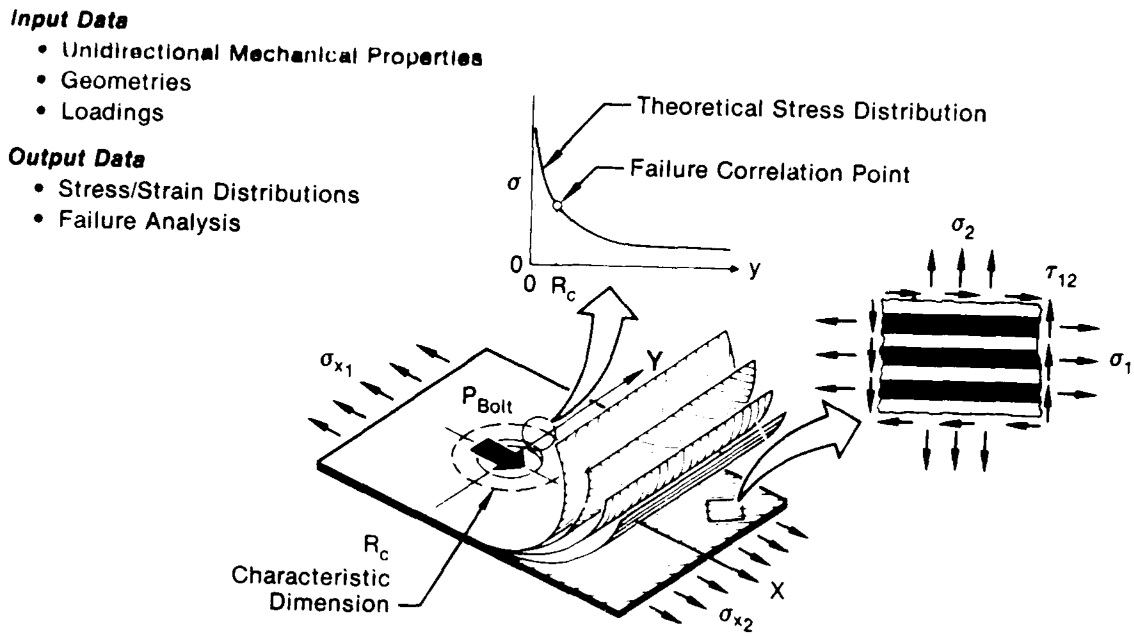

Figure 58. Bolted Joint Stress Field Model GP53-0910-33-R

Correlation of laminate strength predictions with test results for the Cycom 907 resin system are shown in Figure 59, based on the Tsai-Hill failure criteria. For a characteristic dimension of 0.062 inch, correlation of test results with prediction is nearly exact. Strength predictions using the maximum stress failure criteria are compared with test results in Figure 60. Since each of the ply stress components are evaluated independently, the characteristic dimension is much smaller as compared to the interactive Tsai-Hill failure criteria. For an R_c value of 0.023 inch determined using test results from the 50/40/10 layup, predicted strength of the 10/80/10 layup is conservative by 19 percent.

Laminate strength under the combined action of bearing and bypass loads can be predicted using the characteristic dimension determined from theory/test correlation of unloaded hole tests. A predicted bearing/bypass strength envelope for the Cycom 907 resin system is shown in Figure 61. Predictions are based upon the Tsai-Hill failure criteria and a characteristic dimension of 0.062 inch.

Correlation of predicted strength with test results for the 5245C resin system are shown in Figure 62, based on the maximum stress failure criteria. Predictions using a characteristic dimension of 0.011 inch for both the 50/40/10 and 10/80/10 layups are within 6 percent of test results. A bearing/bypass strength envelope for the 50/40/10 layup using the maximum stress failure criteria is shown in Figure 63. Predicted ultimate strength was based on fiber failure; strength predictions based on shear failures are overly conservative. Ply shear failures result only in very localized load redistribution, detectable by increasing nonlinear or discontinuous load-deflection behavior.

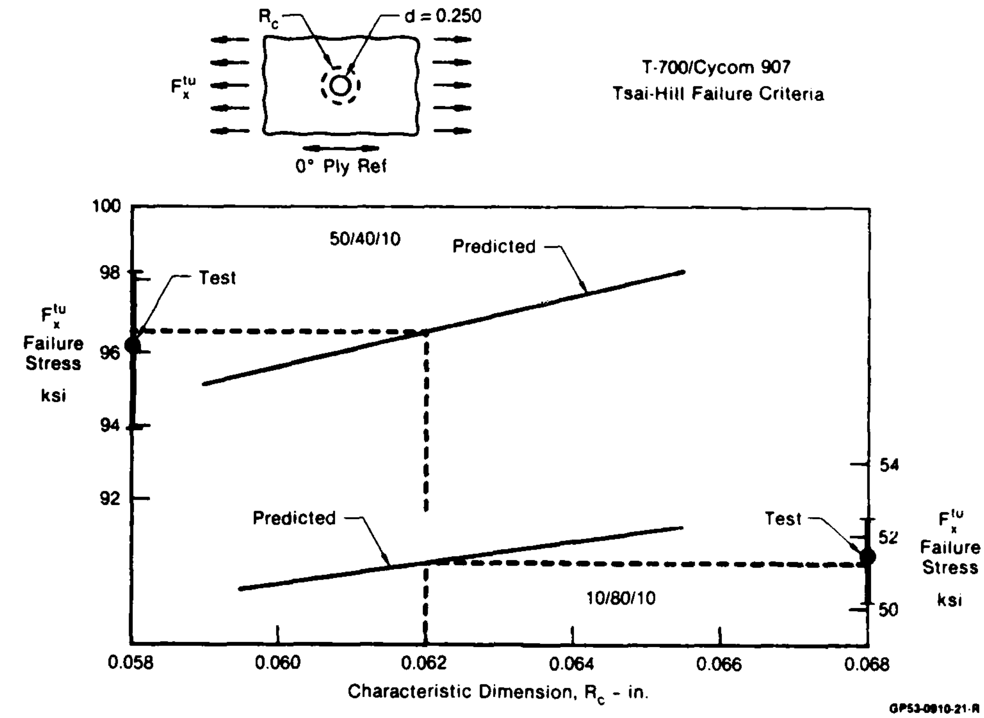

Figure 59. Correlation of Unloaded Hole Static Tension Strength Test Results With Prediction: Cycom 907 Resin System

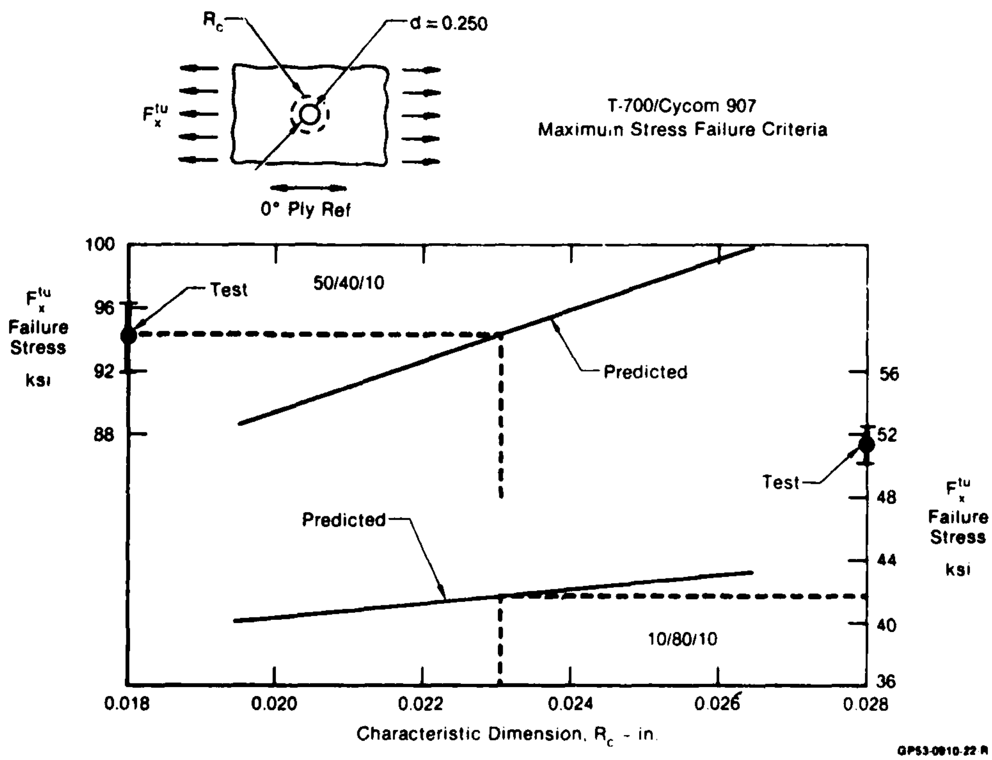

Figure 60. Correlation of Unloaded Hole Static Tension Strength Test Results With Prediction: Cycom 907 Resin System

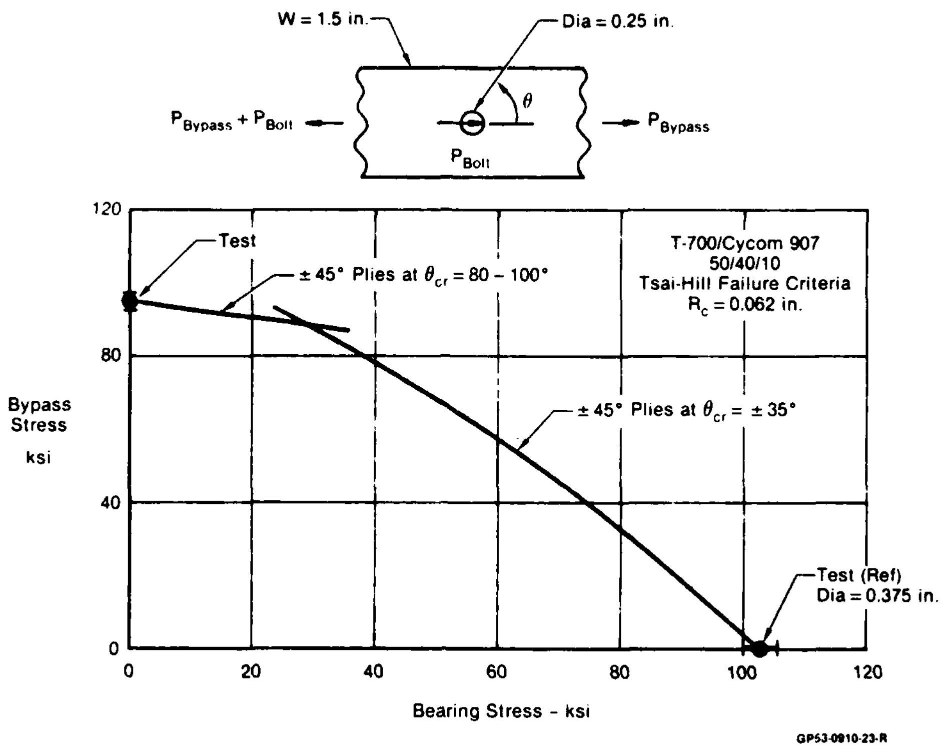

Figure 61. Bearing/Bypass Load Interaction Strength Envelope: Cycom 907 Resin System

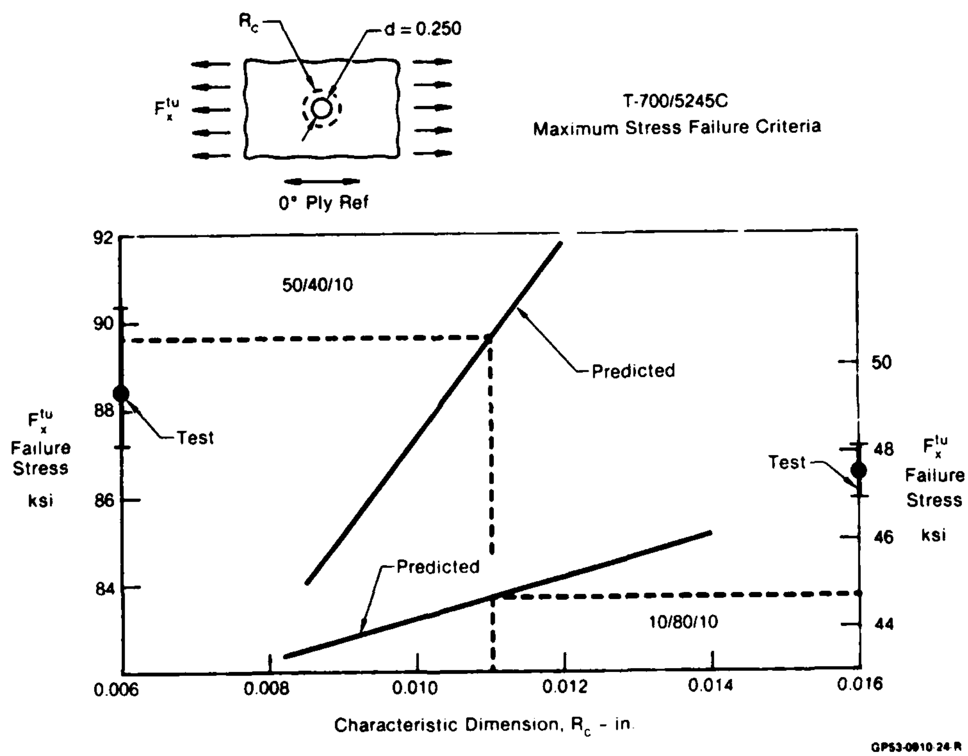

Figure 62. Correlation of Unloaded Hole Static Tension Strength Test Results With Prediction: 5245C Resin System

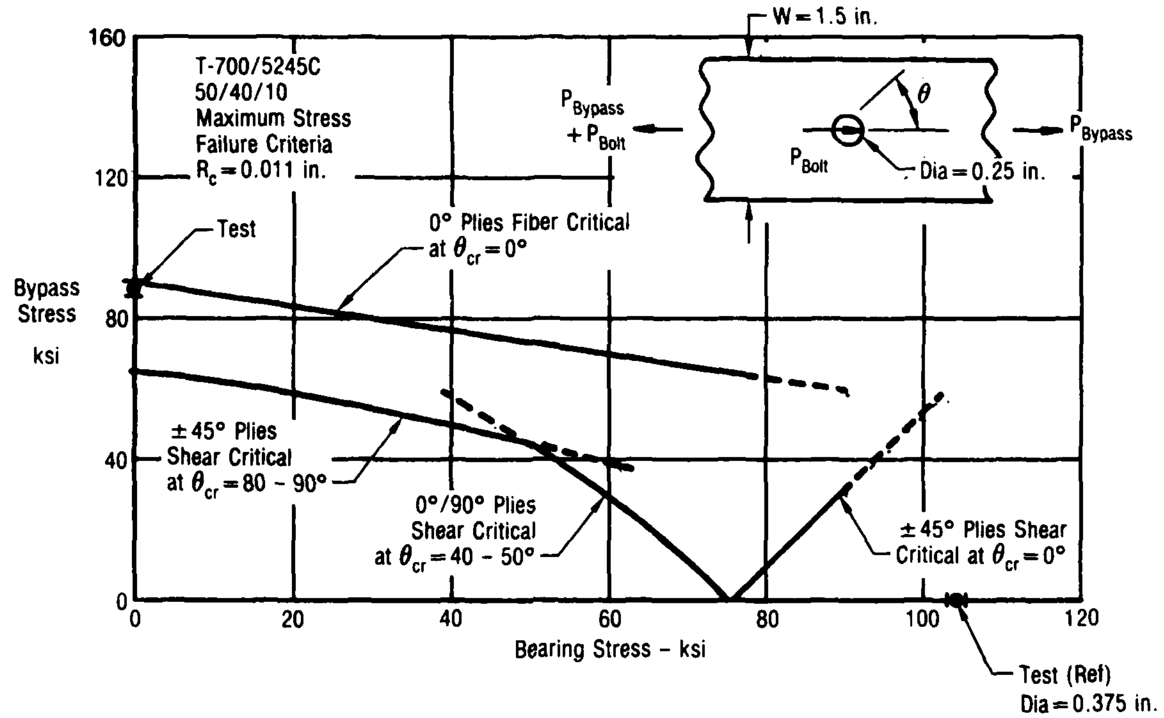

Figure 63. Bearing/Bypass Load Interaction Strength Envelope: 524C Resin System

Correlation of predicted strength with test results for the 50/40/10 layup and Cycom 1808 resin system is shown in Figure 64, based on the maximum stress failure criteria. A characteristic dimension of 0.018 inch was determined for this material.

A summary of unloaded hole static strength theory/test correlations are shown in Figure 65. Results from these studies indicate the characteristic dimension depends on material system, however once the value is determined it can be used to predict strength of arbitrary layups. No consistent advantage in using either the maximum stress or Tsai-Hill failure criteria for predicting unloaded hole tension strength is evidenced by these studies.

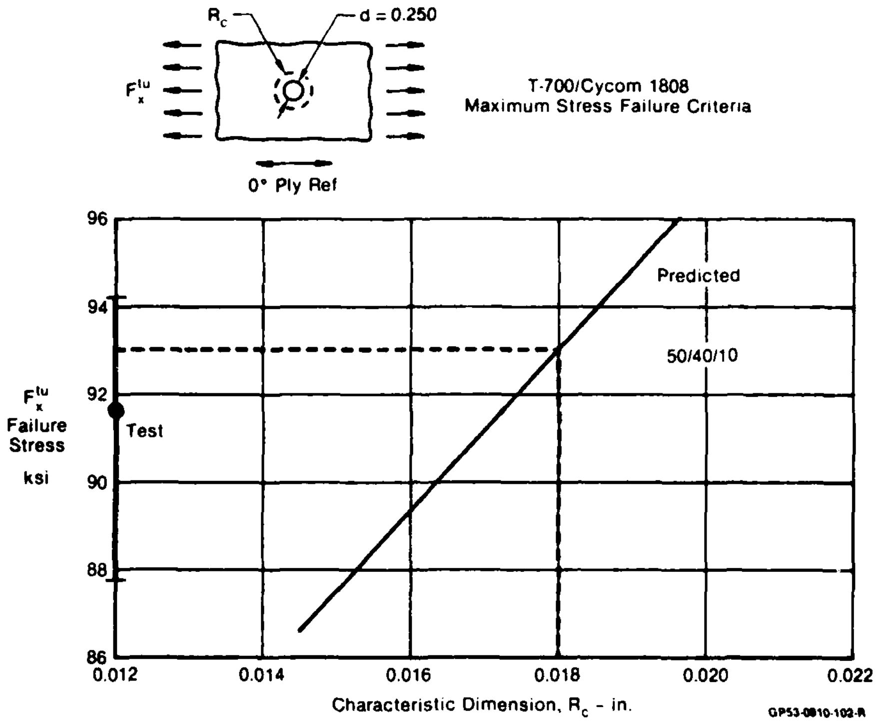

Figure 64. Correlation of Unloaded Hole Static Tension Strength Test Results With Prediction: Cycom 1808 Resin System

Material System	Failure Criteria	Theory/Test Correlation		
		50/40/10 Layup	10/80/10 Layup	
		Characteristic Dimension R_c (in.)	Predicted F_x^{tu} (ksi)	Test F_x^{tu} (ksi)
T-700/Cycom 907	Tsai-Hill	0.062	51.2	51.5
	Maximum Stress	0.023	41.6	
T-700/Cycom 1808	Tsai-Hill	0.093	—	—
	Maximum Stress	0.018		
T-700/5245C	Tsai-Hill	0.093	40.6	47.6
	Maximum Stress	0.011	44.7	

GP53-0810-107-R

Figure 65. Unloaded Hole Tension Strength Theory/Test Correlation Summary

Unloaded hole compression strength test results are summarized in Figure 66; typical failed test specimens are shown in Figure 67. Elevated temperature/wet testing resulted in a strength reduction of 46 percent for the Cycom 1808 resin system; only a 30 percent reduction in strength for the 5245C system was observed.

Resin System	Environment	Layup	Specimen Number	Thickness (inch)	Width (inch)	Hole Diameter (inch)	Failure Load (lb)	Failure Stress (psi) Individual	Failure Stress (psi) Average	Failure Strain (µin/in) Individual	Failure Strain (µin/in) Average	Modulus (msi)
			2-4-27	0.247	1.508	0.250	24,750	78,910		6,780		12.32
Cycom 907	RTD	50/40/10	2-4-28	0.248	1.509	0.250	25,900	82,520	80,160	7,200	7,020	12.49
			2-4-29	0.247	1.508	0.250	24,800	79,070		7,080		12.45
			2-5-11	0.250	1.502	0.250	19,000	60,820		15,150		5.24
	RTD	10/80/10	2-5-12	0.252	1.502	0.250	19,700	63,060	62,100	15,060	15,170	5.17
			2-5-15	0.252	1.502	0.250	19,500	62,420		15,300		5.42
			3-4-48	0.237	1.500	0.250	27,800	90,850		9,380		11.97
Cycom 1808	RTD	50/40/10	3-4-49	0.237	1.500	0.250	27,450	89,710	89,020	8,300	9,210	12.18
			3-4-50	0.237	1.493	0.250	26,350	86,520		9,950		12.16
			3-4-51	0.237	1.501	0.250	14,050	45,880		3,510		13.98
	ETW		3-4-52	0.237	1.492	0.250	13,500	44,350	47,940	3,660	3,590	12.66
			3-4-53	0.237	1.491	0.250	16,300	53,950		6,520		12.69
			4-4-48	0.205	1.505	0.250	23,100	78,310		9,650		11.49
5245C	RTD	50/40/10	4-4-49	0.203	1.505	0.250	22,850	77,460	76,800	8,600	8,830	11.30
			4-4-50	0.205	1.504	0.250	22,000	74,630		8,250		11.60
			4-4-51	0.205	1.509	0.250	16,650	56,300		5,140		12.01
	ETW		4-4-52	0.205	1.508	0.250	16,550	55,990	53,730	7,410	5,630	12.35
			4-4-53	0.205	1.508	0.250	14,450	48,890		4,340		12.06
			4-5-11	0.207	1.507	0.250	16,050	54,300		13,150		4.96
	RTD	10/80/10	4-5-12	0.204	1.508	0.250	16,550	56,030	54,870	13,560	13,100	4.91
			4-5-15	0.205	1.509	0.250	16,050	54,270		12,600		5.00

GP53-0810-87-R

Figure 66. Unloaded Hole Compression Test Results

10/80/10 Layup

Figure 67. Failed Unloaded Hole Compression Test Specimens

Unloaded hole compression strength predictions required evaluating the effect of the installed fastener on laminate stresses. Shown in Figure 68 are predictions of circumferential and radial stresses around a fastener hole for the 50/40/10 layup and Cycom 907 resin system. With a filled fastener hole, pin propping reduces the maximum circumferential stress around the fastener hole. Characteristic dimension values obtained from tension strength theory/test correlation were used for compression strength predictions. As shown in Figure 68, unfilled fastener hole strength predictions correlate well with test results. Manufacturing tolerances allow a maximum of 0.003 inches of clearance, which did not permit support of the fastener hole boundary. Predictions of laminate stresses and strength for the 10/80/10 layup are shown in Figure 69. For this softer laminate, the fastener provided a hole propping effect and strength predictions were within 13 percent of test results.

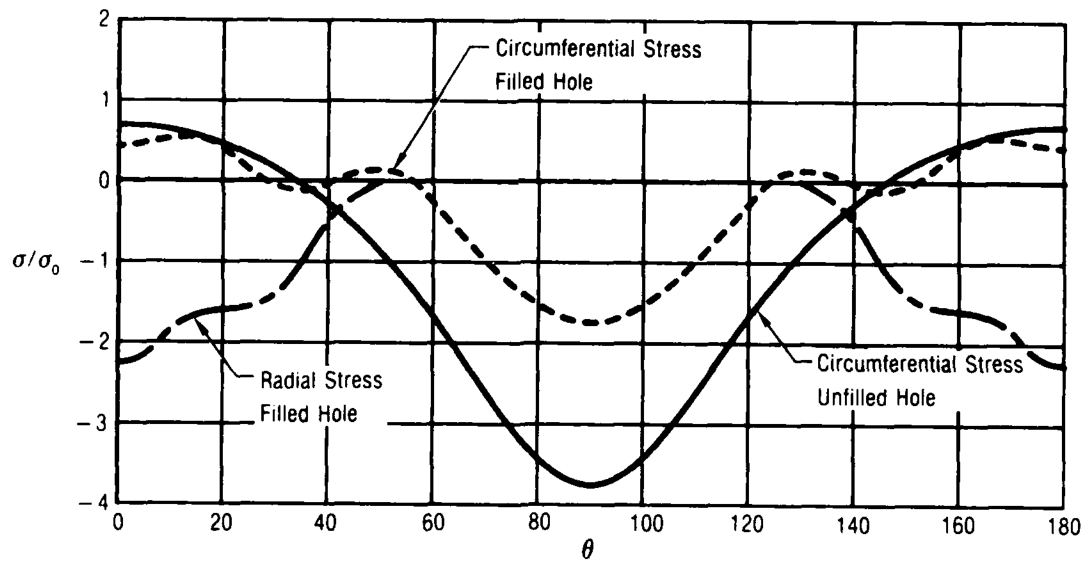

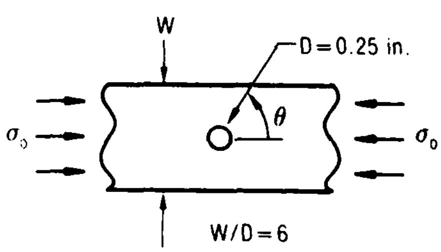

Static Strength (psi)		
Predicted: Tsai-Hill Failure Criteria $R_c = 0.062$ in.		Test
Unfilled Hole	79,500	80,160
Filled Hole	126,100	

GP53-0910-8-R

Figure 68. Correlation of Unloaded Hole Static Compression Strength Test Results With Prediction: 50/40/10 Layup

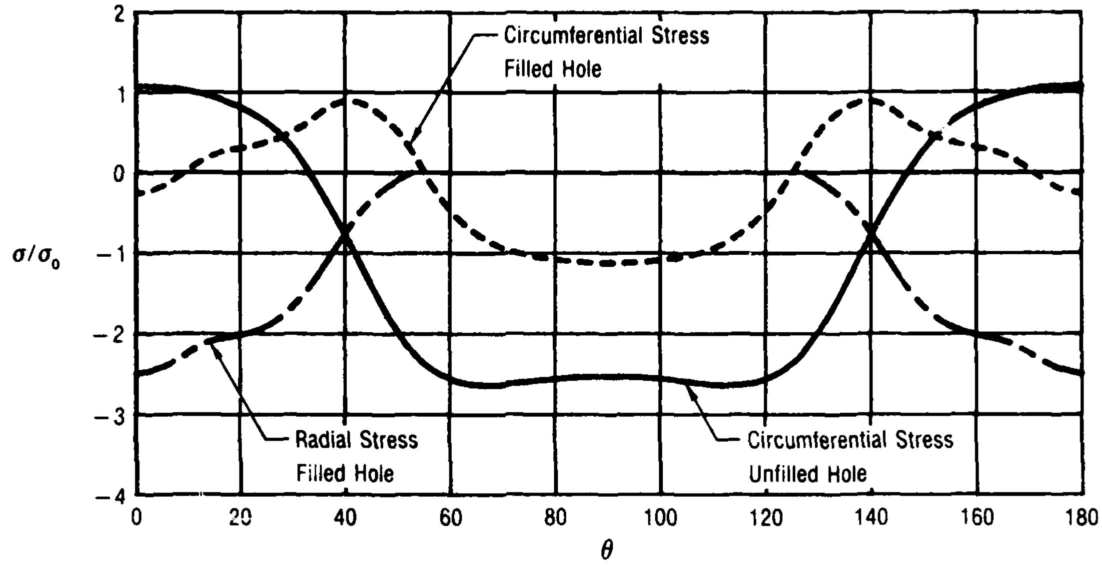

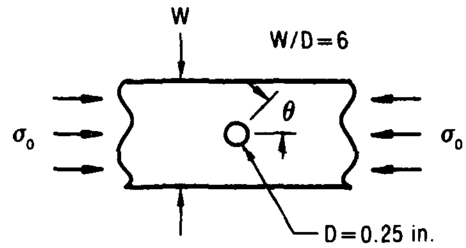

Static Strength (psi)		
	Predicted: Tsai-Hill Failure Criteria $R_c = 0.062$ in.	Test
Unfilled Hole	30,400	62,100
Filled Hole	54,000	

GP53-0910-7-R

Figure 69. Correlation of Unloaded Hole Static Compression Strength Test Results With Prediction: 10/80/10 Layup

The unloaded hole fatigue test specimen is shown in Figure 70. The test objective was to cycle specimens to failure, even though there were instances where high stress levels were required to prevent long lives due to the excellent fatigue characteristics of advanced composites. The common approach of testing to a prespecified life and design limit load, followed by static testing to failure does not identify durability or failure modes, and does not provide data for fatigue life methodology development. Constant amplitude fatigue tests were conducted for the 50/40/10 layup and two stress ratios; tension-compression (R=-1) and compression only (R=-∞). Failure was always catastrophic rupture of the specimen.

Tests were conducted at 5 to 10 cycles per second. Temperatures were maintained at 75°F for the duration of the test by directing refrigerated air on the specimen.

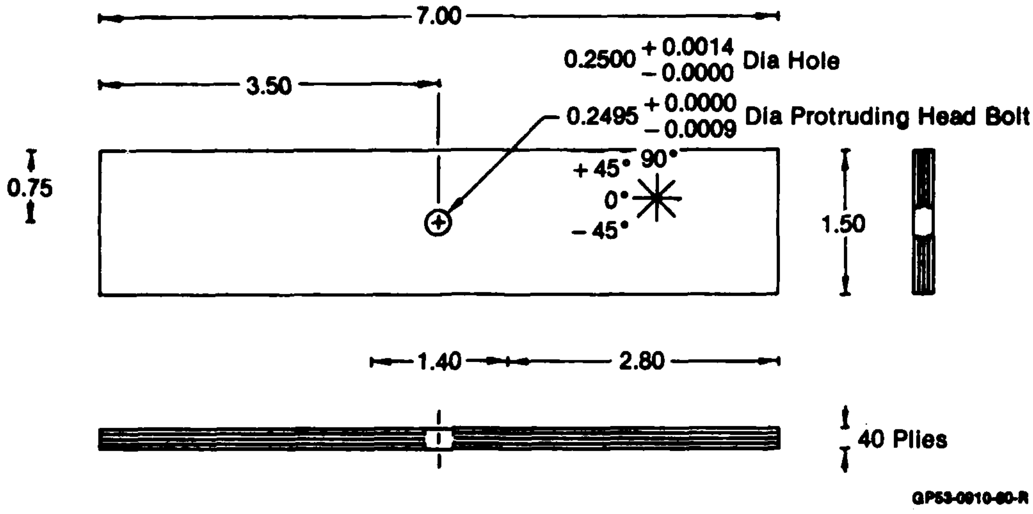

Figure 70. Unloaded Hole Fatigue Test Specimen

Test results are summarized in Figure 71; a typical specimen failure is shown in Figure 72. Fatigue lives under R=-1 constant amplitude fatigue for the three high strain resin systems are shown in Figure 73. Shown for comparison are results for AS-1/3501-6 (Reference 10). The solid symbols in Figure 73 at 1 cycle represent static tension strength; open symbols represent static compression strength. Trend lines are included for each material system. The Cycom 1808 system indicated an order of magnitude improvement in life relative to the baseline 3501-6 resin system.

Resin System	Stress Ratio	Load Level (lb)	Stress Level (ksi)	Specimen Number	Thickness (inch)	Width (inch)	Hole Diameter (inch)	Life (Cycles to Failure)
Cycom 907	-1	22,225	73.5	2-4-3	0.247	1.453	0.250	800
		21,500	68.6	2-4-4	0.245	1.507	0.250	3,430
		18,725	59.6	2-4-9	0.245	1.510	0.250	61,680
				2-4-8	0.245	1.510	0.250	9,310
	-∞	23,625	75.4	2-4-11	0.250	1.509	0.250	260
				2-4-12	0.248	1.504	0.250	380
		23,300	74.3	2-4-13	0.248	1.508	0.250	2,130
		22,500	71.6	2-4-14	0.245	1.511	0.251	1,494,750
Cycom 1808	-1	20,700	67.5	3-4-5	0.242	1.502	0.250	12,600
				3-4-6	0.242	1.504	0.250	24,500
		17,700	57.8	3-4-7	0.241	1.499	0.250	151,000
				3-4-8	0.240	1.502	0.250	113,680
	-∞	24,450	79.8	3-4-17	0.236	1.500	0.250	1,150
				3-4-18	0.237	1.504	0.250	1,040
		22,800	74.4	3-4-19	0.238	1.503	0.250	1,630
				3-4-20	0.237	1.503	0.250	1,520
5245C	-1	18,900	62.9	4-4-5	0.207	1.533	0.250	23,580
				4-4-6	0.208	1.531	0.250	15,160
		16,350	54.8	4-4-7	0.208	1.522	0.250	82,400
				4-4-8	0.205	1.522	0.250	40,190
	-∞	21,150	71.0	4-4-17	0.205	1.521	0.249	86,040
				4-4-18	0.205	1.520	0.250	3,370
		20,250	68.3	4-4-19	0.208	1.520	0.250	207,490
				4-4-20	0.208	1.504	0.250	11,620

GP53-0910-85-R

Figure 71. Unloaded Hole Fatigue Test Results Summary

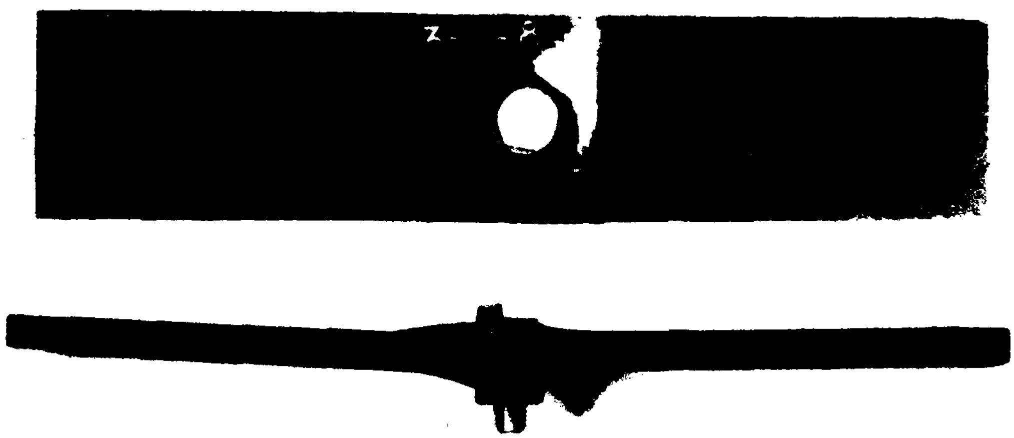

GP53-0910-39-R

Figure 72. Failed Unloaded Hole Fatigue Test Specimen

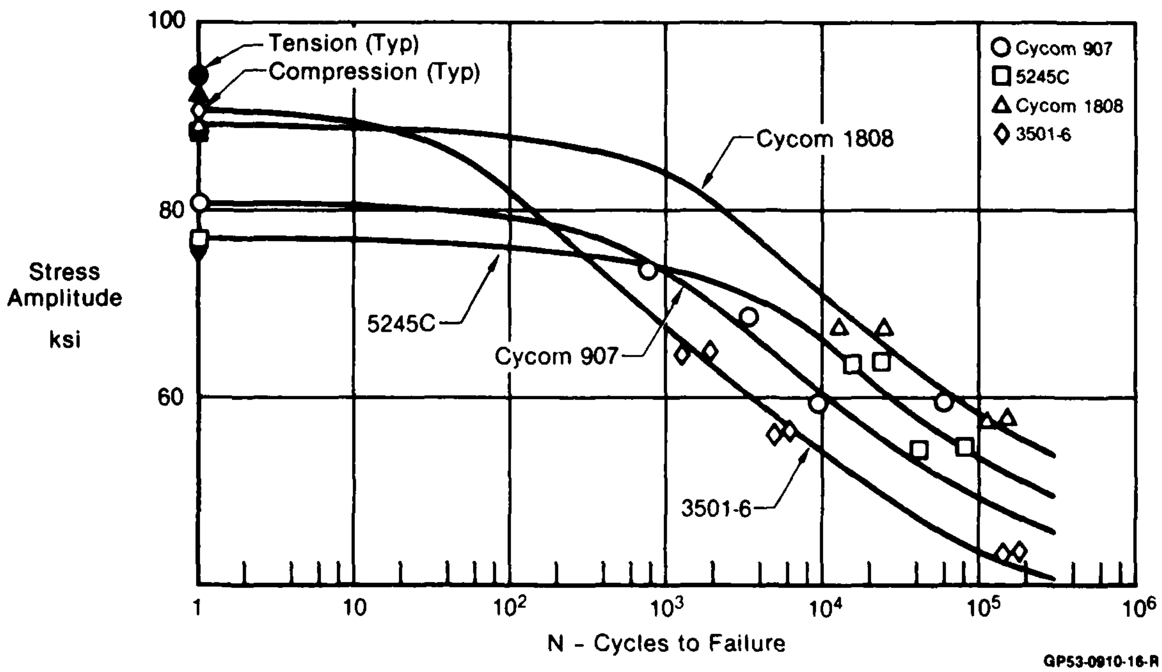

GP53-0910-16-R

Figure 73. Unloaded Hole Fatigue Test Results: R = −1

Selected specimens were examined nondestructively by X-ray photography to observe the type and location of damage during different stages of fatigue life. Figure 74 contains photographs of a specimen fabricated with the 5245C resin system. Examination of fatigue damage was conducted at one-quarter and one-half of expected life. Matrix cracking in the 90° ply can be seen by fine horizontal lines; cracks in the 0° ply can be seen by vertical lines; ±45° ply cracking can also be observed. The white areas are ply delamination zones. Generally, initial damage was matrix cracking at the hole boundary which grew rapidly along the fibers. This was followed by extensive delamination in areas which had accumulated extensive matrix cracking. Matrix cracking and delamination interacted to reduce matrix support and produce eventual crushing of the test section through the hole under compression load. The behavior is similar to that observed for the baseline 3501-6 resin system (Reference 11).

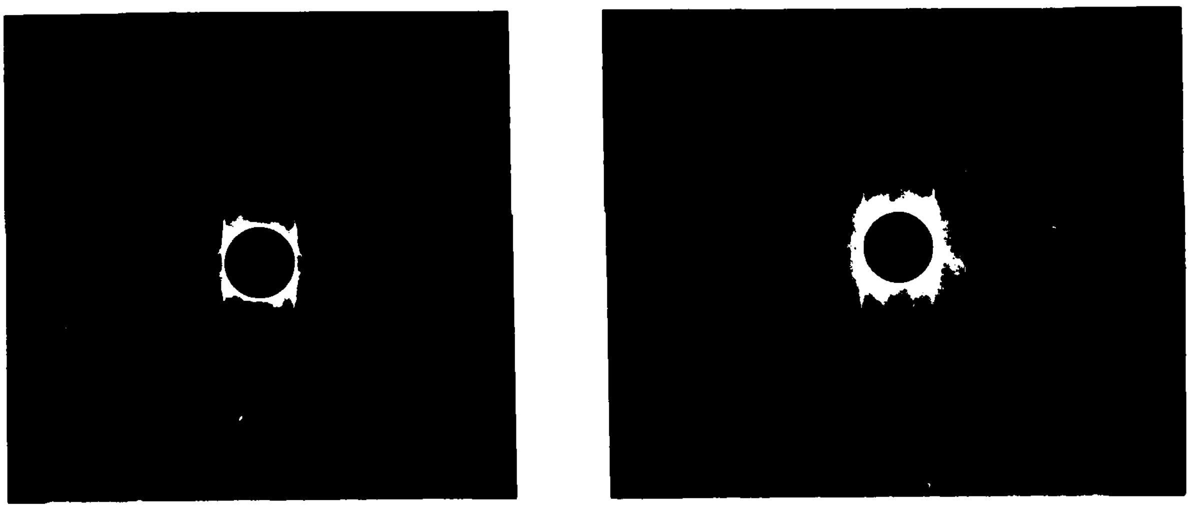

Quarter Life
(4,840 Cycles)

Half Life
(9,680 Cycles)

Specimen 4-4-9
T-700/5245C
50/40/10 Layup
R = −1
83% F_{cu}; 69% F_{tu}

GP53-0910-41-R

Figure 74. X-Ray Photographs Showing Progression of Cracking and Delamination

Test results for compression only fatigue are shown in Figure 75. Stress amplitudes in excess of 90 percent of static strength were required to obtain specimen failures. Life scatter was greater than that for reversed loading tests.

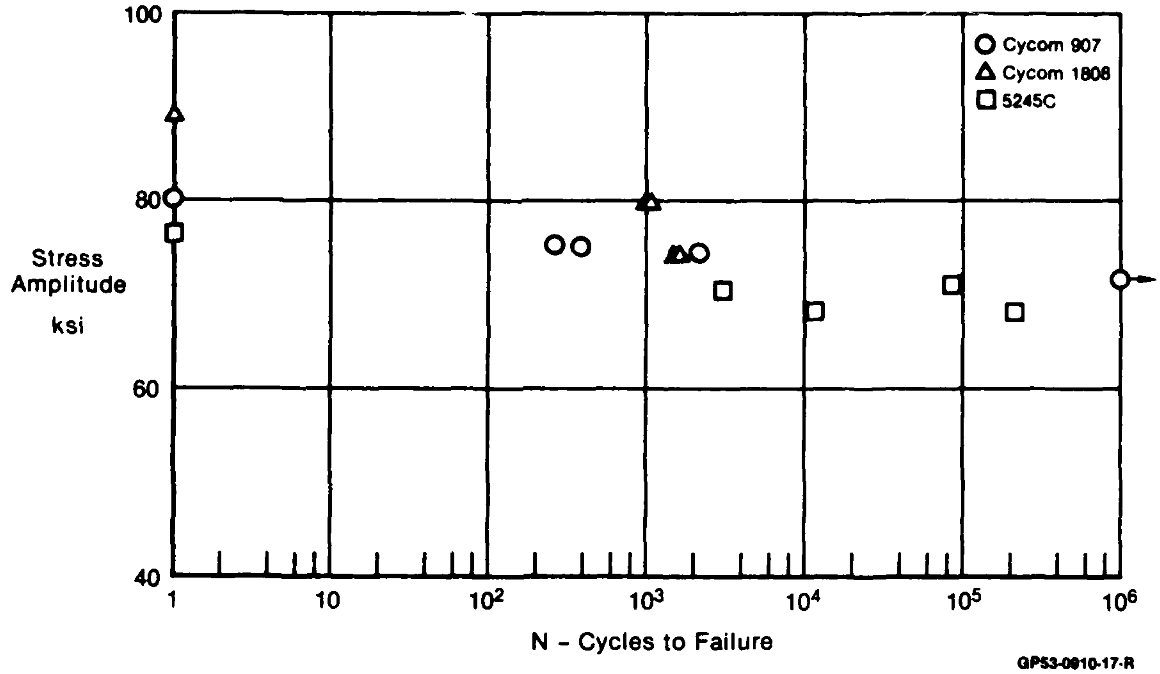

Figure 75. Unloaded Hole Fatigue Test Results: $R = -\infty$

c. <u>Loaded Hole: Static and Fatigue</u> - Pure bearing tests were conducted using the specimen shown in Figure 76; the pure bearing specimen test setup is shown in Figure 77. With this setup, the bearing load is introduced in double shear to obtain uniform bearing stress through-the-thickness of the laminate. Straight shank steel pins were installed with no torque-up to avoid introducing transverse normal forces on the laminate.

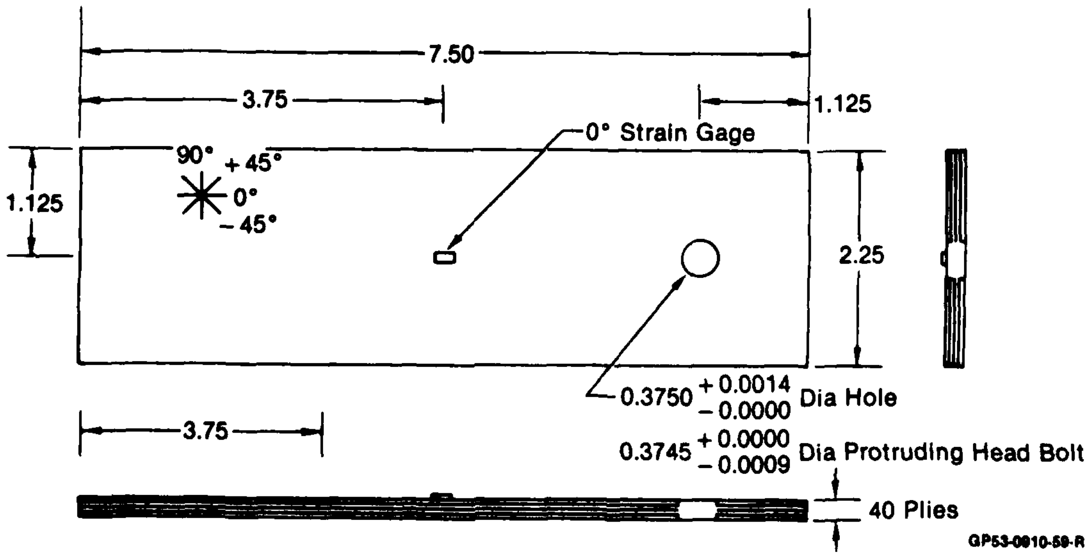

Figure 76. Pure Bearing Test Specimen

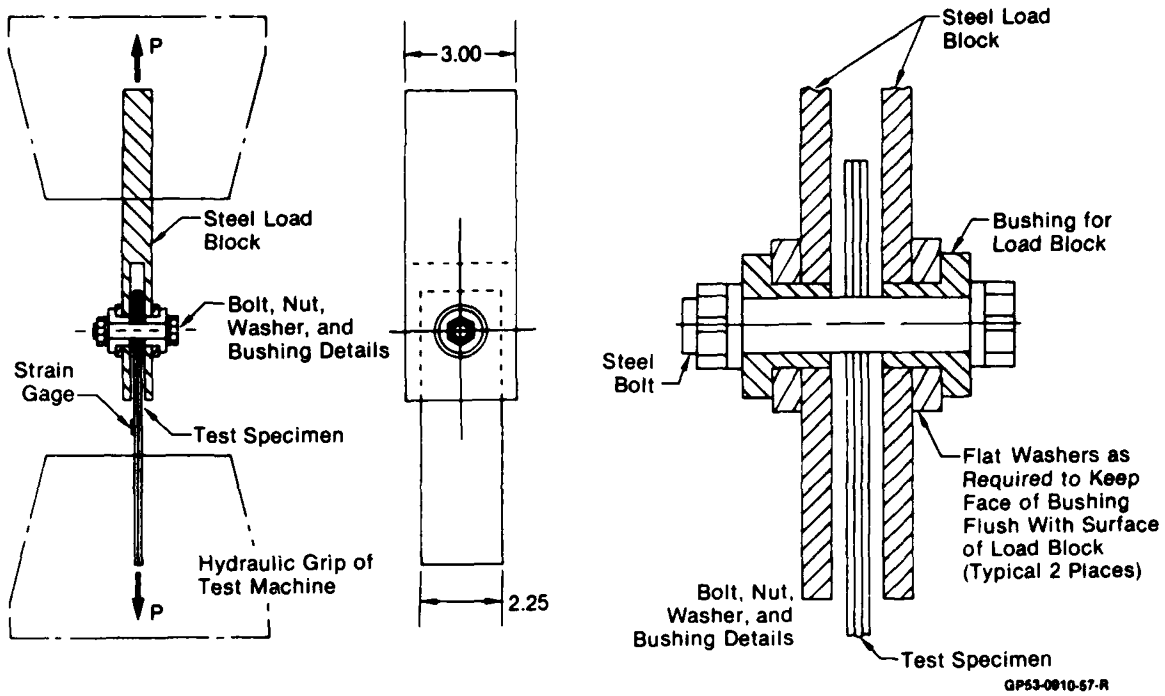

Figure 77. Pure Bearing Specimen Test Setup

Test results are summarized in Figure 78; a typical specimen failure is shown in Figure 79. In all cases, failure was localized crushing of the laminate directly in front of the fastener. Layup and material system had little effect on strength. Elevated temperature/wet test conditions reduced laminate bearing strength by 29 percent for Cycom 1808 and 38 percent for 5245C.

Resin System	Environment	Layup	Specimen Number	Thickness (inch)	Width (inch)	Hole Diameter (inch)	Failure Load (lb)	Bearing Stress at Failure (psi)		Failure Strain (μin/in)		Modulus (msi)
								Individual	Average	Individual	Average	
			2-4-30	0.246	2.258	0.375	7,770	99,620		1,320		12.95
Cycom 907	RTD	50/40/10	2-4-31	0.245	2.261	0.375	7,910	101,920	102,220	1,300	1,330	13.19
			2-4-32	0.245	2.261	0.375	8,200	105,130		1,370		12.90
			2-5-23	0.252	2.259	0.375	7,700	98,660		3,130		5.31
	RTD	10/80/10	2-5-24	0.251	2.259	0.375	7,750	99,360	99,760	3,110	3,150	5.37
			2-5-25	0.253	2.261	0.375	7,900	101,280		3,200		5.31
			3-4-1	0.238	2.254	0.375	7,900	103,200		1,340		12.74
Cycom 1808	RTD	50/40/10	3-4-2	0.252	2.250	0.375	7,450	97,390	100,090	1,250	1,300	13.05
			3-4-3	0.252	2.255	0.375	7,630	99,670		1,300		13.28
			3-4-4	0.238	2.252	0.375	5,830	76,210		960		13.15
	ETW		3-4-13	0.239	2.254	0.375	5,540	72,160	71,290	960	920	12.71
			3-4-14	0.247	2.253	0.375	5,020	65,490		820		13.23
			4-1-1	0.208	2.257	0.375	7,660	104,220		1,230		13.05
5245C	RTD	50/40/10	4-1-2	0.204	2.258	0.375	7,750	105,440	104,290	1,310	1,260	13.35
			4-1-3	0.205	2.256	0.375	7,590	103,200		1,250		12.56
			4-4-4	0.222	2.256	0.375	3,960	53,880		710		13.15
	ETW		4-4-13	0.210	2.256	0.375	4,670	63,540	64,670	730	760	14.17
			4-4-14	0.210	2.257	0.375	2,260	76,600		840		14.68
			4-5-23	0.209	2.254	0.375	6,900	93,880		2,980		5.24
	RTD	10/80/10	4-5-24	0.206	2.259	0.375	6,980	94,900	92,290	2,470	2,720	5.37
			4-5-25	0.206	2.237	0.375	6,480	88,100		2,700		5.29

GP53-0910-86-R

Figure 78. Pure Bearing Test Results

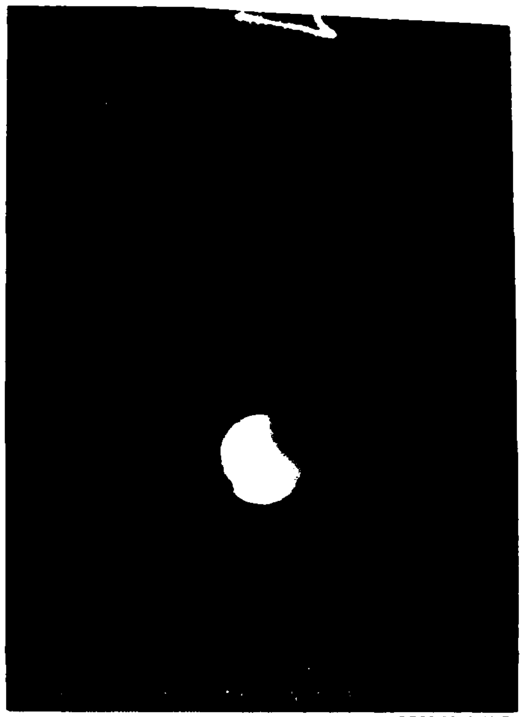

GP53-0910-40-R

Figure 79. Failed Pure Bearing Test Specimen

Strength predictions for both the 50/40/10 and 10/80/10 layups with the Cycom 907 resin system are shown in Figure 80. The characteristic dimension was selected from theory/test correlations of unloaded hole tension strength. Predictions were made using the Tsai-Hill failure criteria; failure ratios given in Figure 80 indicate the relative contribution of each stress component in overall ply failure. For both layups, initial ply failures were predicted well below ultimate, primarily as fiber compression failure. This failure is not catastrophic, resulting only in a local redistribution of bearing stresses. Predicted ultimate strength of the 50/40/10 layup is within 7 percent of test, primarily as matrix compression directly in front of the bearing area. Predicted ultimate strength of the 10/80/10 layup is within 14 percent of test, with failure predominately as matrix shear. Conservatism in predicted strength reflects the conservatism in intralaminar shear strength allowables and due to the local redistribution of bearing stress during material failure.

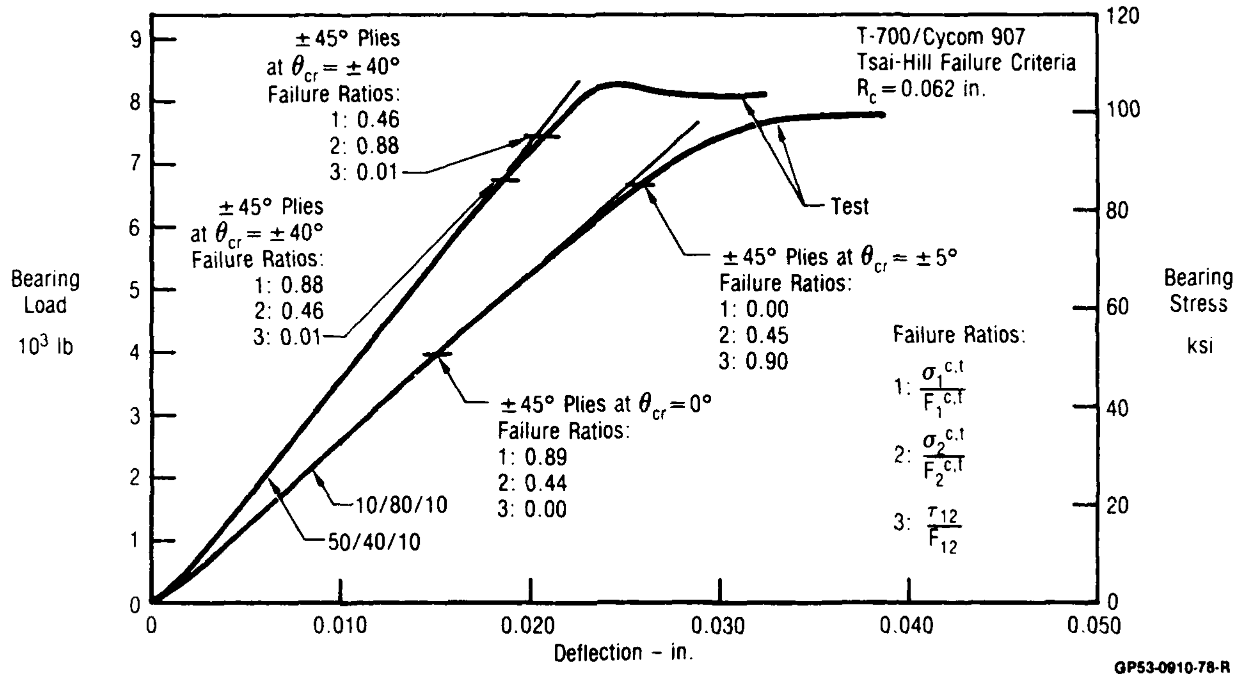

Figure 80. Correlation of Pure Bearing Static Test Results With Predictions

Constant amplitude fatigue tests were conducted for each of the three high strain resin systems using the fiber dominated 50/40/10 layup. Two stress ratios were used: tension-compression (R=-1) and compression only (R=-∞). Specimens were cycled until a total accumulation of 0.02 inch hole elongation was reached. Stiffness and deflection was monitored periodically during test using the set-up shown in Figure 81. Hole elongation measurements were obtained using the data reduction procedures shown in Figure 82. Typical accumulation of hole elongation with fatigue cycling is shown in Figure 83. For much of the specimen life, little or no hole elongation is observed until there is a rapid increase near the end of life.

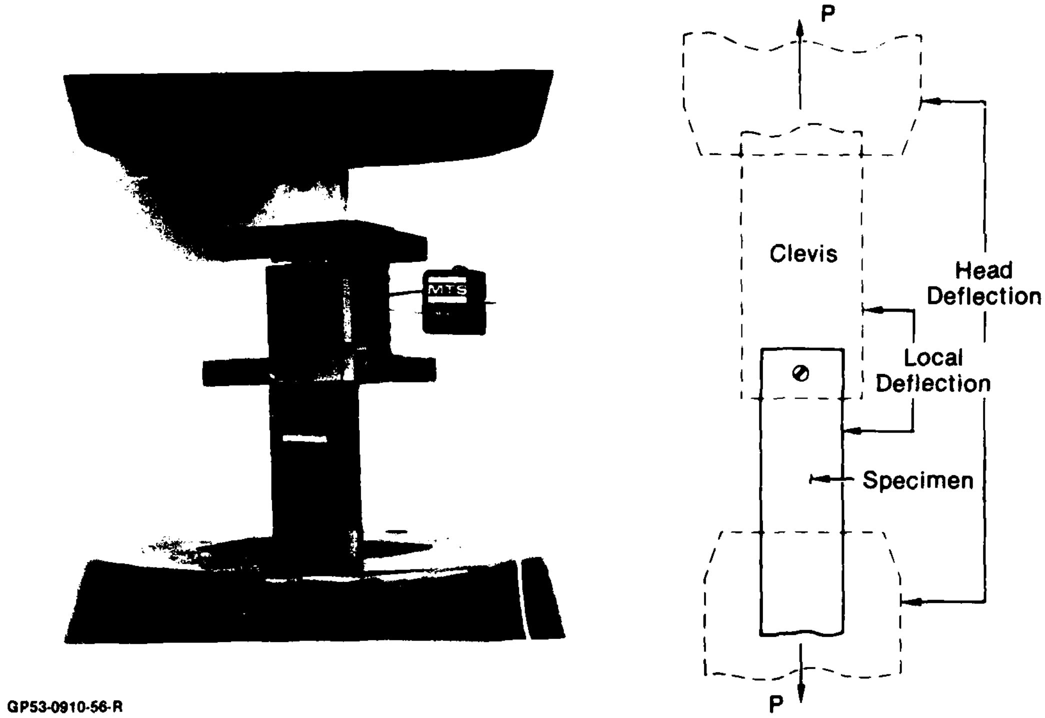

Figure 81. Joint Load-Deflection Test Set-Up

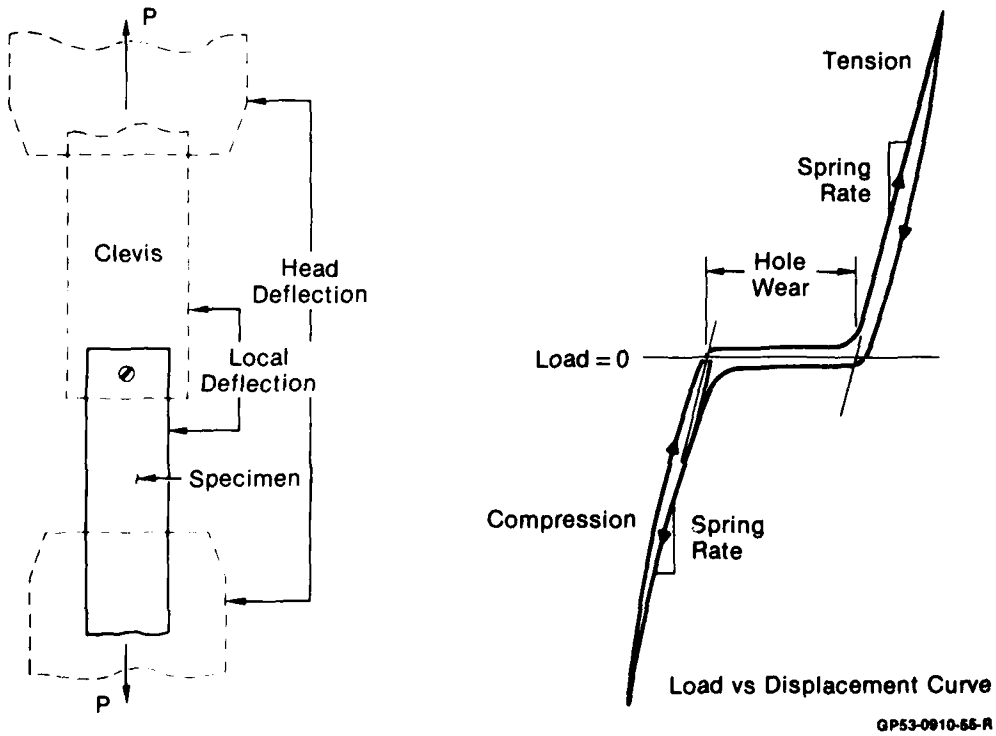

Figure 82. Hole Deformation and Joint Flexibility Monitoring

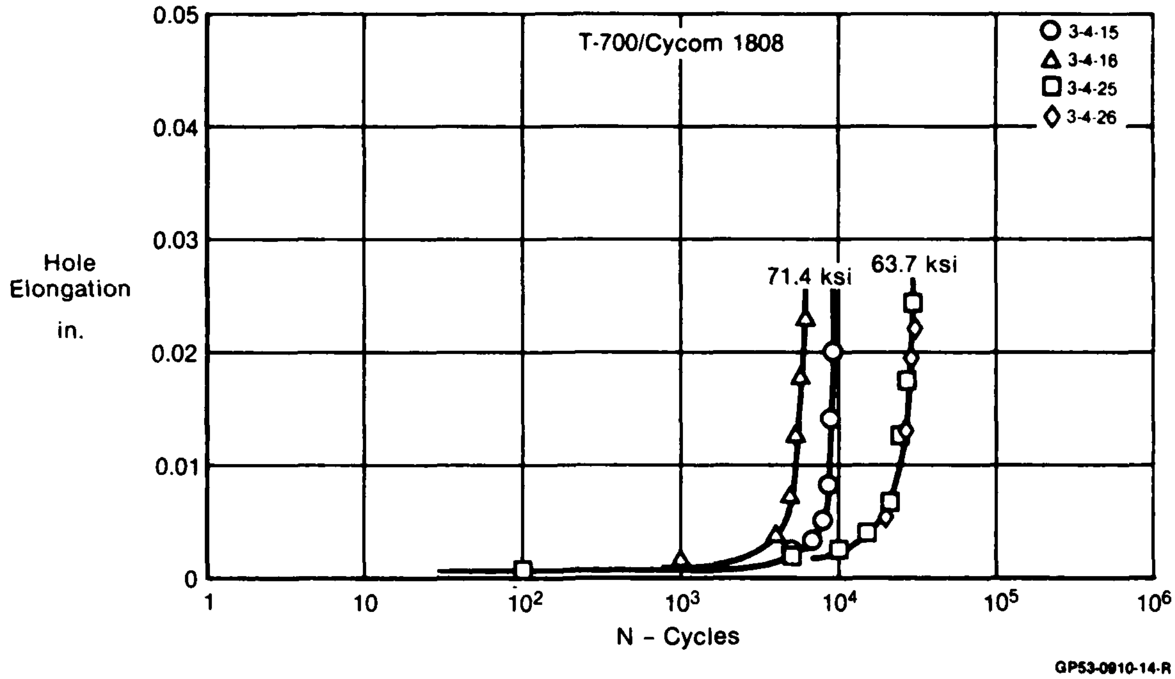

Figure 83. Pure Bearing Fatigue Hole Elongation Measurements: R = −1

Pure bearing fatigue tests are summarized in Figure 84. Specimen failures were similar to a static pure bearing failure. Material stress-life test results for R=-1 fatigue are shown in Figure 85. Test results demonstrate improvement with Cycom 1808 and Cycom 907 over the 3501-6 system. The 5245C system demonstrated reduced fatigue lifes. For all resin systems, the accumulation of hole elongation followed the behavior shown in Figure 83.

Resin System	Stress Ratio	Load Level (lb)	Bearing Stress (ksi)	Specimen Number	Thickness (inch)	Width (inch)	Hole Diameter (inch)	Number of Cycles	Hole Elongation (inch)
Cycom 907	-1	5,460	70.0	2-4-33	0.247	2.259	0.375	12,000	0.0217
				2-4-34	0.249	2.260	0.375	18,600	0.0196
		6,630	85.0	2-4-35	0.245	2.260	0.375	780	0.0200
				2-4-36	0.244	2.259	0.375	500	0.0198
	--	6,240	80.0	2-4-37	0.243	2.257	0.375	250,000	0.02?1
				2-4-38	0.243	2.260	0.375	120,000	0.0183
		7,200	92.3	2-4-39	0.245	2.255	0.375	190,000	0.0183
		7,500	96.2	2-4-40	0.245	2.258	0.375	5,000	0.0149
Cycom 1808	-1	5,460	71.4	3-4-15	0.236	2.253	0.375	9,380	0.0200
				3-4-16	0.238	2.256	0.375	6,220	0.0228
		4,875	63.7	3-4-25	0.237	2.255	0.375	29,840	0.0241
				3-4-26	0.238	2.252	0.375	30,000	0.0222
	--	6,240	81.6	3-4-27	0.237	2.255	0.375	25,000	0.0196
				3-4-28	0.240	2.255	0.375	70,000	0.0186
		6,630	86.7	3-4-43	0.2?9	2.255	0.375	55,000	0.0187
		7,200	94.1	3-4-44	0.240	2.253	0.375	10,000	0.0198
5245C	-1	5,460	74.3	4-4-15	0.206	2.256	0.375	770	0.0222
				4-4-16	0.205	2.258	0.375	1,010	0.0364
		4,680	63.7	4-4-25	0.206	2.256	0.375	6,470	0.0277
				4-4-26	0.205	2.257	0.375	6,340	0.0227
	--	6,240	84.9	4-4-27	0.205	2.255	0.375	260	0.0425
				4-4-28	0.205	2.258	0.375	130	0.0209
		4,680	63.7	4-4-43	0.204	2.256	0.375	33,910	0.0193
				4-4-44	0.207	2.253	0.375	148,110	0.0219

GP53-0810-84-R

Figure 84. Pure Bearing Fatigue Test Results Summary

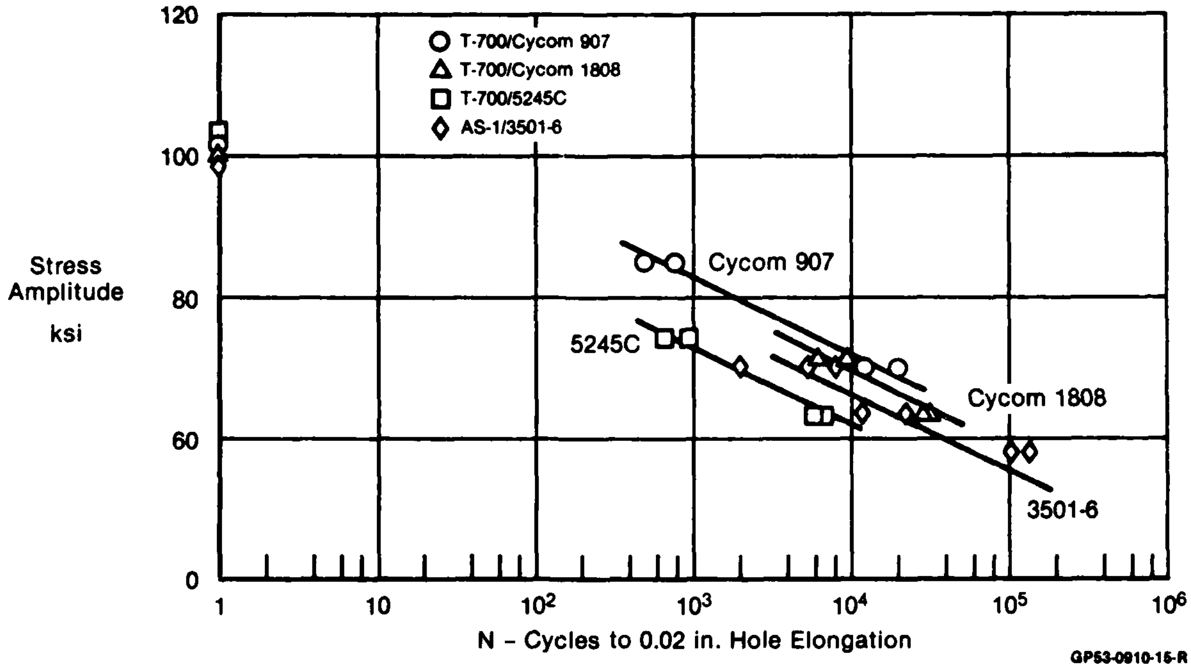

Figure 85. Pure Bearing Fatigue Test Results: R = −1

Compression only fatigue (R=-∞) test results are shown in Figure 86. Cycom 1808 and Cycom 907 resin systems demonstrated similar fatigue lives, with the 5245C system having significantly less life. Accumulation of hole elongation with fatigue for both the Cycom 1808 and Cycom 907 resin systems was gradual as shown in Figure 87. Conversely, the 5245C system exhibited little or no hole elongation up to the point of rapid accumulation, as shown in Figure 88.

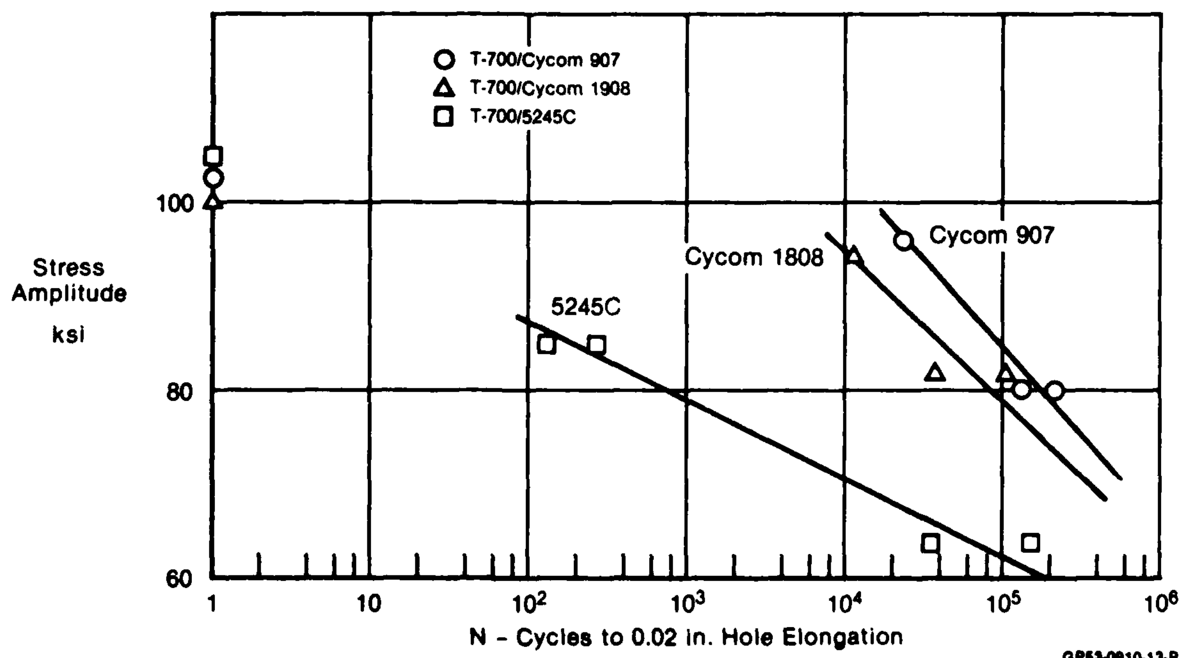

Figure 86. Pure Bearing Fatigue Test Results: R = − ∞

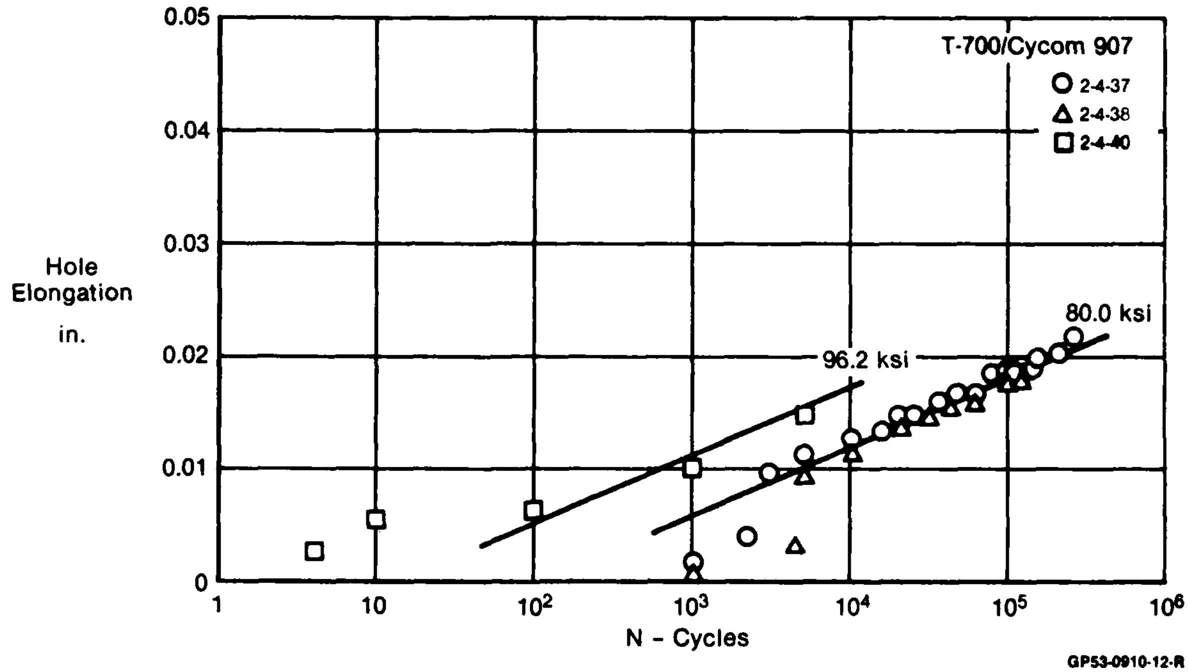

Figure 87. Pure Bearing Fatigue Hole Elongation Measurements: Cycom 907 Resin System

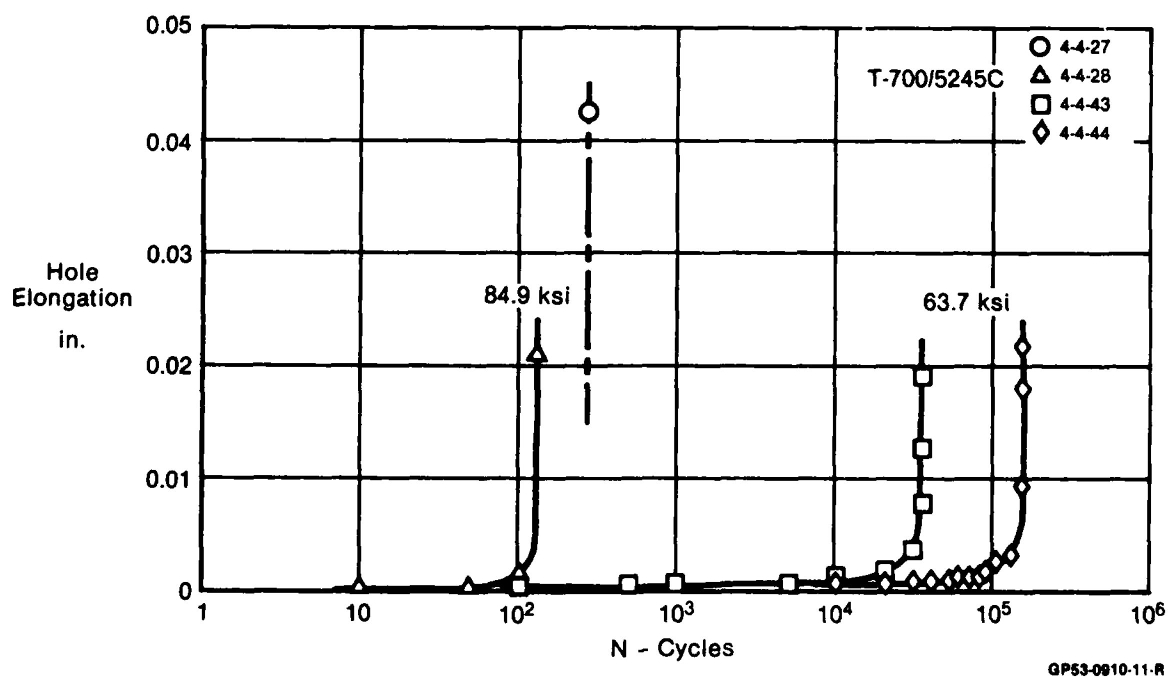

Figure 88. Pure Bearing Fatigue Hole Elongation Measurements: 5245C Resin System

d. <u>Low Energy Impact</u> - Low energy impact damage tolerance tests were performed for each of the three tough resin systems using the specimen configuration shown in Figure 89. Damage tolerance was evaluated nondestructively to determine damage size, and then evaluated on the basis of compression strength after impact. The impact arrangement is shown in Figure 90, in which a rigid picture frame was clamped to the specimen leaving a 3 inch square impact area. An impact energy level of 13 ft-lb was used for all tests.

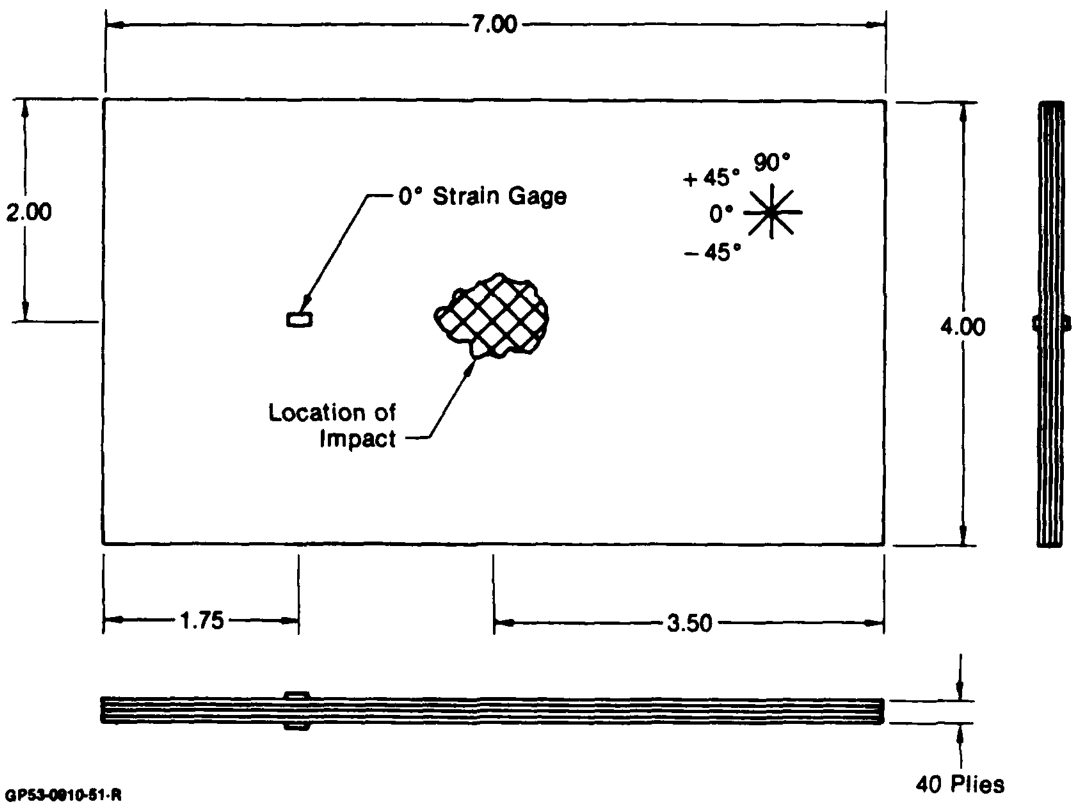

Figure 89. Compression Strength After Impact Test Specimen

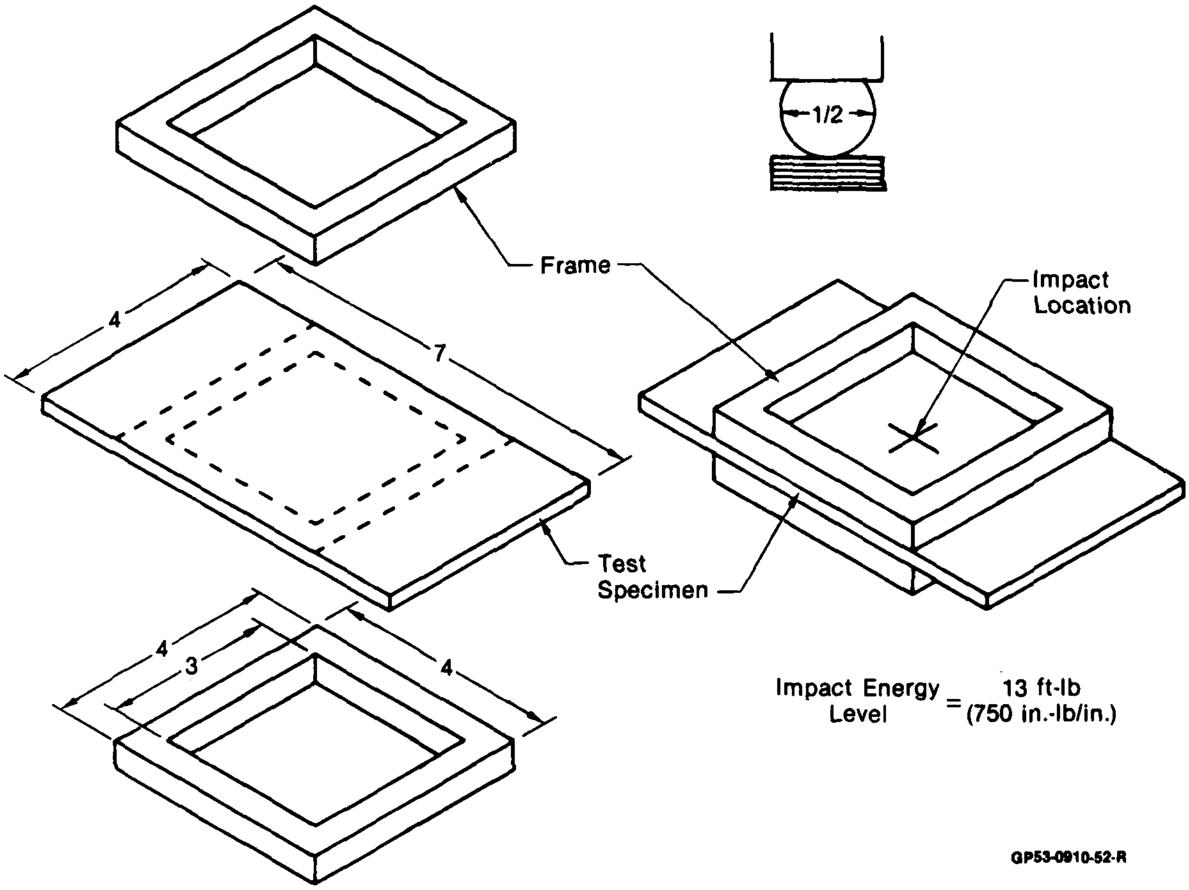

Figure 90. Low Energy Impact Test Arrangement

The C-scan damage size after impact for the 50/40/10 layup is shown in Figure 91 and for the 10/80/10 layup in Figure 92. The Cycom 907 system demonstrated the best tolerance to low energy impact as anticipated. Damage size for the Cycom 1808 and 5245C resin systems was practically the same.

Compression strength after impact was determined using the test arrangement shown in Figure 93; test results are shown in Figure 94. Back-to-back strain gages were averaged to tabulate failing strain. Test specimen failure, shown in Figure 95, occurred directly through the impact damage area.

A comparison of compression strength after impact is shown in Figure 96. Both the Cycom 1808 and 5245C resin systems demonstrated approximately a 60 percent reduction in compression strength after impact while reduction for the Cycom 907 system was approximately 30 percent.

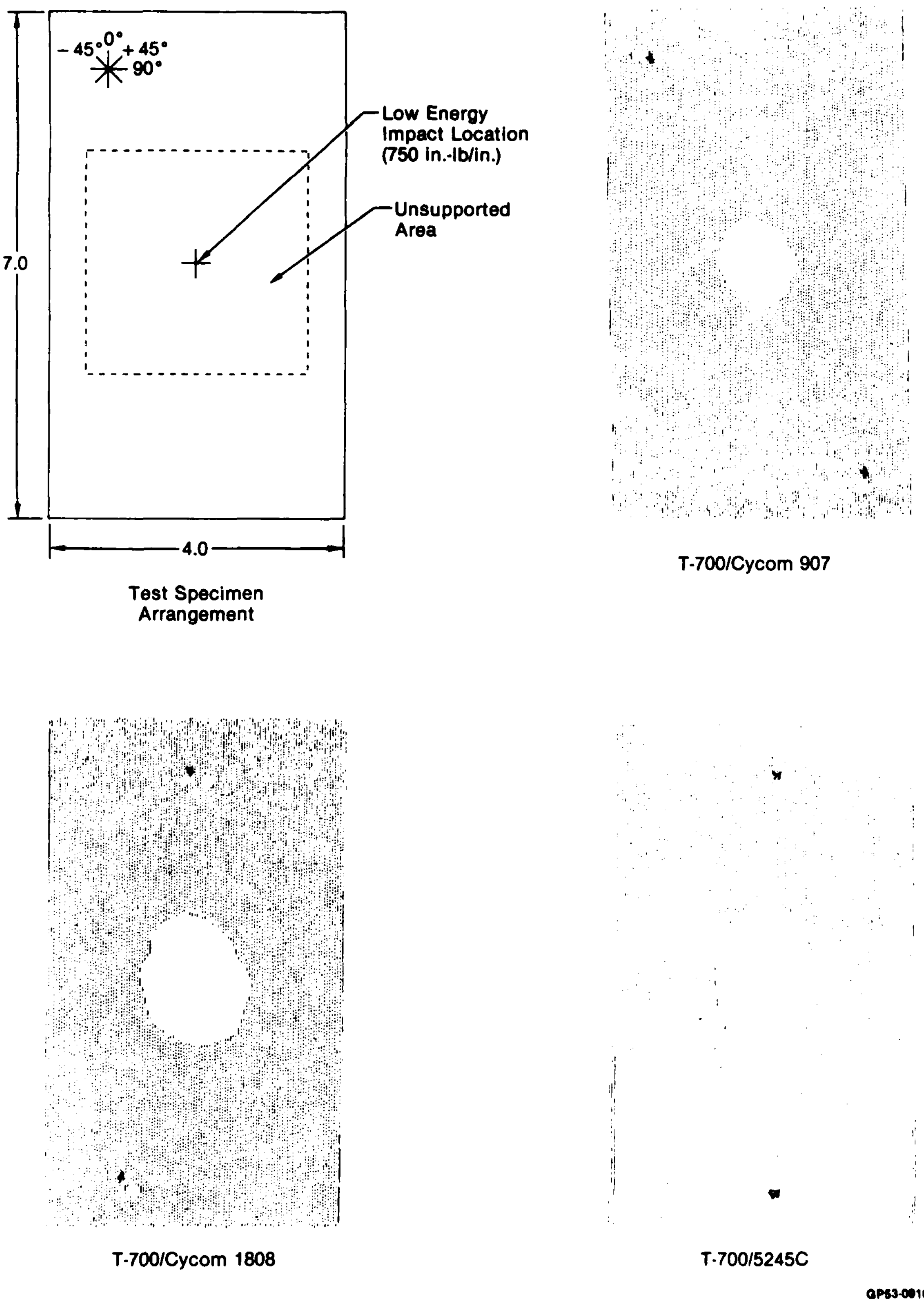

Figure 91. Low Energy Impact Damage: 50/40/10 Layup

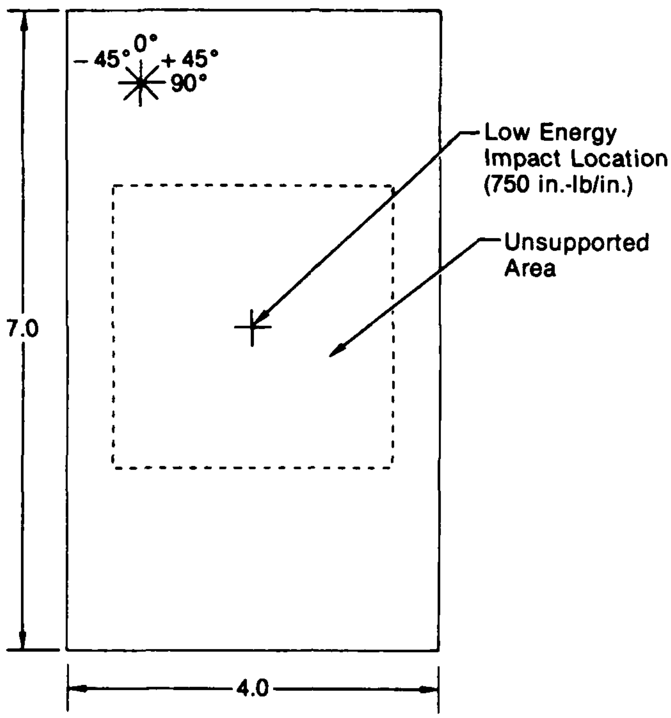

Test Specimen Arrangement

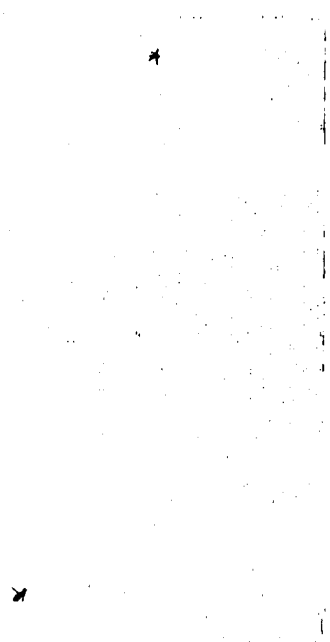

T-700/Cycom 907

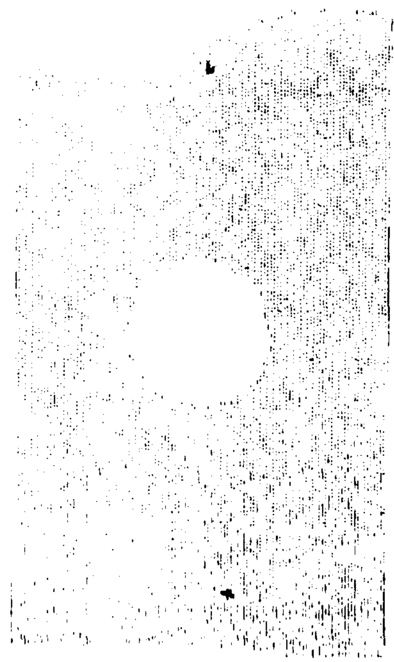

T-700/5245C

GP53-0810-77-R

Figure 92. Low Energy Impact Damage: 10/80/10 Layup

Figure 93. Residual Compression Strength After Impact Test Arrangement

Resin System	Layup	Specimen Number	Thickness (inch)	Width (inch)	Failure Load (lb)	Failure Stress (ksi) Individual	Failure Stress (ksi) Average	Failure Strain (uin/in) Individual	Failure Strain (uin/in) Average	Modulus (msi) Individual	Modulus (msi) Average
		2-4-1	0.244	3.971	57,050	69.1		5,940		12.16	
Cycom 907	50/40/10	2-4-6	0.248	4.010	-	-	70.1	-	5,970	-	12.17
		2-4-16	0.244	4.001	59,110	71.0		5,990		12.19	
		2-5-6	0.249	4.006	46,090	55.3		14,010		4.91	
	10/80/10	2-5-8	0.249	4.007	43,930	52.7	54.7	11,650	12,720	5.22	5.08
		2-5-14	0.250	4.005	46,680	56.0		12,450		5.10	
		3-4-12	0.241	4.006	39,250	48.0		3,560		12.38	
Cycom 1808	50/40/10	3-4-24	0.236	4.006	37,720	46.2	46.9	3,710	3,660	12.17	12.34
		3-4-36	0.238	4.004	37,920	46.4		3,170		12.47	
		4-4-12	0.203	4.003	34,430	43.9		4,010		11.20	
5245C	50/40/10	4-4-12	0.205	4.004	36,110	46.0	44.0	3,740	3,760	11.70	11.68
		4-4-36	0.202	3.995	32,900	42.0		3,530		12.13	
		4-5-1	0.208	4.005	25,810	32.9		6,940		4.71	
	10/80/10	4-5-6	0.206	4.002	24,810	31.6	32.2	6,550	6,660	4.92	4.90
		4-5-8	0.199	4.000	25,040	32.0		6,480		5.08	

Specimen Number 2-4-6 failed in the grip area

GP53-0910-83-H

Figure 94. Compression Strength After Impact Test Results

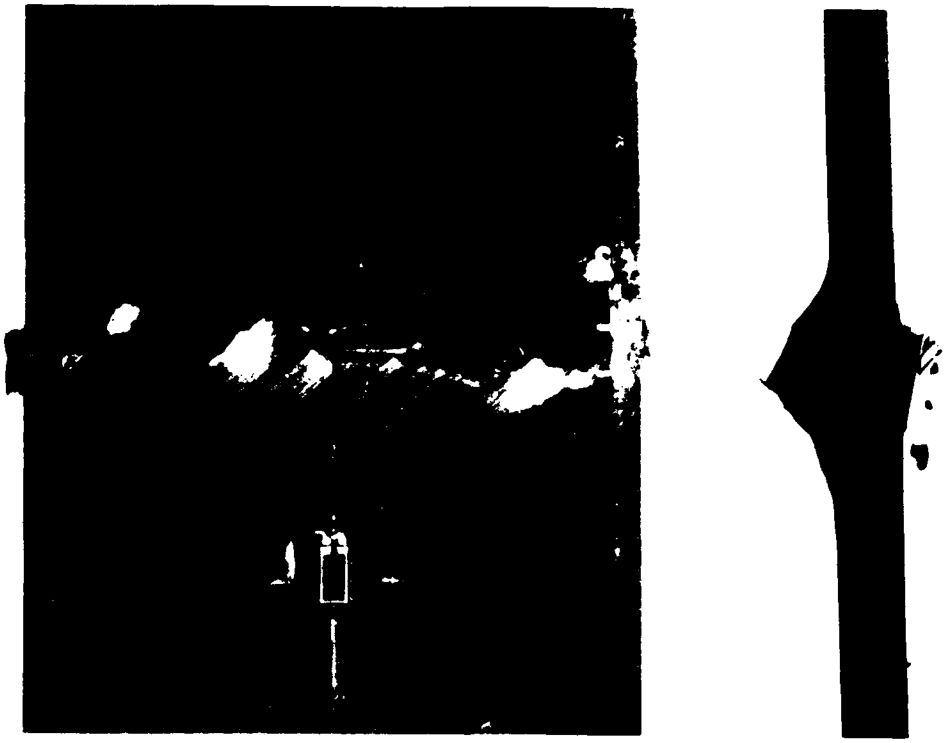

Figure 95. Failed Compression Strength After Impact Test Specimen

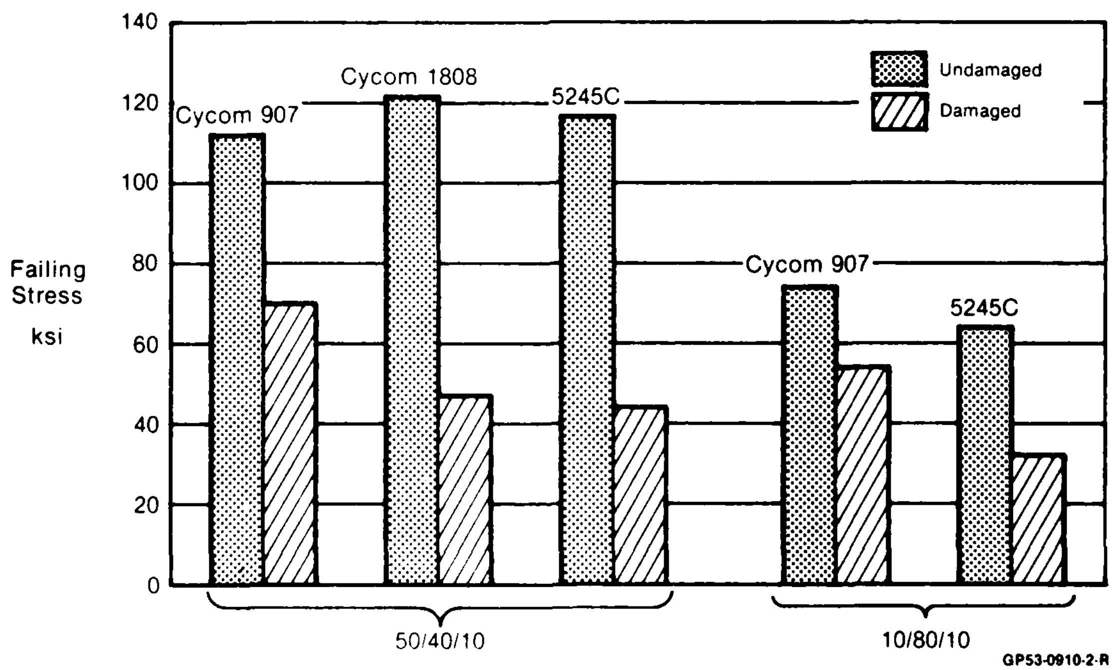

Figure 96. Laminate Compression Strength With and Without Low Energy Impact Damage

5. MULTIFASTENER COMPOSITE-TO-METAL JOINT - Static tests were conducted for a three fastener metal-to-composite splice joint to demonstrate analytic capabilities for predicting fastener load distributions and laminate strength under combined bearing and bypass loadings. Only the Cycom 907 and Cycom 1808 systems were used in this series of tests. The test specimen used in this evaluation is shown in Figure 97, for which a data base on AS-1/3501-6 currently exists (Reference 2). This tapered specimen utilizes three countersunk 0.375 inch diameter in line fasteners to transfer load from a stiff steel loading block to the composite test coupon. The tapered joint was designed to distribute load between fasteners. The taper of the composite coupon was achieved by dropping selected plies along the length; laminate stacking and drop-off sequence is shown in Figure 98. A layup of 50/40/10 was approximately maintained throughout the specimen.

Static tension test results are shown in Figure 99. No significant difference was observed in strength or mode of failure between resin systems. A typical failed specimen is shown in Figure 100. Failure was net section at the fastener location with highest bypass stress.

A bearing/bypass strength envelope for T-700/Cycom 1808 is shown in Figure 101. The value of R_c for this material system was determined from unloaded hole tension strength theory/test correlation. Dashed lines represent predicted ply shear and matrix failures. These predictions result in overly conservative estimates of laminate strength. The solid line is predicted fiber tension failure, representing a net section failure of the composite laminate. Laminate failure is predicted to occur at the first fastener in the joint, which transfers 44 percent of the applied load. Knowing the percent load transfer at this fastener location, predicted load at failure can be determined from the strength envelope. Predicted joint strength compares well with test results.

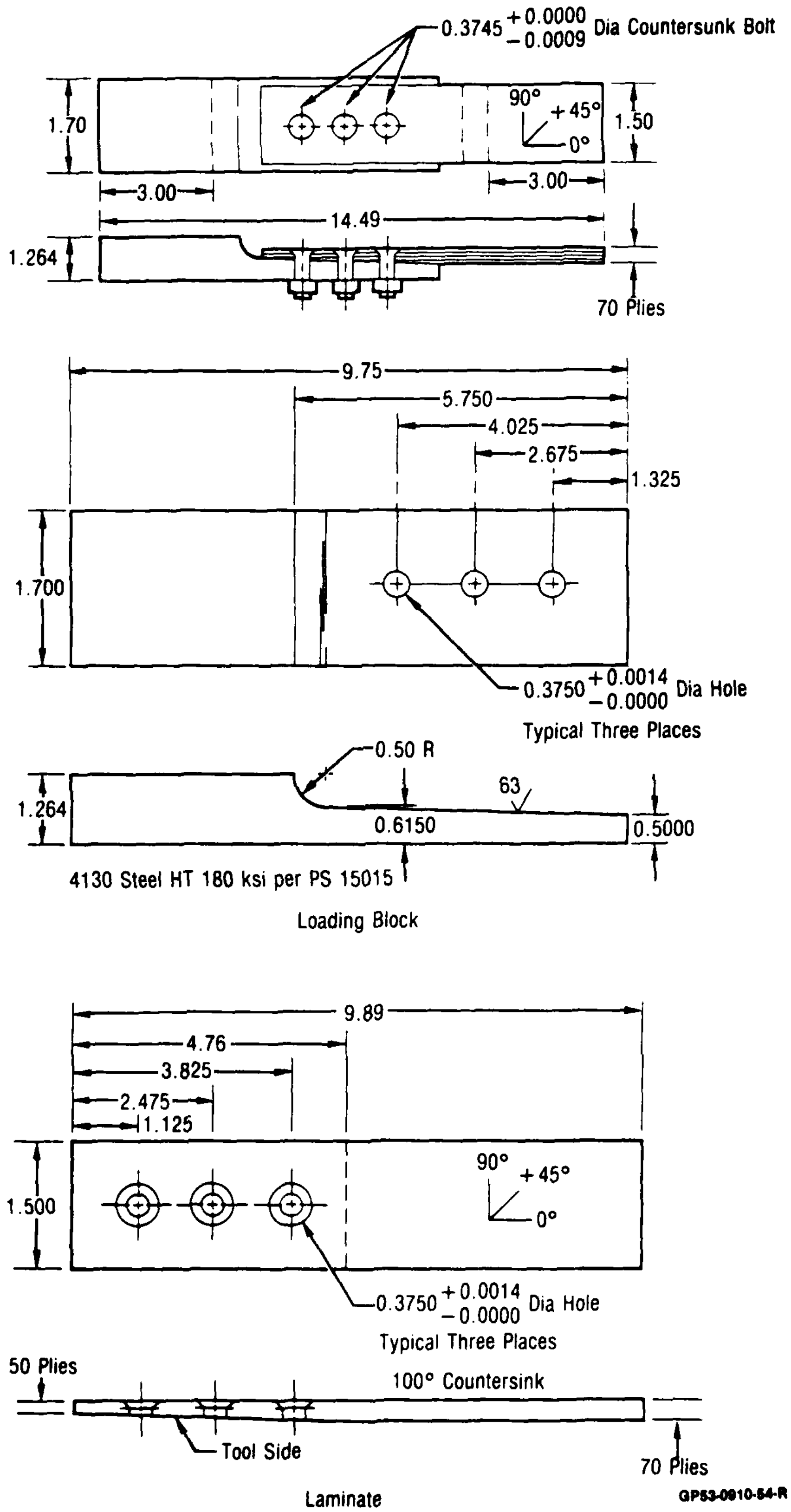

Figure 97. Multifastener Structural Component Test Specimen

Ply Number	Orientation
1	+45
2	0
3	−45
4	0
5	90
6	0
7	+45
10	0
11	+45
13	−45
14	0
15	90
16	0
19	−45
20	0
21	+45
24	0
26	0
27	+45
28	0
29	−45
32	0
33	90
34	0
35	−45
36	−45
37	0
38	90
39	0
42	−45
43	0
44	+45
45	0
47	0
50	+45
51	0
52	−45
55	0
56	90
57	0
58	−45
60	+45
61	0
64	+45
65	0
66	90
67	0
68	−45
69	0
70	+45

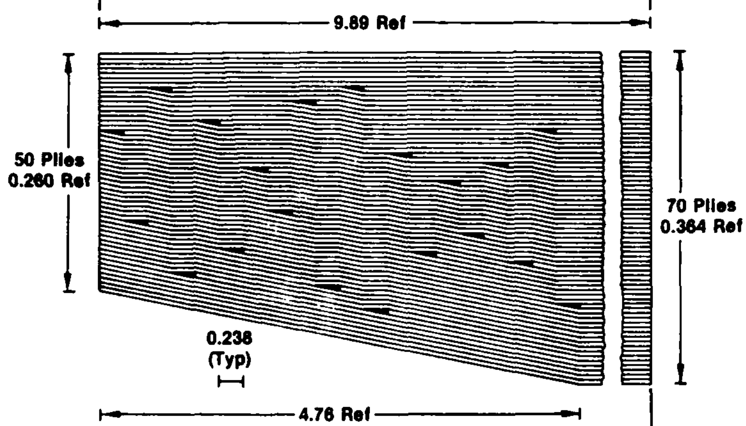

Ply Number	Orientation
1	+45
2	0
3	−45
4	0
5	90
6	0
7	+45
8	0
9	−45
10	0
11	+45
12	0
13	−45
14	0
15	90
16	0
17	+45
18	0
19	−45
20	0
21	+45
22	0
23	−45
24	0
25	90
26	0
27	+45
28	0
29	−45
30	0
31	+45
32	0
33	90
34	0
35	−45
36	−45
37	0
38	90
39	0
40	+45
41	0
42	−45
43	0
44	+45
45	0
46	90
47	0
48	−45
49	0
50	+45
51	0
52	−45
53	0
54	+45
55	0
56	90
57	0
58	−45
59	0
60	+45
61	0
62	−45
63	0
64	+45
65	0
66	90
67	0
68	−45
69	0
70	+45

GP53-0910-53-R

Figure 98. Laminate Stacking Sequence and Ply Drop-Off Schedule for Tapered Specimen

Resin System	Specimen Number	Thickness (inch)	Width (inch)	Failure Load (lb)	Failure Stress (ksi) Individual	Failure Stress (ksi) Average	Failure Strain (µin/in) Individual	Failure Strain (µin/in) Average	First Fastener Stress at Failure (ksi) Individual	First Fastener Stress at Failure (ksi) Average	First Fastener Bearing Stress at Failure (ksi) Individual	First Fastener Bearing Stress at Failure (ksi) Average
	2-6-1	0.436	1.508	29,100	53.0		2,490		56.2		99.9	
Cycom 907	2-6-2	0.437	1.507	29,400	53.6	53.1	2,550	2,510	56.8	56.4	101.0	100.2
	2-6-3	0.435	1.508	29,000	52.8		2,500		56.0		99.6	
	3-5-1	0.433	1.508	29,400	54.6		2,710		57.9		103.0	
Cycom 1808	3-5-2	0.432	1.509	29,300	54.4	54.5	2,810	2,670	57.7	57.8	102.6	102.7
	3-5-3	0.434	1.509	29,300	54.4		2,490		57.7		102.6	

GP53-0910-82-R

Figure 99. Multifastener Joint Static Test Results

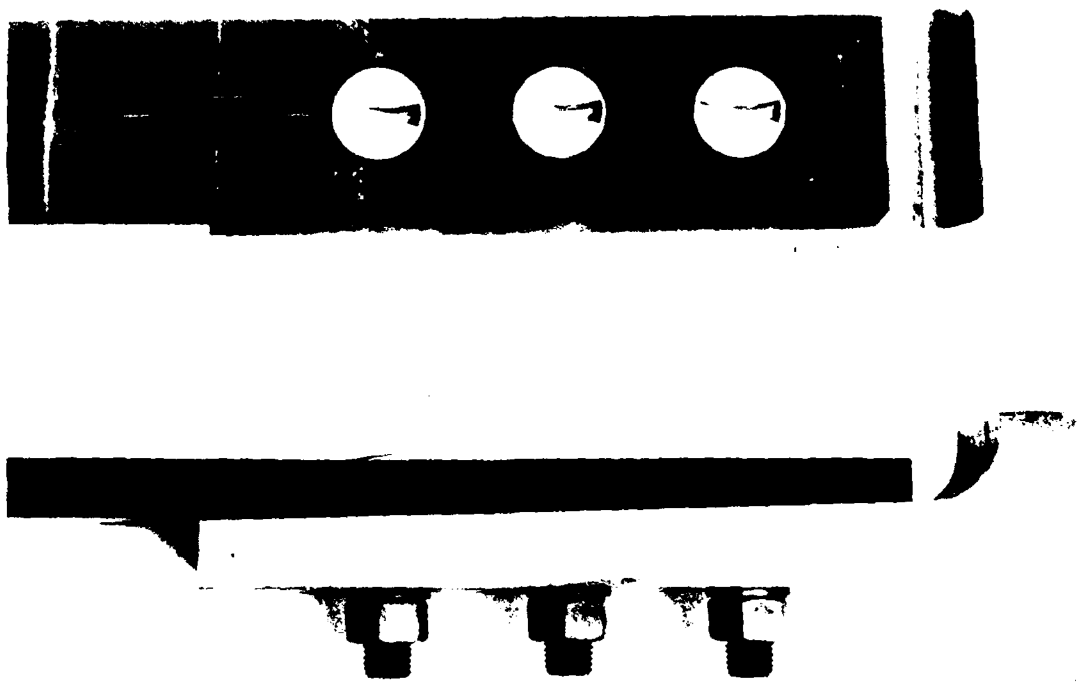

GP53-0910-38-R

Figure 100. Failed Multifastener Joint Static Tension Test Specimen

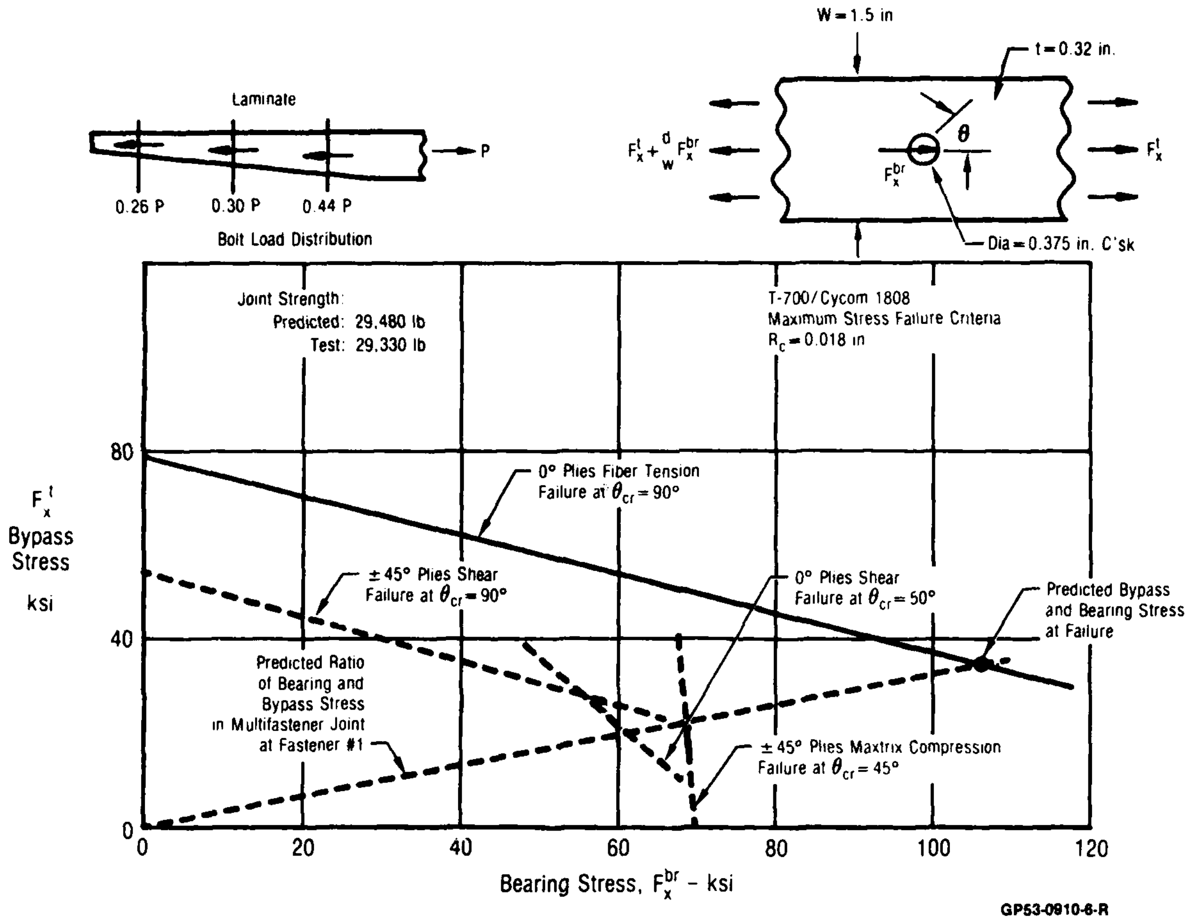

Figure 101. Multifastener Joint Static Strength Prediction

Fatigue tests were conducted for both the Cycom 907 and Cycom 1808 resin systems. Tension-compression (R=-1) cyclic loading was conducted at two stress amplitudes, with a replication of two. In fatigue testing of the multifastener joint there is a small range in stress level where laminate rupture or accumulation of hole elongation precedes fastener failure (Reference 2). Fatigue test results, conducted at 72 and 77 percent of static ultimate strength, are summarized in Figure 102; a comparison of test results are presented in Figure 103. Fatigue failures were of two types: (1) for the lower stress level failure was net section (rupture) at the first fastener location, as shown in Figure 104; (2) for the higher stress level failure was excessive accumulation of hole elongation; specimen failure is shown in Figure 105. Results from measurements of the accumulation of hole elongation with fatigue are shown in Figure 106; failure was defined to be 0.02 inch of total hole elongation, which was the cumulative contribution from each of the three fastener holes. For these limited tests no difference in material systems was observed.

Resin System	Load Level (lb)	First Fastener Stress Level (ksi)	First Fastener Bearing Stress (ksi)	Specimen Number	Thickness (inch)	Width (inch)	Number of Cycles	Mode of Failure
Cycom 907	21,000	40.8	72.1	2-6-4 2-6-5	0.438 0.439	1.508 1.507	2,630 4,860	Net Section
	22,500	43.7	77.3	2-6-6 2-6-7	0.436 0.435	1.507 1.507	2,308 2,208	Hole Elongation : --- 0.0217 inch
Cycom 1808	21,000	41.6	73.5	3-5-4 3-5-5	0.433 0.432	1.508 1.508	4,970 4,420	Net Section
	22,500	44.6	78.8	3-5-6 3-5-7	0.431 0.434	1.508 1.507	1,192 1,090	Hole Elongation : 0.0318 inch 0.0175 inch

GP53-0910-81-R

Figure 102. Multifastener Joint Fatigue Test Results Summary

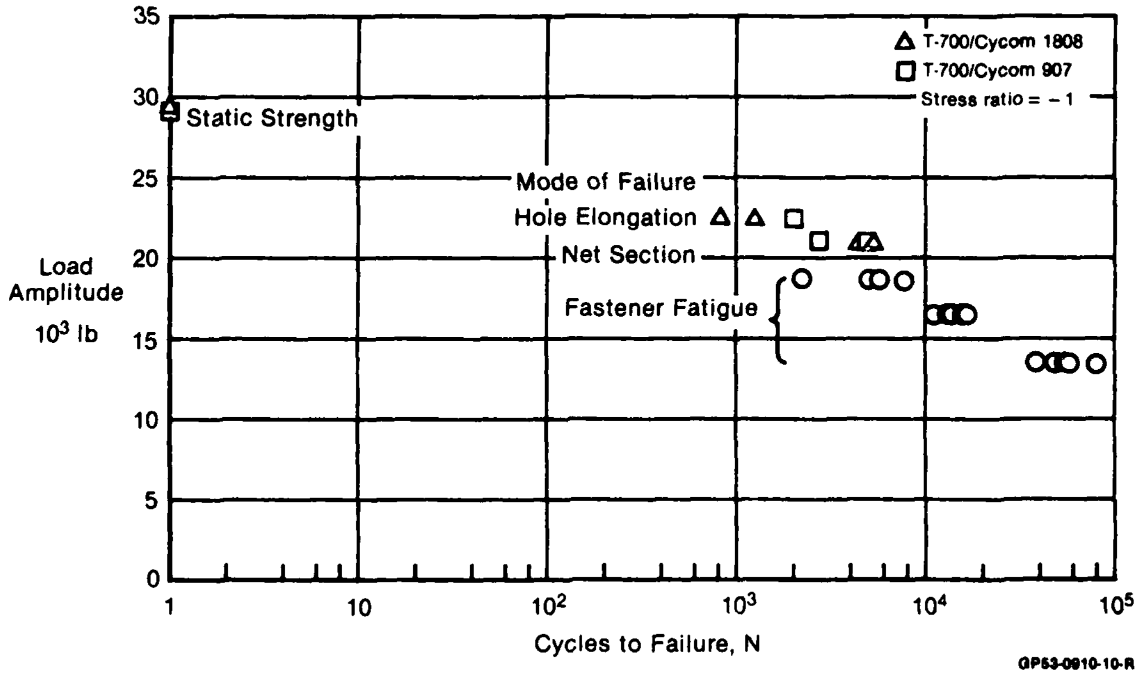

Figure 103. Multifastener Joint Fatigue Test Results

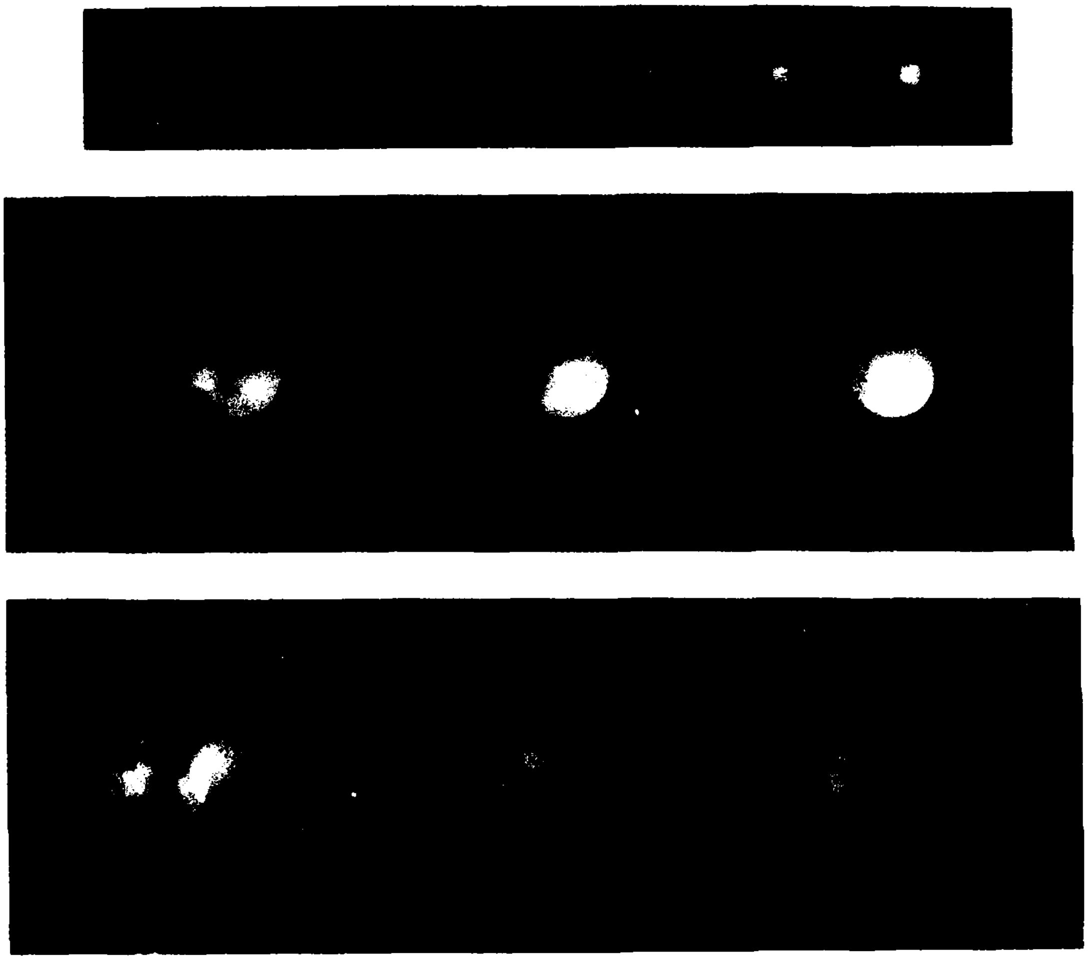

72% F_{tu}
$R = -1$

GP53-0910-108

Figure 104. Multifastener Joint Net Section Fatigue Failure

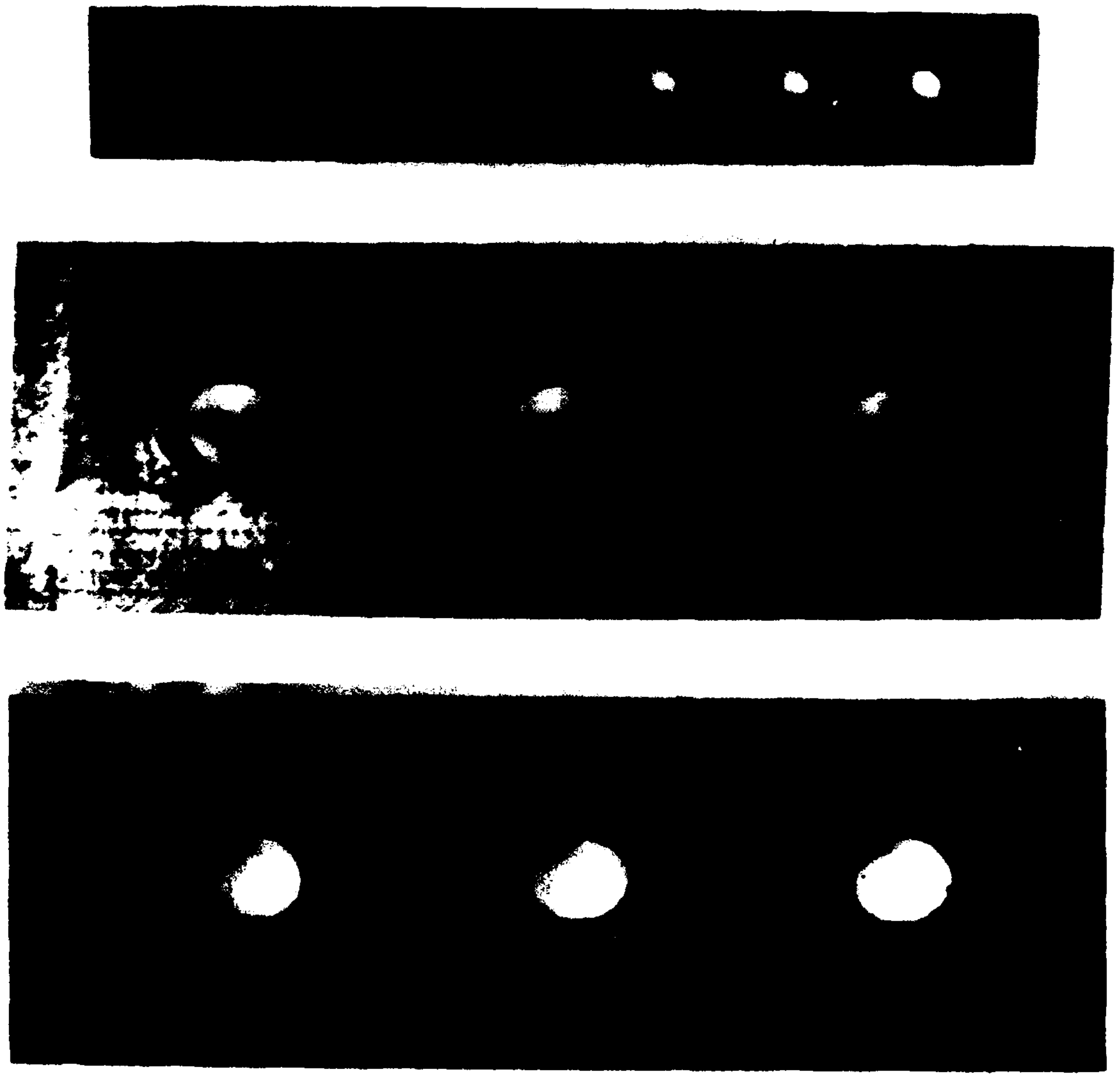

77% F_{tu}
R = −1

GP53-0910-37-R

Figure 105. Multifastener Joint Hole Elongation Fatigue Failure

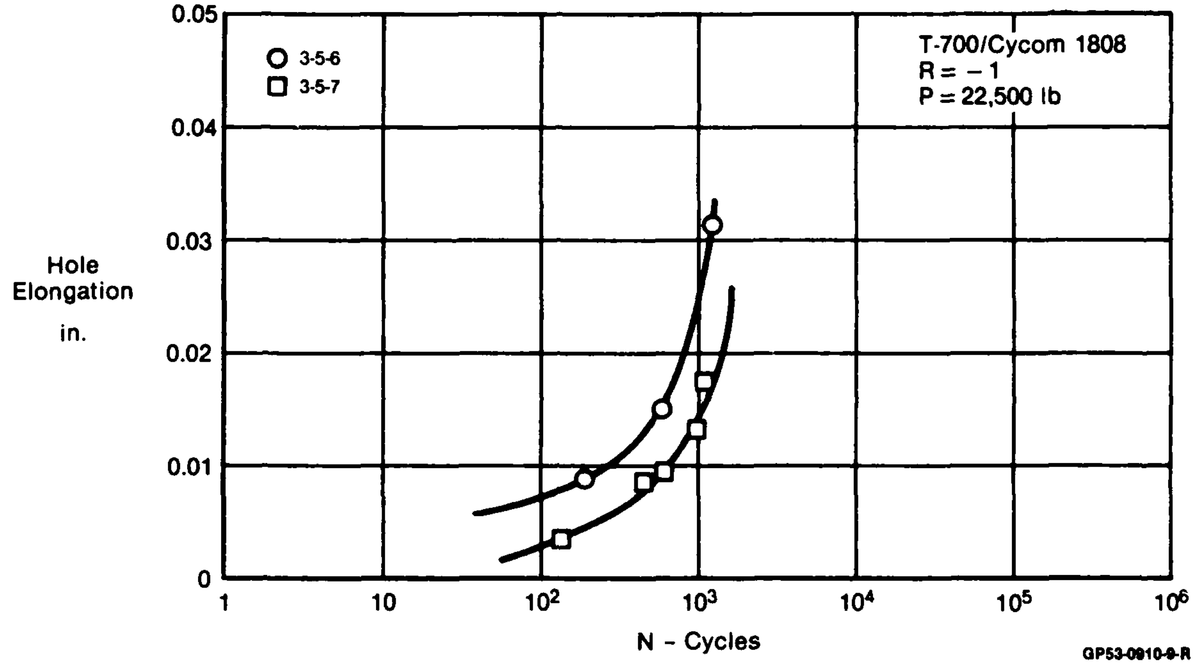

Figure 106. Multifastener Joint Hole Elongation Measurements

SECTION V

CONCLUSIONS AND RECOMMENDATIONS

An evaluation procedure was demonstrated which details tests, test methods, and analysis methods required to conduct a structural evaluation. The procedure includes test evaluation of basic lamina properties, static and fatigue testing of laminates with and without stress concentrations, evaluation of tolerance to low energy impact damage, and static and fatigue testing of a multifastener metal-to-composite splice joint. Also included in the structural evaluation are analytical methods to predict unnotched and notched laminate strength and mode of failure based on unidirectional ply mechanical properties. Four high strain fiber and resin composite material systems were evaluated using this procedure.

1. CONCLUSIONS

Based on the work conducted in this program.

1) The high strain fiber and resin systems demonstrated significant strength improvements in unidirectional mechanical properties relative to a baseline 3501-6 carbon/epoxy system.

2) Laminate strength and stiffness can be predicted using basic lamina mechanical properties and classical lamination plate theory for high strain fiber and resin composite material systems.

3) Unnotched laminate strength predictions using the interactive Tsai-Hill failure criteria demonstrated better correlation with test results than those using the noninteractive maximum stress failure criteria.

Unnotched laminate strength predictions are more conservative as the interlaminar shear stress component in the Tsai-Hill failure criteria becomes large. Ply intralaminar shear strength determined using the $\pm 45^{\circ}$ shear test specimen was conservative, due to the failure mechanisms inherent with this test method.

4) The characteristic dimension (R_c) failure hypothesis is valid for notched laminate strength predictions of high strain fiber and resin composite material systems. The value of R_c was found to be dependent on material system, although once determined can be used to predict laminate strength for various layups.

5) Unloaded hole fatigue durability was improved over baseline 3501-6 systems by an order of magnitude. Pure bearing fatigue durability and the accumulation of hole elongation was

material dependent and was not necessarily improved over the baseline 3501-6 system.

6) Multifastener joint strength can be accurately predicted by extending the characteristic dimension failure hypothesis and unloaded hole theory/test correlation to laminate strength predictions under combined bearing and bypass stress conditions.

2. RECOMMENDATIONS

The results of this program demonstrated the capability of the evaluation procedure to provide early insight into the improved structural efficiency of advanced carbon/epoxy material systems. However, additional work in the following areas is recommended to further improve and predict the performance of composite materials.

1) Although the $\pm 45^{\circ}$ test specimen is well recognized as a method for determining ply intralaminar shear mechanical properties, strength values are generally conservative due to inherent failure mechanisms. In addition, with the advent of tougher resin systems and their associated effect on failure mechanisms of the $\pm 45^{\circ}$ test specimen, comparison of material systems is difficult. Other test methods (Reference 12) should be evaluated as an alternative.

2) Accumulation of hole elongation with fatigue is a limiting factor in the efficient application of bolted joints in composite structures. Failure mechanisms and material properties, and their relation to joint fatigue life, should be further studied.

3) In addition to higher strain carbon fibers, intermediate modulus fibers should be investigated in combination with high strain resin systems. Their associated effect on strength, failure modes, durability, and damage tolerance should be evaluated.

REFERENCES

1. Garbo, S.P. and Ogonowski, J.M. "Effect of Variances and Manufacturing Tolerances on the Design Strength and Life of Mechanically Fastened Composite Joints", AFWAL-TR-81-3041, Volumes 1, 2 and 3, April 1981.

2. Badaliance, R. and Dill, H.D., "Compression Fatigue Life Prediction Methodology for Composite Structures," Report No. NADC-83060-60, September 1982.

3. Chamis, C.C. and Smith, G.T., "Resin Selection Criteria for Tough Composite Structures," 24th Structures, Structural Dynamics and Materials Conference, 2-4 May 1983.

4. Palmer, R.J., "Investigation of the Effect of Resin Material on Impact Damage to Graphite/Epoxy Composites," NASA-CR165677, March 1981.

5. Zimmerman, R.S.; Adams, D.F.; and Walrath, D.E.: Investigation of the Relations Between Neat Resin and Advanced Composite Mechanical Properties. NASA CR-172303, 1984.

6. Rosen, B.W., A Simple Procedure for Experimental Determination of the Longitudinal Shear Modulus of Unidirectional Composites, J. Composite Materials, Vol. 6, October 1972, p.552.

7. Petit, P.H., A Simplified Method of Determining the Inplane Shear Stress-Strain Response of Unidirectional Composites, Composite Materials: Testing and Design,ASTM STP 460, American Society for Testing and Materials, 1969, pp 83-93.

8. Pipes, R.B. and Pagano, N.J., Intralaminar Stresses in Composite Laminates Under Uniform Axial Extension, J. Composite Materials, October 1970, pp 538-548.

9. Wilkins, D.J., "A Comparison of the Delamination and Environmental Resistance of a Graphite-Epoxy and a Graphite-Bismaleimide," NAV-GD-0037, 15 September 1981.

10. Badaliance, R. and Dill, H.D., "Effects of Fighter Attack Spectrum Fatigue on Composite Fatigue Life," AFWAL-TR-81-3001, March 1981.

11. Saff, C.R., "Effects of Layup and Loading Frequency on Fatigue Life of Graphite/Epoxy," NADC-81017-60, October 1982.

12. Lee, S. and Munro, M., "In-Plane Shear Properties of Graphite Fibre/Epoxy Composites for Aerospace

Applications: Evaluation of Test Methods by the Decision Analysis Technique," Aeronautical Note NAE-AN-22, NRC No. 23778, October 1984.

☆U.S.Government Printing Office: 1986 — 646-067/40869